Chromosome walking towards the *Ror1* (Required for *mlo* resistance 1) locus in barley (*Hordeum vulgare* L.)

Inaugural-Dissertation

zur

Erlangung des Doktorgrades

der Mathematisch-Naturwissenschaftlichen Fakultät

der Universität zu Köln

vorgelegt von

Johanna Acevedo García

aus Fusagasugá, Kolumbien

Köln, 2012

Die vorliegende Arbeit wurde am Max-Planck-Institut für Pflanzenzüchtungsforschung in Köln in der Abteilung für Molekulare Phytopathologie (Direktor: Prof. Dr. P. Schulze-Lefert) angefertigt.

Berichterstatter:	Prof. Dr. Paul Schulze-Lefert
	Prof. Dr. Ulf-Ingo Flügge
	Dr. Patrick Schweizer
Prüfungsvorsitzender:	Prof. Dr. Martin Hülskamp
Tag der Disputation:	23. Januar 2012

Lo más importante no es llegar,
es permanecer, y de la mejor manera!
Oct.12.2008

El sueño es personal,
el sacrificio es colectivo.

Dedicada a mis padres y hermana

Table of Contents

Abbreviations

%	percent
(v/v)	volume per volume
(w/v)	weight per volume
°C	degrees Celsius
3’	downstream region (of a gene or sequence)
4MI3G	4-methoxyindol-3-ylmethylglucosinolate
5’	upstream region (of a gene or sequence)
AB1380	a *Saccharomyces cerevisiae* strain
Acc	*Acinetobacter calcoaceticus*
ade2-1	ochre mutation
ADF	actin depolymerizing factor
ADP	adenosine diphosphate
AFLP	amplified fragment length polymorphism
Alu	*Arthrobacter luteus*
Apo	*Arthrobacter protophormiae*
App	appressorium
ARF	ADP-rybosilation factor
At	*Arabidopsis thaliana*
Avr	Avirulence
BAC	bacterial artificial chromosome
Ban	*Bacillus aneurinolyticus*
BC	backcross
Bgh	*Blumeria graminis* forma specialis *hordei*
Bgl	*Bacillus globigii*
BiFC	bimolecular fluorescence complementation
bp	base pair(s)
Bsp	*Bacillus* species H
C	carboxy-terminal
Ca^{2+}	calcium ions
CaM	calmodulin
cDNA	complementary deoxyribonucleic acid
CDPK	calcium-dependent protein kinase
CEN4	a gene required for stable single-copy propagation of a YAC
cM	centimorgan
cm	centimetre
Cm	*Cucumis melo*
CO_2	carbon dioxide
Col-0	*Arabidopsis thaliana* ecotype Columbia-0
Cons	gene encoding a protein of unknown function, DUF1218 family
cv	cultivar
CWA	cell wall apposition

CYP	cytochrome P450
dai	days after infection
DAMP	danger-associated molecular patterns
DAPI	4´,6-diamidino-2-phenylindole
dH_2O	de-ionized water
DNA	deoxyribonucleic acid
dNTP	deoxynucleotide triphosphate
Dpn	*Diplococcus pneumoniae*
Dra	*Deinococcus radiophilus*
DUF	domain of unknown function
Eco	*Escherichia coli*
EDTA	ethylenediaminetetraacetic acid
EMS	ethyl methanesulfonate
ER	endoplasmic reticulum
EST	expressed sequence tag
ETI	effector-triggered immunity
f. sp.	forma specialis
F1GH	family 1 glycosyl hydrolase
Far1	far-red impaired response 1
FISH	fluorescence *in situ* hybridization
FL	full length
FRET	förster resonance energy transfer
g	gram
Gb	gigabase (s)
GDP	guanosine diphosphate
GFP	green fluorescent protein
GTP	guanosine triphosphate
hai	hours after infection
Hinc	*Haemophilus influenzae Rc*
Hinf	*Haemophilus influenzae Rf*
HIS	histidine selectable marker
Hph	*Haemophilus parahaemolyticus*
HR	Hypersensitive response
Hv	*Hordeum vulgare*
I10	near isogenic barley line in Ingrid background
IBSC	International Barley Genome Sequencing Consortium
IGV	integrative genomic viewer
ILV	intraluminal body
kb	kilobase(s)
l	liter
LRR	leucine rich repeat
LTP	lipid transfer protein
LTR	long terminal repeat
m	milli

M	molar (mol/l)
MAMP	microbe-associated molecular patterns
MAPK	mitogen activated protein kinase
MATH	Meprin and TRAF homology protein
Mb	megabase (s)
Mbo	*Moraxella bovis*
min	minutes
min	minutes
Mla	mildew locus a
Mlg	mildew locus g
Mlo	mildew locus o
Mnl	*Moraxella nonliquefaciens*
mol	mole
MTI	MAMP-triggered immunity
MVB	multivesicular body
n	nano
N	amino-terminal
NB	nucleotide binding site
NGS	next generation sequencing
NO	nitric oxid
No.	number
NOC2	nucleolar complex protein 2
Os	*Oryza sativa*
p	pico
P01	near isogenic barley line in Pallas background
PAMP	pathogen-associated molecular patterns
PCR	polymerase chain reaction
PDR	pleiotropic drug resistance
PEN1	penetration 1
PEN2	penetration 2
PEN3	penetration 3
PFGE	pulse field gel electrophoresis
PGT	primary germ tube
pH	negative decimal logarithm of H^+ concentration
Pol	gene encoding a DNA-directed RNA polymerase I subunit 2 protein
PP	penetration peg
Pp	*Physcomitrella patens*
PRR	pattern recognition receptor
Ps	*Pisum sativum*
PTI	PAMP-triggered immunity
Pvu	*Proteus vulgaris*
pYAC4	a yeast artificial chromosome vector for cloning *Eco* RI fragments
R	resistant
Rar1	required for *Mla12* resistance

RFLP	restriction fragment length polymorphism
RNA	ribonucleic acid
Ror	Required for *mlo*-resistance
ROS	reactive oxygen species
Rpg1	stem-rust resistance gene 1
rpm	rounds per minute
Rsa	*Rhodopseudomonas sphaeroides*
RT	room temperature
S	susceptible
SDS	sodium dodecyl sulphate
sec	seconds
Sl	*Solanum lycopersicum*
SMCN5	structural maintenance of chromosomes N-terminal domain containing protein
SNAP	synaptosomal-associated protein
SNARE	soluble N-ethylmaleimide-sensitive factor attachment protein receptor
SNP	single nucleotide polymorphism
STS	sequence-tagged site
SUP4	a gene required for stable single-copy propagation of a YAC
SYP	syntaxin of plants
Ta	*Triticum aestivum*
Taq	*Thermophilus aquaticus*
TEL	*Tetrahymena* telomere sequence for telemore formation in yeast
TEs	transposable elements
TIGR	The Institute of Genomic Research
TIR	terminal inverted repeat
TM	transmembrane
TRAF	TNF-receptor associated factor
TRP	tryptophan selectable marker
Tsp	*Thermus* species
U	unit
UGP	UDP-glucose pyrophosphorylase
URA	uracil selectable marker
UV	ultraviolet
V	volume
VAMP	vesicle-associated membrane protein
vir	virulence
Vrs1	six-rowed spike gene 1
Vv	*Vitis vinifera*
Xap	*Xylophilus ampelinus*
Xcm	*Xanthomonas campestris*
YAC	yeast artificial chromosome
Zm	*Zea mays*
µ	micro

Summary

The presence of the seven-transmembrane (7-TM) domain Mlo (mildew resistance locus o) protein is a prerequisite for successful colonization of barley (*Hordeum vulgare* L.) by the biotrophic powdery mildew fungus, *Blumeria graminis* f.sp. *hordei* (*Bgh*). The *mlo*-mediated resistance response is dependent on at least two genes, *Ror1* and *Ror2* (required for *mlo* resistance). Double mutant *mlo ror1* partially restores susceptibility to the fungus and exhibits reduced spontaneous leaf cell death. The *Ror1* gene represents an interesting target for characterization, since its isolation could reveal an unknown pathway or additional molecular components necessary for effective *mlo* resistance. Nevertheless, despite extensive prior efforts to clone the *Ror1* gene, its nature remains unknown. In this project, we pursued an alternative approach to isolate the *Ror1* gene performing chromosome walking using a barley YAC library combined with Next Generation Sequencing (NGS) techniques. Previously, the *Ror1* gene was located on barley chromosome 1H to an interval of ~0.15cM between two predicted flanking genes, *Cons* and *Pol*. These two genes were used to design primers to screen a barley YAC library by PCR. The isolated YAC clones and additional overlapping ones, discovered by chromosome walking, formed the basis of our YAC contig at the *Ror1* region. The YAC clones were paired-end sequenced by Illumina. Thorough analysis of the sequences revealed that we obtained two non-overlapping YAC contigs around the *Ror1* locus. Eight annotated genes present in the contigs were selected as candidate genes. However, by "pseudo-mapping" in a *Ror1* recombinant population and positioning in the YAC contigs, seven of the eight genes were excluded to encode *Ror1*. Furthermore, comparative genomics of barley with three other model grasses, *Oryza sativa*, *Brachypodium distachyon* and *Sorghum bicolor* revealed re-arrangements in the *Ror1* region. Additionally, for the first time, we could physically locate the *Ror1* region on barley chromosome 1H using Fluorescence *In Situ* Hybridization. Further chromosome walking steps are required to bridge the gap between *Pol* and *Cons* and complete the *Ror1* YAC contig. The analysis of newly isolated YAC clones/pools that can be used to extend the YAC contigs is currently in progress. Our approach combining classical genetics and second-generation sequencing technologies has opened a new door that can potentially lead to the isolation of the *Ror1* gene.

Zusammenfassung

Die Gegenwart des sieben Transmembrandomänen Proteins Mlo (mildew resistance locus o) ist Vorraussetzung für eine erfolgreiche Kolonialisierung von Gerste (*Hordeum vulgare* L.) durch den biotrophen Mehltaupilz *Blumeria graminis* f. sp. *hordei* (*Bgh*). Die *mlo*-vermittelte Mehltauresistenz hängt dabei von mindestens zwei Genen ab, *Ror1* und *Ror2* (required for *mlo* resistance). Die Doppelmutante *mlo ror1* ist wieder partiell anfällig gegenüber dem Mehltaupilz und weist verminderten spontanen Blattzelltod auf. Die Isolierung und Charakterisierung des *Ror1* Gens ist von großer Bedeutung, weil dadurch bisher unbekannte Prozesse sowie neue molekulare Komponenten enthüllt werden könnten, welche für eine effektive *mlo* Resistenz erforderlich sind. Trotz extensiver Bemühungen, das *Ror1* Gen zu klonieren, ist die Natur des Gens bis heute unbekannt. Daher wurde in der vorliegenden Arbeit ein alternativer Ansatz zur Isolierung von *Ror1* gewählt, bei dem ‚chromosome walking' einer genomischen YAC-Bibliothek aus Gerste mit Hilfe der Next Generation Sequenzierung (NGS) durchgeführt wurde. Es wurde zuvor gezeigt, dass das *Ror1* Gen auf dem Chromosom 1H in einem Intervall von ~ 0.15 cM zwischen den flankierenden Genen *Cons* und *Pol* lokalisiert ist. Mit Hilfe dieser beiden Gene wurden Oligonukleotide hergestellt, um die Gerste YAC-Bibliothek mittels PCR zu analysieren. Die dabei isolierten YAC-Klone sowie weitere überlappende Klone, die mittels ‚chromosome walking' identifiziert wurden, formten dabei die Basis für das YAC-Kontig um den *Ror1* Lokus. Die YAC-Klone wurden anschließend mit der ‚paired-end' Methode der Illumina-Technologie sequenziert. Ausführliche Sequenzanalysen ergaben die Identifizierung von zwei nicht-überlappenden YAC-Kontigs in der Nähe der *Ror1* Region, sowie acht annotierten Genen, die als *Ror1* Genkandidaten in Frage kamen. Sieben dieser Kandidaten wurden jedoch mittels ‚pseudo-mappings' einer rekombinanten *Ror1* Population sowie ihrer Positionierung in den YAC-Kontigs als putatives *Ror1* Gen ausgeschlossen. Zudem konnte mit Hilfe komparativer Genomanalysen von Gerste mit den drei Modellpflanzen *Oryza sativa*, *Brachypodium distachyon* und *Sorghum bicolor* eine Umorganisierung der *Ror1* Region festgestellt werden. Des Weiteren haben wir mittels der Fluoreszenz-in-situ-Hybridisierung zum ersten Mal die physikalische Lokalisation der *Ror1* Region auf dem Gerste Chromosom 1H bestätigt. Dennoch ist weiteres ‚chromosome walking' notwendig, um die Lücke zwischen den flankierenden Genen *Pol* und *Cons* zu schließen und das vollständige *Ror1* YAC-Kontig zu erhalten. Dazu wird die Analyse neu isolierter YAC-

Klone zurzeit weiter verfolgt. In der vorliegenden Arbeit haben wir gezeigt, dass der Ansatz klassische Genetik mit den Sequenziertechnologien der zweiten Generation zu kombinieren, neue Wege zur Isolierung des *Ror1* Gens eröffnet.

1. Introduction

Powered by the sun, plants are the only higher organism that can convert water and CO_2 into stored, usable chemical energy in carbohydrates, proteins and fatty acids. All animals including humans depend on these plant substances for survival (Agrios, 2005). Plants are considered "healthy" when they can carry out physiological functions to the best of their genetic potential. However, plants either cultivated or wild, are continuously exposed to various detrimental environmental factors, including pathogenic microorganisms, unfavourable environmental conditions and competitors of their own kind. These factors disrupt, alter or inhibit plant processes and cause disease (Agrios, 2005). Plant pathogens can be broadly divided into organisms that kill the host and feed on the contents (necrotrophs) and those that require a living host to complete their life cycle (biotrophs) (Dangl and Jones, 2001). An entire plant species exerts broad-spectrum resistance to the majority of genetic variants of a nonadapted pathogen species. Termed as "nonhost resistance", this phenomenon defines the most robust, highly effective and durable form of plant immunity (Thordal-Christensen, 2003; Nürnberger and Lipka, 2005; Lipka et al., 2010). Both host and nonhost pathogens have to breach the initial line of host defence. Firstly, the presence of preformed (chemical, enzymatic or structural) barriers forms an early obstacle for the ingress of the pathogens (Thordal-Christensen, 2003; Nürnberger et al., 2004). Secondly, if the pathogen manages to overcome these preformed barriers, it may become subjected to recognition of its pathogen/microbe associated molecular patterns (PAMPs/MAMPs) via pattern recognition receptors (PRRs) located at the plasma membrane (Thordal-Christensen, 2003; Nürnberger et al., 2004; Jones and Dangl, 2006). Plants also respond to endogenous self-molecules released by pathogen invasion, called danger-associated molecular patterns (DAMPs) (Dodds and Rathjen, 2010). PAMP-triggered immunity (PTI) comprises an array of early defence responses, which includes: the occurrence of ion fluxes across the plasma membrane, the generation of reactive oxygen species (ROS), nitric oxide (NO) and ethylene. At later steps in the defence response, cell walls are reinforced locally and antimicrobial compounds are synthesized and secreted. PAMPs trigger activation of

calcium-dependent protein kinases (CDPK), activation of mitogen–activated protein kinase (MAPK) cascades, and lead to changes in the transcription of many defence-related genes (Bittel and Robatzek, 2007; Aslam et al., 2009). Thirdly, the pathogens adapt and become able to suppress PTI through the deployment of "effector" proteins that interfere with early defence responses. Plants in turn adapt to this microbial innovation by evolving a class of polymorphic nucleotide-binding site leucine-rich repeat (NB-LRR) protein products encoded by *R* genes that recognize effectors either directly or indirectly. This recognition triggers a signal-transduction cascade that culminates in the activation of defence mechanisms and the arrest of pathogen growth (effector-triggered immunity -ETI-), an amplified version of PTI that often passes a threshold for induction of hypersensitive cell death (HR) (Dangl and Jones, 2001; Jones and Dangl, 2006). NB-LRR-mediated resistance is effective against obligate biotrophic pathogens or hemibiotrophic pathogens, but not against necrotrophic pathogens (Jones and Dangl, 2006).

1.1 Barley (*Hordeum vulgare* L.)

Kingdom: Viridiplantae / Phylum: Streptophyta / Class: Liliopsida / Family: Poaceae[1]

Barley is a worldwide extensively cultivated cereal crop. It is one of the first domesticated cereals and evolved from the wild progenitor *Hordeum spontaneum,* most likely, originating in the Fertile Crescent from Israel and Jordan to south Turkey, Iraqi Kurdistan and south-western Iran (Salamini et al., 2002). It is a diploid, self-pollinating plant with seven pairs of chromosomes (Jørgensen, 1994) and a large genome, with a size of 5.1 Gb, of which more than 80% is composed of repetitive DNA and has not been completely sequenced yet (Sreenivasulu et al., 2008; Mayer et al., 2009). Barley is used as raw material for the brewing and distilling industry, animal feed grain and is planted in more than 57 million hectares of agricultural land around the world (Mayer et al., 2011).

[1] http://www.ncbi.nlm.nih.gov/Taxonomy/Browser/barley

1.2 Powdery mildews

Kingdom: Fungi / Phylum: Ascomycota / Class: Leotiomycetes / Order: Erysiphales[2]

Powdery mildews are probably, the most common, conspicuous, widespread, plant pathogenic fungi. Powdery mildews appear as spots or patches of a white to greyish powder. They infect leaves, young shoots and stems, buds, flowers and young fruits of nearly 10,000 species of angiosperms (Agrios, 2005; Glawe, 2008). They are obligate biotrophic pathogens, which exclusively colonize the epidermal cell layer. The asexual powdery mildew life cycle commences with the landing of spores on the plant surface (Figure 1.1). Within 1-2 hours after inoculation (hai), from the spore the primary germ tube (PGT) is initiated and produces a minute "cuticular peg" that penetrates the plant cuticle but not the cell wall beneath it. By 8-9 hai, the PGT initiates the production of the appressorium (App). Around 10-12 hai from the penetration peg (PP) a mature App emerges and penetrates the wall of the host by using a combination of high turgor pressure and enzymatic degradation of the cell wall. Afterwards, beneath the App, the plant forms a cell wall apposition (CWA), (termed papilla), in response to the fungus. If the pathogen successfully breaches this barrier, the fungus will produce a feeding organ called "the haustorium" inside the living host cell (15-18 hai). The plant plasma membrane is not punctured but invaginated around the growing haustorium. After infection of the host, the pathogen continues its growth epiphytically by generating and elongating secondary hyphae (36-48 hai), from which it penetrates additional distant epidermal cells. Eventually, conidiophores arise from the superficial mycelium and new spores will spread and start a new infection cycle (Zhang et al., 2005; Eichmann and Hückelhoven, 2008; Glawe, 2008; Micali et al., 2011). Several economically important crops are affected by powdery mildews including cereals, such as barley -*Blumeria graminis* f.sp. *hordei*- (Mathre, 1997) and wheat -*Blumeria graminis* f.sp. *tritici*- (Bockus et al., 2010); but also tomato -*Oidium neolycopersici*- (Jones et al., 2001), pea -*Erysiphe pisi*- (Kraft and Pfleger, 2001), grapes -*Erysiphe necator*- (Gadoury et al., 2011); ornamentals like roses -*Podosphaera pannosa*- (Horst and Cloyd, 2007); and the model plant *Arabidopsis*

[2]http://www.ncbi.nlm.nih.gov/Taxonomy/Browser/powdery

thaliana -*Golovinomyces orontii* and *Golovinomyces cichoracearum*- (Adam and Somerville, 1996). The recent sequencing of the barley powdery mildew genome provided insight into the basis of the biotrophic life-style of this pathogen. In comparison with autotrophic ascomycetes, the *Bgh* genome exhibited loss of genes encoding enzymes of primary and secondary metabolism, carbohydrate-active enzymes, and transporters. In addition, massive retrotransposon proliferation and a four times expansion in genome-size larger than the median of other ascomycetes were observed (Spanu et al., 2010).

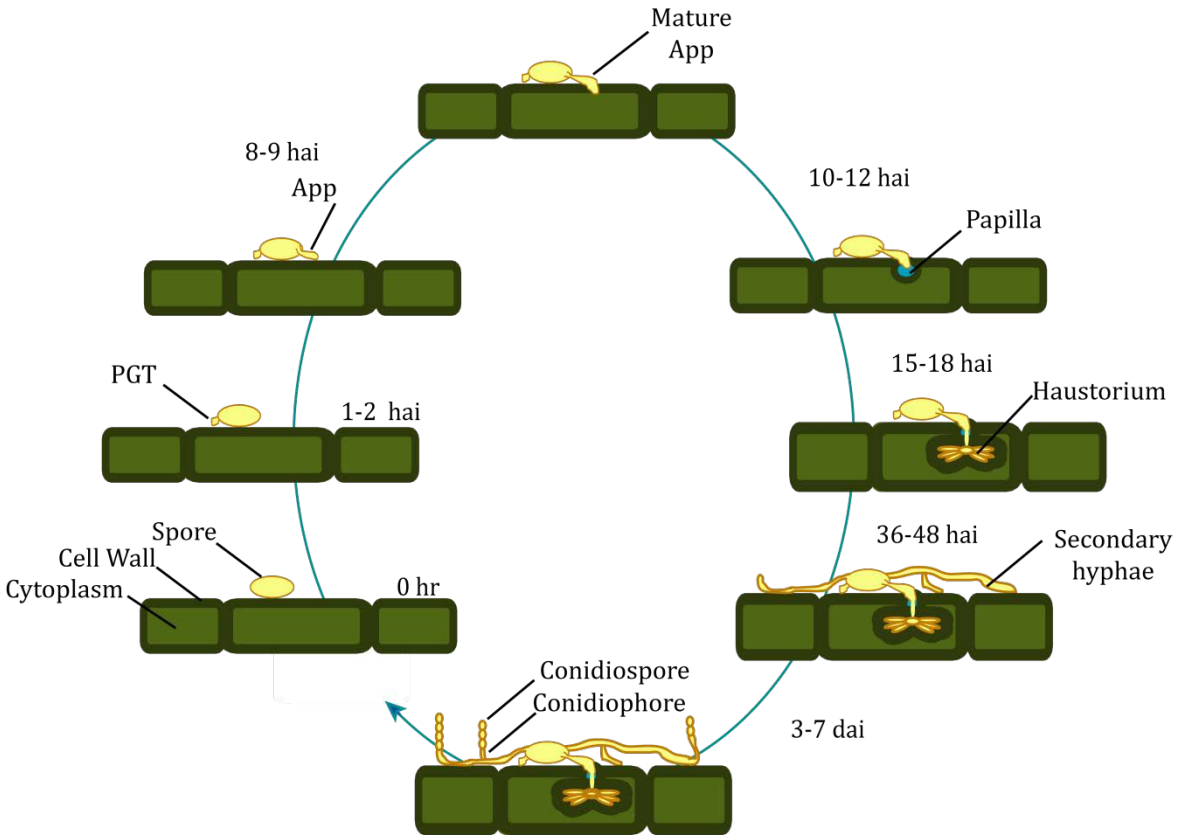

Figure 1.1. Schematic representation of the asexual powdery mildew life cycle in barley. The scheme represents the chronological order of events after the landing of a spore on the leaf surface. Within 1–2 hours after infection (hai), from the spore a primary germ tube (PGT) is formed, which differentiates into an appressorium (App) for host cell penetration. Penetration attempts are typically associated with the formation of a cell wall apposition (CWA), termed papilla. At about 15-18 hai, sporelings that successfully penetrated the host cell wall establish a haustorium within the epidermal cell enabling epiphytic growth of secondary hyphae. At 3–7 days after infection (dai) conidiophores with new conidiospores are formed and new spores will spread to start a new cycle.

1.3 Barley-powdery mildew interaction

The genetic basis of resistance to powdery mildew infection has been intensively studied in barley. Three modes of resistance gene action can be distinguished in the mildew/barley interaction (Görg et al., 1993): (1) loci at which only a single acting allele determines resistance specificity (e.g. mildew locus g -*Mlg*); (2) loci at which several dominant acting alleles each determine a different resistance specificity (e.g. mildew locus a -*Mla*); (3) a locus at which all analysed recessive acting alleles each confer resistance to all known powdery mildew isolates (e.g. mildew locus o -*Mlo*).

1.3.1 *Mlo*

Monogenic resistance mediated by recessive mutant alleles (*mlo*) of the *Mlo* locus was originally discovered in a mutagen-induced powdery mildew-resistant barley mutant in 1942 and it has been recovered many times from mutation experiments. In 1970, an additional allele was discovered as a spontaneous mutation in barley landraces from Ethiopia (Jørgensen, 1992a; Jørgensen, 1994). The presence of the recessive mutant alleles *mlo* confers broad-spectrum resistance to almost all known powdery mildew isolates and it is durable in the field despite extensive cultivation in Europe (Jørgensen, 1992b). A negative aspect of *mlo* mutations is enhanced susceptibility to the hemibiotrophic fungus *Magnaporthe grisea* (Jarosch et al., 1999) and the necrotrophic fungus *Bipolaris sorokiniana* (Kumar et al., 2001). In the absence of pathogens plants with the *mlo* allele spontaneously form CWA in the short cell type of the epidermis (Wolter et al., 1993). In addition, mesophyll cells in *mlo* mutants undergo spontaneous cell death, which suggests leaf senescence is accelerated in these plants (Peterhänsel et al., 1997; Piffanelli et al., 2002).

The barley *Mlo* gene was mapped to the middle of the long arm of chromosome 4 and was isolated by high resolution genetic mapping. The deduced protein of 533 amino acids has a molecular weight of 60.4 kDa. All induced mutant alleles show amino acid substitutions or truncated versions of the predicted wild type protein (Büschges et al., 1997). Mlo is a seven-transmembrane (7-TM) domain protein with the N terminus

located extracellularly and the C terminus intracellularly (Devoto et al., 1999). The susceptibility conferring activity of Mlo is enhanced by Ca^{2+} dependent Calmodulin (CaM) binding to a CaM binding domain present in the C-terminal cytoplasmic tail (Kim et al., 2002).

To present, homologs of barley *Mlo* are found in different plant species and they can be involved in processes other than pathogen resistance. In wheat (*Triticum aestivum*) seven *Mlo* members have been identified (*TaMlo1* to *-7*) (Konishi et al., 2010); in rice (*Oryza sativa*) 12 members (*OsMLO1 to -12*) (Liu and Zhu, 2008); in maize (*Zea mays*) 9 members (*ZmMlo1* to *-9*) (Devoto et al., 2003; Panstruga, 2005); in *Arabidopsis thaliana* 15 members (*AtMLO1* to *-15*) (Devoto et al., 2003; Panstruga, 2005); in tomato (*Solanum lycopersicum*) two members (*SlMlo1-SlMlo2*) (Bai et al., 2008); in moss (*Physcomitrella patens*) one member (*PpMlo1*) (Elliott et al., 2005); in melon (*Cucumis melo*) a recently cloned single member (*CmMlo1*) (Cheng et al., 2011); in grapevine (*Vitis vinifera*) 17 members (*VvMLO1* to *-17*) (Feechan et al., 2008); and a recently confirmed single member in pea (*Pisum sativum*) (*PsMLO1,* formerly *Er1*) (Humphry et al., 2011; Pavan et al., 2011).

In *Arabidopsis thaliana* the mutant *Atmlo2* presents incomplete resistance and a diminished rate of entry into host epidermal cells when challenged with the virulent powdery mildew *G. orontii*. *AtMLO2* belongs to a plylogenetic clade of three genes (*AtMLO2*, *AtMLO6* and *AtMLO12*) that represents co-orthologous of barley *Mlo*. When challenged with *G. orontii*, *Atmlo6* and *Atmlo12* single mutant lines and *Atmlo6 Atmlo12* (*Atmlo6/12*) double mutant lines support wild type levels of secondary hyphae formation and conidiophore production, whereas *Atmlo2 Atmlo6* (*Atmlo2/6*) and *Atmlo2 Atmlo12* (*Atmlo2/12*) double mutant lines support lower levels of fungal growth than *Atmlo2*. The *Atmlo2 Atmlo6 Atmlo12* (*Atmlo2/6/12*) triple mutant is resistant to the fungal pathogen. However, these mutants are susceptible to the biotrophic oomycete *Hyaloperonospora parasitica* and the bacterium *Pseudomonas syringae*. *Atmlo2/6* double and *Atmlo2/6/12* triple mutants result in enhanced disease symptoms when they are challenged with the necrotroph *Alternaria alternatae* or the hemibiotroph *Phytophtora infestans.* The unchallenged mutants *Atmlo2*, *Atmlo2/6*, *Atmlo2/12* and *Atmlo2/6/12* show developmentally controlled spontaneous callose

deposition as the barley *mlo* mutants. These findings demonstrate that broad spectrum immunity against powdery mildew based on loss-of-function *mlo* alleles can be achieved in a distant dicot species and suggest a highly conserved mechanism(s) preventing fungal ingress, which evolved before the monocot-dicot split, approximately 200 million years ago (Consonni et al., 2006).

1.4 Genes required for *mlo* resistance

Seeds from a resistant backcross (BC) line carrying the *mlo* allele (BCIngrid *mlo*-5) were mutagenized using ethyl methanesulfonate (EMS) and sodium azide (NaN_3) to identify genes required for *mlo*-mediated resistance. Six M2 individuals (A39, A44, A89, C36, C69, and C88) were susceptible to the powdery mildew fungus isolate K1. The susceptibility of these individuals was monogenic and inherited recessively. The mutants could be assigned to two independent complementation groups: A39, A89, C36, C69 and C88 (C82 and C33, not published) represented one group (Figure 1.2) and A44 represented the second group. The respective loci were designated *Ror1* and *Ror2* (required for *mlo* resistance), respectively (Freialdenhoven et al., 1996).

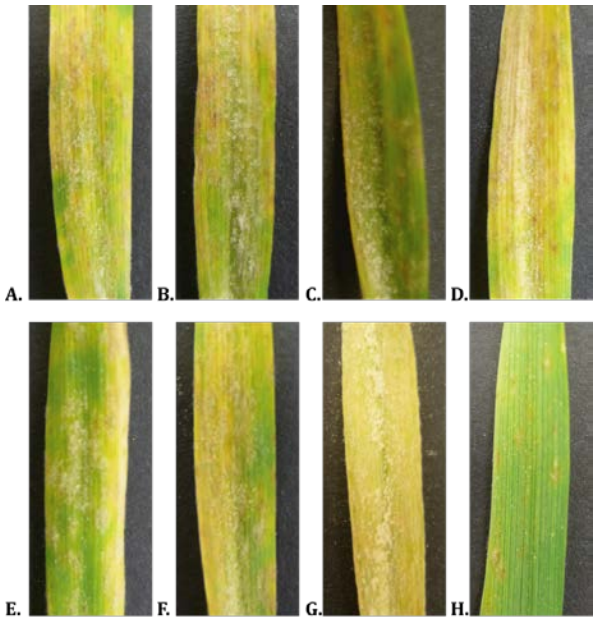

Figure 1.2. Powdery mildew infection phenotype of *ror1* mutants, Ingrid and BCIngrid *mlo*-5 seedlings at seven days after inoculation with *Blumeria graminis* f.sp. *hordei* (*Bgh*) isolate K1. (A-F) *ror1* mutants (partially susceptible) **(A)** A89. **(B)** C33. **(C)** C36. **(D)** C69. **(E)** C82. **(F)** C88. **(G)** Ingrid (susceptible). **(H)** BCIngrid *mlo*-5 (resistant).

The *Ror* genes are required for full resistance of different tested *mlo* alleles in barley. After *Bgh* infection, the resistant BCIngrid *mlo*-5 (*mlo Ror1 Ror2*) cultivar exhibits a maximal penetration frequency of 0.5%; in contrast, a penetration frequency of ~70% is observed in the susceptible (*Mlo Ror1 Ror2*) near-isogenic cultivar Ingrid; the alleles from the *ror1* mutant (*mlo ror1 Ror2*) show approximately 20-30% of host cell penetration and (*Mlo ror1 Ror2)* approximately 80%; the *ror2* mutant (*mlo Ror1 ror2*) 10% and (*Mlo Ror1 ror2)* close to 80% (Freialdenhoven et al., 1996; Collins et al., 2003). The combined mutations in *ror1* and *ror2* have an additive effect on susceptibility, suggesting separate defence pathways (Collins et al., 2003). The *ror* mutants act in a non-race specific manner; they confer susceptibility not only to the powdery mildew isolate K1 but also to the isolates A6 and R146 (Freialdenhoven et al., 1996). The function of *Ror1* and *Ror2* involves the accumulation of H_2O_2 in *mlo* barley during *Bgh* attack. *ror* mutants show less H_2O_2 accumulation beneath the appressorium, but more interaction sites with whole cell H_2O_2 accumulation and hypersensitive cell death response than resistant BCIngrid *mlo*-5 (Hückelhoven et al., 2000). Race-specific resistance specified by *Mla* or *Mlg* is not compromised by mutations in *Ror* genes (Peterhänsel et al., 1997). Findings from (Trujillo et al., 2004) support that the *ror* effect is uncoupled from the *mlo* effect in non-host resistance to *Blumeria graminis* f.sp *tritici* (*Bgt*). In this case, *mlo*-5 *ror* and *Mlo Ror* showed similar degrees of penetration and HR, in contrast *mlo*-5 *Ror* was less often penetrated and showed less HR (Peterhänsel et al., 1997), whereas *Mlo ror* was more often penetrated and showed high HR (Trujillo et al., 2004). This might indicate that HR is expressed as a second line of defence in barley cells successfully penetrated by *Bgt*. Regarding other pathogens, on the one hand, mutants defective in *ror (mlo*-5 *ror)* are more sensitive to necrosis-inducing toxin from *B. sorokiniana* than wild-type (*Mlo Ror*) but show less symptoms than *mlo*-5 (*mlo*-5 *Ror*) (Kumar et al., 2001); on the other hand, barley *mlo* (*mlo*-5 *Ror*) shows enhanced susceptibility to *M. grisea*, but the combined mutations of *mlo ror1* have no influence on the *mlo*-mediated phenotype after *M. grisea* infection (Jarosch et al., 1999). Interestingly, (Jarosch et al., 2005) revealed that the as-yet-uncloned *Ror1* gene limited entry of *M. grisea* into barley epidermal cells, most evident in *Mlo* genotypes, as the *Mlo ror1* genotype exhibited a significant increase in lesion number and a reduced formation of effective papillae compared to *ror2* mutants that showed unaltered interactions with *M. grisea*.

These combined findings from various groups show that *Ror1* is essential for *mlo*-mediated resistance to adapted biotrophic fungi, but also contributes to the natural basal resistance to non-adapted biotrophic or hemibiotrophic fungi independent of *Mlo*.

1.5 Barley *Ror2*

The *Ror2* gene, located on barley chromosome 5HL, was isolated using a barley-rice syntenic-map-based cloning approach. *Ror2* encodes a syntaxin, a member of the soluble *N*-ethylmaleimide-sensitive factor attachment protein receptor (SNARE) superfamily. This class of proteins mediates membrane fusion events. Subcellular fractionation revealed that the Ror2 protein localizes to the plasma membrane (Collins et al., 2003). The *ror2*-1 (A44) mutation has a 31-amino-acid in-frame deletion covering most of the Hc helix (Collins et al., 2003). Ror2 forms a binary t-SNARE complex with the synaptosomal-associated protein 25 -SNAP25-like protein (SNAP34) which in turn interacts with the R-SNARE vesicle-associated membrane protein 721 (VAMP721) (Collins et al., 2003; Kwon et al., 2008). Pairwise *in vivo* interaction studies of this ternary SNARE complex in epidermal cells were performed by bimolecular fluorescence complementation (BiFC) and Förster resonance energy transfer (FRET) (Kwon et al., 2008; Kwaaitaal et al., 2010). Biochemical analysis showed that Ror2 is present in a heat-sensitive, but SDS-resistant SNARE complex. Furthermore, the combined use of FRET and BiFC showed that Ror2, SNAP34 and VAMP721 can form an authentic ternary SNARE complex *in planta* (Kwaaitaal et al., 2010). A genetic screen for *Arabidopsis* penetration (*pen*) mutants that permit an elevated entry frequency of the non-adapted powdery mildew fungus *Bgh*, resulted in the identification of multiple genes (*PEN1*, *PEN2* and *PEN3*) needed for full penetration resistance. Map-based cloning of *PEN1* revealed that the gene encodes the *A. thaliana* syntaxin SYP121 and it is a functional orthologous of barley Ror2 (Collins et al., 2003). The PEN1 protein was shown to reside in the plasma membrane (Collins et al., 2003). These data indicate a specialized antifungal resistance function conserved between monocot and dicot plants and provide a mechanistic link between basal and nonhost penetration resistance. In *Arabidopsis* PEN1 was found to interact with SNAP33 and VAMP721/ VAMP722, which together form a SDS-resistant/heat-

sensitive ternary SNARE complex. This interaction was validated *in planta* by co-immunoprecipitation experiments (Kwon et al., 2008). The ternary SNARE complexes focally accumulate at sites of attempted pathogen ingress, beneath the fungal appressorium, in the papillae and through its extension in the haustorial encasements. Continued pathogen entry and growth is likely inhibited through secretion of cell wall components and anti-fungal compounds derived from the ER/Golgi protein secretory pathway and facilitated by the PEN1/SNAP33/VAMP(721/722) protein complex (Kwon et al., 2008; Meyer et al., 2009).

PEN2 was isolated by map-based cloning and was initially suggested to encode a deduced family 1 glycosyl hydrolase (F1GH) which localizes to peroxisomes and accumulates at *Bgh* entry sites. Interestingly, after infection with *Bgh*, entry rates in the *pen1 pen2* double mutant are higher than wild type or single mutants, suggesting that PEN1 and PEN2 act in separate defence pathways (Lipka et al., 2005). Bednarek et al., (2009) showed that indole glucosinolate biosynthesis is needed to restrict the fungal entry. The functionally redundant gene products of *CYP79B2* and *CYP79B3* mediate the conversion of tryptophan to indole-3-acetaldoxime, a precursor of 4-methoxynidol-3-ylmethylglucosinolates (4MI3G) by CYP81F2 P450 monooxygenase-catalized conversion. Subsequently, the 4MI3G is hydrolysed by the atypical myrosinase, PEN2. The focal accumulation of PEN2 plus its biochemical function suggest a localized synthesis of, and concentration of the glucosinolate-derived products at fungal entry sites.

PEN3 encodes a putative pleiotropic drug resistance (PDR)–like ABC transporter (formerly annotated as PDR8), which was isolated by map-based cloning. The gene encodes a 1469 amino acid protein with 13 transmembrane domains, which localizes to the plasma membrane, accumulates beneath the fungal appressorium and partially surrounds the haustorium after *Bgh* infection. The *pen3* mutant supports the establishment and growth of secondary hyphae by *Bgh*. Like *pen1* and *pen2*, the *pen3* mutant allows high fungal entry rates (~23%, 27% and 20%, respectively) compared with the Columbia-0 (Col-0) wild-type (Stein et al., 2006). PEN2 and PEN3 limit growth of a broad spectrum of pathogens, including the nonadapted oomycete *P. infestans*, the adapted powdery mildew *G. orontii* and *G. cichoracearum* and the

necrotrophic fungus *Plectosphaerella cucumerina* (Lipka et al., 2005; Stein et al., 2006). It is suggested that the bioactive end-products of the PEN2 metabolic pathway are transported to the apoplast by the ABC transporter PEN3, poisoning the fungus as its attempts to breach the cell wall (Stein et al., 2006). Mlo, Ror2 and PEN1, co-localize and become concentrated at attempted pathogen entry sites (Bhat et al., 2005). Thus specific isoforms of Mlo and syntaxins represent ancient and antagonistically acting components, promoting or restricting powdery mildew ingress, respectively. In contrast, the peroxisome-associated PEN2 and the ABC transporter PEN3 seem to be a recent innovation of *A. thaliana* (Consonni et al., 2006).

Böhlenius et al., (2010) revealed a functional link between the t-SNARE Ror2 and the small GTPase ADP-rybosilation factor (ARF) subfamily A1b and A1c (ARFA1b/1b) in penetration and callose deposition in barley. Using transient-gene silencing and transient expression of constitutive GDP- and GTP-locked forms of ARF GTPases they showed that ARFA1b/1c is required for Ror2-mediated penetration resistance against *Bgh* and that the proteins function in the same membrane trafficking pathway. Green fluorescent protein (GFP) fusions of ARFA1b/1c localized to multivesicular bodies (MVBs). In addition, ARFA1b/1c function was found to be required for callose deposition into papillae of attacked barley cells. High frequency of haustorium formation in barley epidermal cells expressing the GTP- or GDP-locked ARFA1b/1c versions, suggested that one or more MVB-dependent, but undiscovered components interfere with fungal penetration. Which papillae constituents next to callose are transported to fungal attack sites by the Ror2 syntaxin/MVB pathway is still unknown.

1.6 Barley *Ror1*: progress on map-based cloning

Crosses between *ror1* mutants (*mlo*-5 *ror1* in cv. Ingrid) and *mlo Ror1* lines from different genetic backgrounds were used for mapping *Ror1*: (1) A89 x BCPallas (*mlo*-5); (2) C69 x Grannenlose Zweizeilige (*mlo*-11); (3) A89 x Malteria Heda (*mlo*-3). The gene was located to the centromeric region of chromosome 1H using amplified fragment length polymorphism (AFLP) and restricted amplified length polymorphism

(RFLP) markers. Over 2,300 segregants from the three populations were used in *Ror1* linkage analysis; fine genetic mapping by sequence-tagged site (STS) markers located *Ror1* to a 0.2- to 0.5-cM marker interval (Collins et al., 2001).

Since the initial *Ror1* mapping described by (Collins et al., 2001), the population derived from the *ror1* mutant A89 (*ror1*-2) x Malteria Heda (*mlo*-3) cross was expanded, because patterns of linkage disequilibrium were such that this was the only one of the three populations in which sequence polymorphism was present on both sides of *Ror1.* This brought the total number of segregants analysed to more than 3,000 (6,000 gametes). By using a synteny-based comparison with rice (*Oryza sativa*) the *Ror1* region in barley was identified as syntenic to a region of rice chromosome 10, which had been partially sequenced by The Institute of Genomic Research (TIGR). *Ror1* was mapped in barley between two genes, one recombinant above (towards the telomere), encoding a protein of unknown function DUF1218 family protein (Os10g0495900 [RAP-DB nomenclature]) from here named *Cons*, and 7 recombinants below the other (towards the centromere), encoding a DNA-directed RNA polymerase I subunit 2 (Os10g0495600 [RAP-DB nomenclature]), from here named *Pol*. The interval between these two genes in rice is only 2 kb, contains the promoters for both (head-to-head oriented) genes, and contains no predicted genes (Figure 1.3). Sequencing of both of the flanking genes from the *ror1* mutant lines indicated that these genes are not *Ror1* (Nicholas Collins, Australian Centre for Plant Functional Genomics, personal communication, unpublished data). Therefore, it appears that rice either does not contain an orthologous of *Ror1*, or that an orthologous is located in a non-syntenic/non-collinear region of the rice genome. Furthermore, these findings suggest that the *Ror1* gene might be an inversion or insertion in the interval between *Pol* and *Cons* on the barley genome.

Next to the approaches discussed above, a Bacterial Artificial Chromosome (BAC) library of *Brachypodium sylvaticum* was used to facilitate the identification of the *Ror1* gene. Two BACs containing *Pol* and *Cons* flanking genes were identified (BAC 78G14 and BAC 77I12); the interval between the two genes is about 4.5 kb and contains no predicted genes (Figure 1.3). Suggesting a similar situation as was found in rice (Mariam Benjdia, unpublished data).

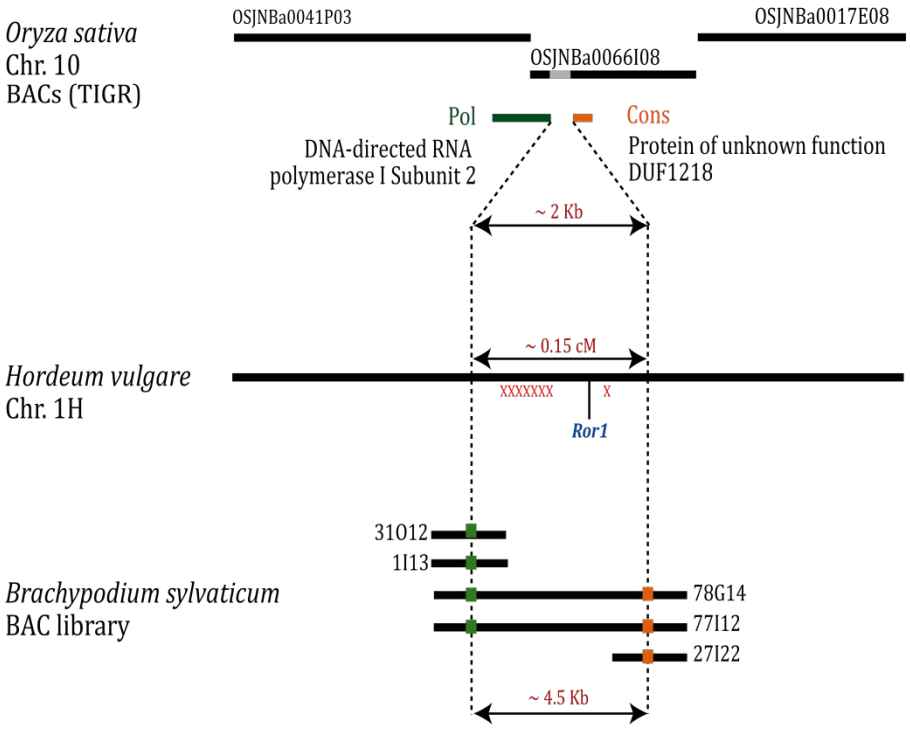

Figure 1.3. Progress on *Ror1* cloning. In barley (*Hordeum vulgare*) the *Ror1* gene was located on chromosome 1H. Based on the synteny with rice (*Oryza sativa*) the barley *Ror1* region was identified in a region of rice chromosome 10. The *Ror1* gene was mapped in barley between two genes, one recombinant above (towards the telomere), encoding a hypothetical protein (*Cons*), and 7 recombinants below (towards the centromere), encoding the DNA-directed RNA polymerase I subunit 2 (*Pol*). The interval between these two genes in rice (*Oryza sativa*) is only 2 kb, and contains no predicted genes. In *Brachypodium sylvaticum* two BAC contigs containing *Pol* and *Cons* flanking genes were identified (BAC 78G14 and BAC 77I12), the interval between the two genes is about 4.5 kb and contains no predicted genes. Suggesting a similar situation as was found in rice.

1.7 Thesis Aim

The barley *Ror1* gene is required for full expression of the broad-spectrum *mlo* resistance to the powdery mildew fungus *Bgh*. Mutations in this gene partially disable other known effects of *mlo*-mutations like spontaneous formation of CWA and spontaneous mesophyll cell death. The *Mlo ror1* genotype exhibit a super-susceptible phenotype with respect to penetration resistance to *Bgh*. Combined *ror1* and *ror2* mutations have an essentially additive effect on increasing powdery mildew penetration frequency, indicating two separate pathways. Furthermore, the *ror1* mutation does not alter the function of race-specific powdery mildew resistance

genes and its effect is uncoupled from *mlo* in nonhost resistance, suggesting that *Ror1* is not only relevant for *mlo* resistance, but also contributes to the natural basal resistance present in wild-type (*Mlo*) genotypes. The *Ror1* gene represents an interesting target for isolation and characterization, since its isolation could reveal an unknown pathway and additional molecular components necessary for effective *mlo* resistance. However, despite extensive prior efforts to clone the *Ror1* gene, its nature remains unknown. In this project we pursue an alternative approach to isolate the *Ror1* gene: the use of a barley YAC library and Next Generation Sequencing (NGS) techniques combined with a "pseudo-map-based" cloning approach. The screening of a barley Yeast Artificial Chromosome (YAC) library provides large-insert genomic clones from which DNA sequence information can be readily unravelled by Illumina sequencing. Subsequently, candidate genes identified on the YAC clones can either be verified or discarded by pseudo mapping in a *Ror1* recombinant population. With this approach we open a new door which potentially will lead us to find our gene of interest, *Ror1*.

2. Materials and Methods

2.1 Materials

2.1.1 Plant Material

The following barley (*Hordeum vulgare* L.) lines were used in this study: Golden Promise (*Mlo*); P01 (near-isogenic line in "Pallas" background containing *Mla1*); I10 (near-isogenic line in "Ingrid" background containing *Mla12*); BCIngrid *mlo*-5 containing the *mlo*-5 resistance allele from cv Carlsberg II backcrossed into cv Ingrid; Malteria Heda *mlo*-3 containing the *mlo*-3 resistance allele induced by γ irradiation (Favret, 1965); *ror1* mutants A39 (*ror1*-1), A89 (*ror1*-2), C36 (*ror1*-3) C69 (*ror1*-4), C88 (*ror1*-5), were generated by ethyl methanesulfonate (EMS) or NaN_3 mutagenesis of the line BCIngrid *mlo*-5 (Freialdenhoven et al., 1996); C33 (*ror1*-6) and C82 (*ror1*-7) were found later and are not published. *Ror1*-recombinant population (C473, 74-2, 51, 77-5, 111, 21-2, 26-3, C487 and 102-1) was derived from a cross between the partially susceptible *ror1* mutant line A89 (*ror1*-2; *mlo*-5) and a fully resistant line carrying a wild type *Ror1* allele and the Malteria Heda *mlo*-3 resistance allele (*Ror1*; *mlo*-3) (Collins et al., 2001).

2.1.2 Pathogen material

Barley powdery mildew (*Blumeria graminis* f.sp. *hordei, Bgh*) isolate K1 was used for plant-pathogen inoculation assays (Section 2.2.1.3). This isolate contains the following avirulence (*Avr*)/virulence (*vir*) profile: *Avr*: *AvrMla1, AvrMla3, AvrMla7, AvrMla22, AvrMlLa, AvrMl*(Ab) and *vir*: *virMla6, virMla9, virMla10, virMla11, virMla12, virMlg, virMl(CP), virMlH, virM1K, virMlra*) (Shen, 2004).

2.1.3 Barley Yeast Artificial Chromosome (YAC) library

A four-genome-equivalent barley Yeast Artificial Chromosome (YAC) library with an average insert size of 480 kb was screened. The library was constructed using barley genomic DNA cv. Ingrid, the YAC vector pYAC4 and the *Saccharomyces cerevisiae* strain AB1380 (Simons et al., 1997).

2.1.3.1 YAC vector pYAC4

The pYAC4 vector contains all necessary elements to be replicated as a circular plasmid in *Saccharomyces cerevisiae* (Figure 2.1). It carries a unique *Eco* RI cloning site in the SUP4 gene (an ochre-suppressing allele of a tyrosine tRNA), a centromere (CEN4) required for stable single-copy propagation of the YAC, an ARS1 site (autonomous replication sequence, naturally adjacent to TRP1 gene), selectable markers on both sides of the centromere TRP1 (tryptophan), HIS3 (histidine) and URA3 (uracil) and two sequences derived from *Tetrahymena* telomeres (TEL) for telomere formation in yeast. The transformants were screened for the presence of inserts in SUP4 using a colour assay where colonies with the *ade2*-1 ochre mutation suppressed by SUP4 are white, and colonies with inserts in SUP4 are red because SUP4 is inactivated (Burke et al., 1987; Foote and Denny, 2001).

2.1.4 Chemical and reagents

Laboratory grade chemicals and reagents used are listed in Table 2.1.

Table 2.1. Laboratory grade chemicals and reagents

Name	Source
2-mercaptoethanol	Merck, KGaA, Darmstadt, Germany
Agarose	Bio-Budget Technologies GmbH, Krefel, Germany
Ammonium acetate	Merck, KGaA, Darmstadt, Germany
Bacto agar	Becton Dickinson GmbH, Heidelberg, Germany
Bacto peptone/triptone	Carl Roth GmbH, Karlsruhe, Germany
Bacto yeast extract	Becton Dickinson GmbH, Heidelberg, Germany
Bromophenol blue	Sigma, Deisenhofen, Germany

Table 2.1. Continued

Name	Source
Citric acid	Carl Roth GmbH, Karlsruhe, Germany
Deoxynucleotide triphosphates (dNTPs)	Carl Roth GmbH, Karlsruhe, Germany
Disodium ethylenediaminetetraacetate (Na_2EDTA)	Merck, KGaA, Darmstadt, Germany
Ethanol	J. T. Baker, Griesheim, Germany
Ethidium bromide	Carl Roth GmbH, Karlsruhe, Germany
Glacial acetic acid	Carl Roth GmbH, Karlsruhe, Germany
Glucose	AppliChem GmbH, Darmstadt, Germany
Hydrochloric acid	J. T. Baker, Griesheim, Germany
Maleic acid	Merck, KGaA, Darmstadt, Germany
N-lauroylsarcosine	Fluka Chemie AG, Buchs, Germany
Phenol/chloroform/isoamylalcohol	Carl Roth GmbH, Karlsruhe, Germany
Potassium acetate	Merck, KGaA, Darmstadt, Germany
Potassium phosphate	Merck, KGaA, Darmstadt, Germany
Sodium acetate	Merck, KGaA, Darmstadt, Germany
Sodium chloride	Carl Roth GmbH, Karlsruhe, Germany
Sodium citrate	Merck, KGaA, Darmstadt, Germany
Sodium dodecyl sulphate (SDS)	Gibco, Life Technologies, Karlsruhe, Germany
Sodium hydroxide	Carl Roth GmbH, Karlsruhe, Germany
Sorbitol	Carl Roth GmbH, Karlsruhe, Germany
Tris base	Carl Roth GmbH, Karlsruhe, Germany
Tween®20	Sigma, Deisenhofen, Germany
Urea	Sigma, Deisenhofen, Germany
Xylene cyanol	Sigma, Deisenhofen, Germany
Yeast nitrogen base w/o amino acid	Becton Dickinson GmbH, Heidelberg, Germany
Yeast synthetic drop-out medium supplement without uracil or tryptophan	Sigma, Deisenhofen, Germany

2.1.5 Media

Media were sterilized by autoclaving at 121°C for 20 min. Glucose was added after autoclaving (cooling down of the media to ~55°C). Glucose stock solution (40%) was filter sterilized. The recipes in this section are each for 1L unless otherwise stated.

YPD (yeast extract, peptone, and dextrose) medium, pH 6.5: Undefined medium that supports the growth of most yeast strains, irrespective of their auxotrophic requirements.

10 g/L Bacto yeast extract

20 g/L Bacto peptone/triptone

20 g/L	Agar for solid medium
50 ml	40% Glucose stock

Yeast drop-out medium, pH 5.8: Selective media for yeast strains expressing a functional gene that complements an auxotrophic mutation in the host. The appropriate supplement is excluded from the media.

6. 70 g/L	Yeast nitrogen base without amino acids
1. 92 g/L	Yeast synthetic drop-out medium supplement without uracil or tryptophan
15 g/L	Agar for solid medium
20 g/L	Glucose

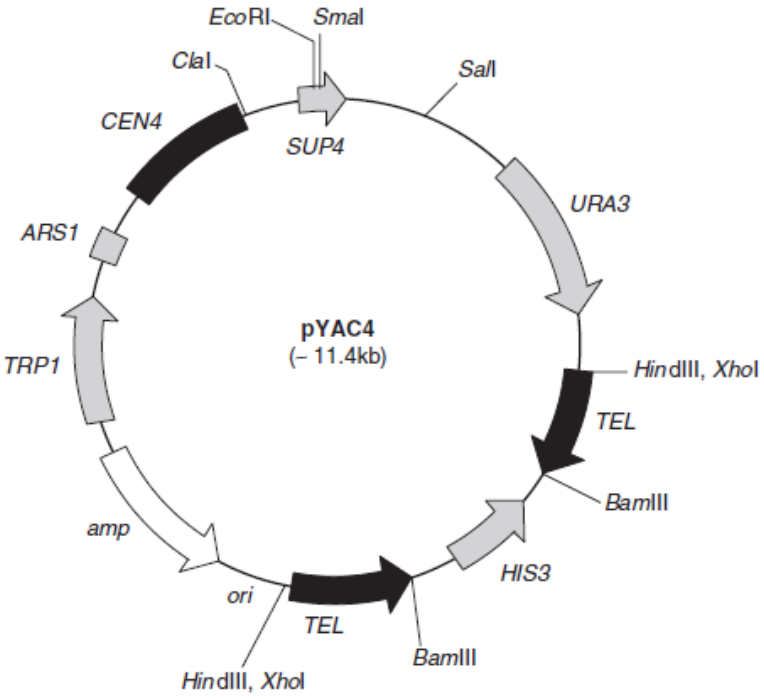

Figure 2.1. pYAC4. The pYAC4 vector is propagated as a circular plasmid in *Saccharomyces cerevisiae*. It contains a unique *Eco* RI cloning site in the SUP4 gene, an ARS1 and CEN4 elements required for stable propagation of the YAC as well as the TRP1, HIS3, and URA3 selectable markers. TEL sequences function as telomeres in yeast. Selected restriction sites (not necessarily unique) are indicated. Black bars represent chromosomal function elements; grey bars label yeast genes and the white bar represents the amp sequence from pBR322. The transformants are screened for the presence of inserts in SUP4 using a colour assay. (Modified from Foote and Denny, 2001).

2. 1.6 Buffers and solutions

The recipes in this section are each for 1L unless otherwise stated.

2.1.6.1 General solutions

EDTA (ethylenediaminetetraacetic acid) 0.5M

186. 1 g Disodium ethylenediaminetetraacetate (Na_2EDTA)

Na_2EDTA was dissolved in H_2O. The pH to 8.0 was adjusted by adding ~20 g of NaOH (sodium hydroxide) pellets. Subsequently, the volume of the solution was adjusted with dH_2O and sterilized by autoclaving.

NaCl (sodium chloride) 5M

292. 2 g NaCl

NaOH (sodium hydroxide) 1M

40 g NaOH

Potassium acetate 5 M

490. 75 g Potassium acetate

pH 4.8

Sodium acetate 3M

246. 09 g Sodium acetate

pH 5.2

Tris-HCl (1M)

121. 1 g Tris base

The Tris base was dissolved in dH_2O. The pH to 8.0 was adjusted by adding ~ 42 ml of concentrated HCl. Subsequently, the volume of the solution was adjusted with dH_2O and sterilized by autoclaving.

2.1.6.2 Plant DNA extraction

Urea Buffer

420 g/L	Urea
5 ml	5M NaCl
50 ml	1M Tris-HCl pH 8.0
40 ml	0.5M EDTA pH 8.0
50 ml	20% Sarkosyl NL-30

NH_4Ac (Ammonium acetate) 4.4 M

339. 163 g	NH_4Ac
pH 5.2	

2.1.6.3 YAC DNA pools for PCR

TE (Tris-HCl/EDTA) with 20% glycerol

10 mM	Tris-HCl pH 8.0
1 mM	EDTA pH 8.0
20%	Glycerol

Extraction buffer

200 mM	Tris-HCl pH 8.0
250 mM	NaCl
25 mM	EDTA pH 8.0
10%	SDS (sodium dodecyl sulphate)

2. 1.6.4 Polymerase Chain Reaction (PCR)

dNTPs (deoxynucleotide triphosphates) 10mM

Each dNTP was dissolved in sterile H_2O at a concentration of 10 mM. The desired final volume was adjusted with sterile H_2O.

SB Buffer

10X Taq Buffer with $(NH_4)_2SO_4$ (Fermentas GmbH, St. Leon-Rot, Germany)

2.1.6.5 Agarose gel and electrophoresis

TAE (Tris/acetate/EDTA) buffer (50X)

1. 2 kg	Tris base
285. 5 ml	Glacial acetic acid
93 g	$Na_2EDTA{\cdot}2H_2O$

Add dH_2O to 10 L

Agarose gel

1- 4% (w/v)	Agarose
0.2 µg/L	Ethidium bromide (10mg/ml)

Dissolve in 1X TAE buffer

5X DNA gel loading dye

50% (v/v)	Glycerol
0. 1% (w/v)	Xylene cyanol
0. 1% (w/v)	Bromophenol blue

2.1.6.6 Southern blot

SSC (saline-sodium citrate) buffer (20X)

87. 65 g	NaCl
44. 10 g	Trisodium citrate dihydrate

pH 7.0 by adding HCl

Low stringency washing buffer (SSC 2X)

100 ml	SSC 20X buffer
10 ml	10% SDS solution

High stringency washing buffer (SSC 0.2X)

10 ml	SSC 20X buffer
10 ml	10% SDS solution

Maleic acid buffer

11. 60g	Maleic acid
8. 76 g	NaCl

pH 7.5 by adding NaOH pellets

Blocking buffer

Maleic acid buffer + 10% (w/v) blocking reagent

Washing buffer

Maleic acid buffer + 0.3% Tween 20

Detection buffer

100 mM	Tris-HCl pH 8.0
100 mM	NaCl

pH 9.5 by adding HCl

2.1.7 YAC DNA extraction

SCE Buffer

0.9 M	Sorbitol
0.1 M	Sodium citrate
0.06 M	EDTA, pH 8.0

pH 7.0

SCEM buffer

4. 9 ml	SCE buffer
0. 1 ml	2-mercaptoethanol
250 U	Lyticase (see below)

Lyticase

2. 8 mg	Lyticase
0.05 M	Potassium phosphate pH 7.5
50%	Glycerol
Resuspend at 10 U/µl	

Lysis Buffer

0.5 M	Tris-HCl, pH 8.0
3% (V/V)	N-lauroylsarcosine
0.2 M	EDTA, pH 8.0
1 mg/ml	Proteinase K, before use

2.1.8 Fluorescence *In Situ* Hybridization (FISH)

Nick translation buffer

50 mM	Tris-HCl, pH 7.8
5 mM	$MgCl_2$
10 mM	2-mercaptoethanol

2X SSC buffer as section 2.1.6.6

Citrate buffer (0.01M)

2.941 g	Sodium citrate
2.101 g	Citric acid
pH 4.5	

Enzyme mixture

0.7 % (w/v)	Cellulase R10
0.7 % (w/v)	Cellulase
1% (w/v)	Pectolyase
1% (w/v)	Cytohelicase

The enzymes were dissolved in 0.01 M citrate buffer by incubation overnight at 4°C (adjusted to 10 ml) and stored at -20°C.

2.1.9 Molecular biological kits

The following kits were used in this study:
PCR product purification: Nucleo Spin Extract II Kit (Macherey-Nagel GmbH & Co. KG, Düren, Germany). YAC DNA isolation from yeast growth cultures: E.Z.N.A. Yeast DNA Isolation Kit (Omega Bio-tek, Norcross, GA, USA). Preparation of agarose-embedded YAC DNA plugs: CHEF Yeast Genomic DNA Plug Kit (BIO-RAD, Hercules, USA). DIG labelling and detection of probes for Southern blotting: PCR Dig Probe Synthesis Kit; DIG Easy Hyb Solution; Blocking Reagent; DIG DNA Labelling and Detection Kit; CDP-*Star* (Roche, Mannheim, Germany). PCR product extraction from the gel and cleanup of PCR products for FISH probes: MinElute Gel Extraction Kit and the QIAquick PCR purification kit (both kits were obtained from Qiagen GmbH (Hilden, Germany).

2.1.10 Oligonucleotides

All the oligonucleotides used in this study (Table 2.2) were purchased from Invitrogen (Karlsruhe, Germany).

2.1.11 Enzymes

2.1.11.1 Restriction enzymes

Restriction enzymes were purchased from New England Biolabs GmbH (Frankfurt, Germany), Fermentas GmbH (St. Leon-Rot, Germany) or Roche (Mannheim, Germany). Reaction conditions were according to manufacturer recommendations in the provided 10X buffer.

Table 2.2. Oligonucleotides

Primer ID	Sequence	Primer ID	Sequence
JA50-CONS1F	AGG AGT GGA CCT ACT GCG TG	JA51-CONS1R	TGC TGA AGG AGT GGT GCC TG
JA52-CONS2F	CTT CCT TCC CTG CTC GAA GC	JA53-CONS2R	TCC ACC AAA ACA ACC ACC TGA
JA54-CONS3F	CTT ATG TTT AGG GCT ACC CTG T	JA55-CONS3R	GCA CTA TGC ATT TCA CTG ATG G
JA56-CONS4F	CAA GCA TTG CCC CGT GGT TCA	JA57-CONS4R	AAT CTA CGG CCG GGT GGT GTG
JA58-CONS5F	AAA GGT CCG TCG GTG CGG TTA G	JA59-CONS5R	TTC GTT CCT CGC CGG TAA GA
JA60-CONS6F	GTG CGT GAA GAT TCC ACC CA	JA61-CONS6R	GTA GAC GCC ACA CAT CCG GT
JA62-CONS7F	TTG AGA ACC CAC CGG ACT GT	JA63-CONS7R	TCT CGC GTA CAG GAA CCG GA
JA64-CONS8F	TAG ATT CCC GTC CCT TGT GT	JA65-CONS8R	ACA GCA GCA GTC GAG GAA CG
JA66-POL1F	GTT GGG ACA ACC GCT CTA CC	JA67-POL1R	ATA AGC CTT GGA ACA GTG CA
JA68-POL2F	AAT GAT GGG GCG CCA ATC AGA	JA69-POL2R	TGG GAC CAT AGA AGG CCA AGC
JA70-POL3F	TTC ACA GTT GTG GCC TGA CA	JA71-POL3R	TGC CAA AAA GCC CAC TGT AC
JA72-POL4F	GGG TCA GTC CAT ACT CCA TAG GGA	JA73-POL4R	TGT CAG TCA GTG AAG GTG CA
JA74-ABG452F	GGG AGT ATG TGA TAT TGT GGG CAT C	JA75-ABG452R	GCA TGG AGT GTG CAA GTA CGT GGT C
JA76-BCD386F	GTG AGC AGT GCA ACA TGT ATA GAG	JA77-BCD386R	CTG GAG AAT GCG GAG GTA TCA TCA G
JA78-CDO98F	AAT GAG TTG TTT AAG CAC ACG AGA AGA G	JA79-CDO98R	CTT GTG CTT ATG TTG TCT ACA ACG TAT G
JA80-RsaI-top	GAA GGA GAG GAC GCT GTC TGT CGA AGG TAA GGA ACG GAC GAG AGA AGG GAG AG	JA81-univ-bottom	CTC TCC CTT CTC GAA TCG TAA CCG TTC GTA CGA GAA TCG CTG TCC TCT CCT TC
JA82-224-primer	CGA ATC GTA ACC GTT CGT ACG AGA ATC GCT	JA83-HinfI-top	ANT GAA GGA GAG GAC GCT GTC TGT CGA AGG TAA GGA ACG GAC GAG AGA AGG GAG AG
JA84-HYAC-C	GCT ACT TGG AGC CAC TAT CGA CTA CGC GAT	JA85-HYAC-D	GGT GAT GTC GGC GAT ATA GGC GCC AGC AAC
JA86-RA-2	TCG AAC GCC CGA TCT CAA GAT TAC	JA87-LS-2	TCT CGG TAG CCA AGT TGG TTT AAG G
JA88-Bubbleseq	CGC TGT CCT CTC CTT C	JA89-158LPF	CTC TAT GCT TCT GCA ACA AGT G
JA90-158LPR	GGC GAG AGA GTT TGA GGA ATG TG	JA91-158LNF	TGC ATC CCT TAA TTG TGA CAC G
JA92-158LNR	AAC ATT GTC CTG CGC TTA CTG	JA93-82RPF	GGG TAA ATG TGA CAC GCC
JA94-82RPR	AGA AGT CCA AAC CCC AAT TA	JA95-82RNF	AAC AAG TCA CCT CAC TAG
JA96-82RNR	TTG TGT GTA TCT CCC TCC	JA97-87RPF	GTC AAA TTC ATC AAA GCA TAG

Table 2.2. Continued

Primer ID	Sequence	Primer ID	Sequence
JA98-87RPR	ATG AGT CTG AGA CGT TCA	JA99-87RNF	GAA TTC ACT TCC ACT ACC
J100-87RNR	AAG GAT GAT GCT AAA GG	J102-R1	ATA GGC GCC AGC AAC CGC ACC TGT GGC G
J103-R2	CTT GCA AGT CTG GGA AGT GAA TGG AGA C	J104-SR	GTC GAA CGC CCG ATC TCA AG
J105-L1	GTG TTA TGT AGT ATA CTC TTT CTT CAA C	J106-L2	CTT CAA CAA TTA AAT ACT CTC GGT AGC C
J107-SL	GTT GGT TTA AGG CGC AAG	J108-UNIV-TOP-STK	GAT CGA AGG AGA GGA CGC TGT CTG TCG AAG GTA AGG AAC GGA CGA GAG AAG GGA GAG
J109-82R_2_PF	CGC TGG GTA GTG GGT GGT TCC	J110-82R_2_PR	GGT GTG TGT TTT CCG ACG GCC A
J111-82R_2_NF	CAC AAT GAG TGC ATC CAT CCT	J112-82R_2_NR	CTC AAC CCT ACC GGA TGG AGT
J113-82LPF	AGT GGA TTC ATA TCC AGC CCC A	J114-82LPR	GGT TGC CAG TAG AAA TGC TCC T
J115-82LNF	CGC GGT TCT TTC TTT GCT CTC A	J116-82LNR	AGT AGC AAC GCT AGT TTG GAC
J117-87LPF	AGA TGT CCA TGA TGG GGG AGC	J118-87LPR	TTG AGC ACA GCA AGA ACC AGC
J119-87LNF	ATG CAA AGG TGC CAA GAC TCC	J120-87LNR	GTG CCA GAA GTT GAC TTG CGA
J121-158L_2_PF	GCC AGG ATC TGA CAA ATG CCA	J122-158L_2_PR	GTA CAG ACT CGT CAC CAG AGG
J123-158L_2_NF	TTT TTG ATC CGC CAA TGG TGT	J125-158L_2_NR	GGT GCA TAA GGC CCA ATC ACC
J126-Os4953PF	ATC ATT CGG ACC CAG GCA GAG	J128-Os4953PR	CCA AGA GAT TCC AGT TGC CTC
J129-Os4953NF	GCT GAA GGA AAT GGA CTT GCC T	J130-Os4953NR	CAT TCC CAT CCA AGG ACA TGA
J131-Os4969PF	GAT CTG GCC TCC CTC GAC AGC	J132-Os4969PR	CCA GCT CCA GTA GAC GCC GGA
J133-Os4969NF	CAG CTC GAC ATG CCC ATC GAC	J134-Os4969NR	TCG GAC ACG TAC CCC TTG GTG A
J135-42973-FP1	ATG CTC TGG CTA AAG CCC T	J136-19977-RP1	TCC ACG AGT CAA AGT TCT GCT
J137-42973-FN2	GGC AAG GCT TTC GCT GTC CGT	J138-19977-RN2	CGA CCG CAT CTG CTT CTG CCA
J139-19977-FP3	AGG CGT CAT TCC TGG CTG AGC	J140-19977-RP3	AAT GGC ACT GAG CAA ACC CCA
J141-19977-FN4	CGA GAT GCT ACA CCA GCG GCT C	J142-19977-RN4	AGA AGC AGC CCC CCA GTG GAA G
143J-87L_2_PF	TCG TAT GAT AAT GAC CTG TTT G	144J-87L_2_PR	GTG AAG AGT GAT ACG CAG TTC
145J-87L_2_NF	TCC AAT GCC TAC CAA CGG CCA CGT CG	146J-87L_2_NR	TGC GAT CCA CAC GGT CAC CAG C
148J-42973-RP5	GGA CAG CGA AAG CCT TGC CTC	149J-42973-FN6	CTT TCA GTT GGC AAG CGT C
150J-42973-RN6	GTG TCA AGA TGT TGC TTG AGC	151J-42973-FP7	CGA CTT CTT GGC TGC AGT A
152J-42973-RP7	GAC TCA AAG CCG TAG ATG TC	153J-42973-FN8	TTG TCA AAG CGG CAC ATG AA

Table 2.2. Continued

Primer ID	Sequence	Primer ID	Sequence
154J-42973-RN8	TCC CAG TTC GAC GCT TGC CAA	155J-34977-FP9	GCA TCA TTA GGC CAA TGG GA
156J-34977-RP9	TCT TCA CAG GAA CAC CTC C	157J-34977-FN10	GGT TTT AGC TGG GTT GAT GC
158J-34977-RN10	ACT TCA GTG CAG AAT GAC AG	159J-26899-FP11	GTG ATG CGT AGG CTG GAC G
160J-26899-RP11	AAA GTG GAA CCC AAG TTG GT	161J-26899-FN12	AGT ACG GAT CCA AGG TGG GA
162J-26899-RN12	TCC TAG CGG AAT CAT GAC C	163J-2581-FP13	TGA CTC TGT CCA TCC TGG ACC
164J-2581-RP13	ACC GAC ATA GCT GCA TCA TCC	165J-2581-FN14	GTT TAC GGG TGG ACA CGG CTG
166J-2581-RN14	GGA TGT AAG GGC ACA TCA T	167J-26899-FP15	AGG ATT TGC AAT GCT TAG GG
168J-26899-RP15	CGT CTT TGG TGC TCA AAC C	169J-2581-FP16	GTG AAT CCA GTG CGT AAA GAA
170J-2581-RP16	CCA AGT GTA TGT CCC TTT GAC	171J-6091-FP17	CTC TGA TTA GGT TTG GTG TG
172J-6091-RP17	GAG GTT CAG ATA TAG CTG CAC	173J-6091-FN18	TGA TAT TTG GCC TGA GTG GA
174J-6091-RN18	AAA TCC ATG AGA ACA CCG T	175J-18727-FP	GCT TGT TGA CCG GGG AGT T
176J-18727-RP	CAT CCC AGC GTT GCT TGT G	177J-18727-FN	CGA TTC TGT GGC TGG TCG TC
178J-18727-RN	TGC GTC CAT CTG ATA GCC GAG	179J-22190-FP	TAG CTT GTC CCG TTG ACG TG
180J-22190-RP	TCG TAG TCC TGG TAG GCG A	181J-22190-FN	TAG GCT GTG GAG ATC GGC A
182J-22190-RN	CTT TGG TCG GGT CCA GGT A	183J-1649-FP	CTG TCA GGT CGC AGC AGA C
184J-1649-RP	GGA CGC CAT TTG CGA ACC TC	185J-1649-FN	GAG TCC CAC CTC CGG TAC GA
186J-1649-RN	TCT AAG AAC CGG AGC GGG TC	187J-18727-2RP	CCT CAT TGC GCG GAC CCA GTC
188J-18727-2RN	GAC CCT GGA GAG GGA GCG CAT	189J-16367-FP	ACC ACT TCC ATC AAC GCC A
190J-16367-RP	CCC ATG GTA GGA CAC ACT GC	191J-16367-FN	CAT CAG GGC TTG CCA ATG G
192J-16367-RN	CAC ATG CCA GGA GCA GAC G	193J-21139-FP	ACC CTC GAC ATC GGG AGT A
194J-21139-RP	CAG CAG ATC TCC ACG TCT C	195J-21139-FN	GGG ACC AAG GTT CCG TCG T
196J-21139-RN	AGT ACA GCC ACT GGT CCT C	197J-2346-FP	GCA CCA ACC CTA GAG CCC A
198J-2346-RP	TGA TGG AGA TCA GTG TCC A	199J-2346-FN	AGA AGC CAT GGA CAC CTC C
200J-2346-RN	TGG TCC ATG TGG CGA AGA AGC	205J-141026-FP	CCA GAA TCA GCC TGT GCC TC
206J-141026-RP	TGC GGA AAC GTG AGT CCG T	207J-141026-FN	GCC ACA ATC ACC TCC AGA CGT
208J-141026-RN	ATA TGA AGC CGC GCC AAG TG	209J-141239-FP	TTA GGC CTT CCG ACA TGT GG

Table 2.2. Continued

Primer ID	Sequence	Primer ID	Sequence
210J-141239-RP	CCT CCA AGA TTT GGC CAT GGA	211J-141239-FN	GAA TGC GTC TGT GGC GAC TT
212J-141239-RN	TTT GGT ACA GCA TCG CTC C	213J-141664-FP	TAA AGG GCG TGG GTG TCC A
214J-141664-RP	TTC ACA TGC GCT TGC AGT C	215J-141664-FN	TTA GGG TTG TCC ACC AGC T
216J-141664-RN	TGT GGT AGC TTG CAC AGA G	217J-305LPF	ATT CAA TGG GAG TCA CAC C
218J-305LPR	GAG TAG CAA CGC TAG CTT GG	219J-305LNF	CTC ATC ACG AGA ACA CGC CT
220J-305LNR	GAC GAT TTG GCT AAG AGC GTT	221J-305RPF	ACT TGG GAT CAA TCC CCG TC
222J-305RPR	AGG ATG CTT GAT ACG TCT CC	223J-305RNF	ACG ATG AAG ACC TTC ATG GA
224J-305RNR	AGC AGA ATT GCC ATC GTG TT	225J-354LPF	CCC CTA ACG CTC CAT GAG C
226J-354LPR	AAA GAC CAT GCC AAG CCT G	227J-354LNF	TCT TCG TTA GGA TGT CCG GT
228J-354LNR	TTG CTA GCC TTC GCC TGT A	229J-354RPF	AAT CCC ATG AGC GAA ACG T
230-354RPR	AGT GGG ATT GGA GAA GTC AT	231J-354RNF	GTT TTG CTT GGC TCA AAC AC
232J-354RNR	TGA AGA GCG TCA ACT TTG C	233J-1807-PF	ACT CAA AGA GCA CCA GAC AA
234J-1807-PR	TTG CAA CAG CCT TAG GAG G	235J-1807-NF	CAT CCA GCA AGG AAT GAT GCA
236J-1807-NR	CCA TGT GAC AAG GCT CTG C	237J-20658-PF	ACG ACG CCG TCT GCA TGT C
238J-20658-PR	AAC GTT GAC ACG TGA GCC A	239J-20658-NF	TAC GTG GCG TTC GGA AGC A
240J-20658-NR	TCT ACC TTC CCA TGG ACT CC	241J-CONS-PR	TAG TAG CAC CCG GTG AGC A
242J-POL-PR1	TAG GAA GCG CCA TGA GCA A	243J-POL-PR2	CGA GAA CCA GGC GGA ACA T
244J-25890-PF	ATG ATG TGC CTG CAG AGG A	245J-25890-PR	CTC CTG ACA GGC AGG TGT T
246J-AK363338.1PF	GCA AAA CGT TCG AAA CCC A	247J-AK363338.1PR	CTC TAG TCA CCG TGT CAG AA
248J-AK363338.1NF	CAG CGA GTC GCC ATG ATC G	249J-AK363338.1NR	CCA TCC CTG TCA AGT GGC T
250J-AK363338.2PF	TGC AAA GTG CTG CAT TCC T	251J-AK363338.2PR	TCA AGG AGG CCA TGG TGT T
252J-AK363338.3PF	TCA CCT CTT CTG AGG ACA GC	253J-AK363338.3PR	ACC GAA ACA GCA CAG ATG C
254J-25890-NF	GAT CGG ACG AGG ATG GCT C	255J-25890-NR	AAC AGC CTT TGC CCA GTA CTA
256J-AK363338-PR	CGC GAA ATT GAC CTC GTC GA	257J-AK363338-PF	GCA AAT GAT GTC AAA GCA CCA
258J-AK363338-PR	ACA ATT CCC TCC AGT GAG G	259J-AK363338-PF	AGA ATG GTG ACG AGG TCT C

Table 2.2. Continued

Primer ID	Sequence
260J-AK363338-PR	AGG TGA GAA GGA GCA CGC A
261J-AK371545-PF	TGG TGG AAG ACC GTT TCA GC
262J-7604-PF	ATC TGA CGG TCG AGA AGC GCG TC
263J-7604-PR	GGA GGT GCA GAT CCC GAG CA
264J-7604-PF	ACG CTC ATG GAG GCC GAG GAG TA
265J-AK363338.2PF	ATA ACC TTC CGC TGA ACC A
266J-AK363338.2PR	CCT GAC TTC CAA TCC CAC GA
267J-AK363338-PF	TGT CCA AAA TGG CTT GCT T
268J-AK363338-PR	TGT GAT AGG CCA ACA TCA CTG
269J-540-FP	CGG CAA GAT GTC TCG GCT CG
270J-540-FR	TGC TAC GGC ATC GTC CAC C
271J-540-NF	CTG TGA CGG GTC CGG CAA GCT
272J-540-NR	CTC AGC CGG CAT GTT CCT GC

2.1.11.2 Other enzymes

Standard PCR reactions were performed using homemade *Taq* DNA polymerase or commercially available enzymes: *Taq* DNA polymerase, Qiagen GmbH (Hilden, Germany). Ligation of DNA fragments was performed using T4 DNA ligase, Roche (Mannheim, Germany) the enzyme was used according to manufacturer recommendations. Lyticase, Proteinase K and DNA-free RNAse A used in YAC DNA extraction were purchased from Sigma (Deisenhofen, Germany). The enzyme mixture for FISH experiments contained Cellulase R10, C8001 (Duchefa, Haarlem, The Netherlands), Cellulase 319466 (CalBioChem, Merck, BioSciences, Darmstadt, Germany), Pectolyase P3026 (Sigma, Deisenhofen, Germany) and Cytohelicase C8274 (Sigma, Deisenhofen, Germany).

2.1.12 Software and web resources

The software and web resources used in this study are listed in Table 2.3 and Table 2.4.

Table 2.3. Software resources

Software	Specification	Reference
Adobe Photoshop	Pseudo colour and merged of images (FISH)	Adobe Systems Incorporated
ABySS	Sequence assembler for short reads	Genome Sciences Centre, British Columbia Cancer Agency, Vancouver, Canada. (Simpson et al., 2009)
BioEdit	Sequence alignment editor	Ibis Biosciences Carlsbad, CA, USA (Hall, 1999)
Bowtie	Short DNA reads aligner	University of Maryland, MD, USA (Langmead et al., 2009)
DNASTAR	Alignment of sequences	Lasergene 8: MegAlign DNASTAR, Inc. Madison, USA
Excel 2007	Interpolation of PFGE data	Microsoft Corporation, USA
FastPCR	Primer design	Ruslan Kalendar, Helsinki, Finland (Kalendar et al., 2009)
Gene Runner	Restriction site analysis	Version 3.05. Michael Spruyt and Frank Buquicchio http://www.generunner.net/
IGV	Integrative Genomics Viewer	Broad Institute of Massachusetts Institute of Technology and Harvard Cambridge, MA, USA (Robinson et al., 2011)

Table 2.4. Web resources

Resource	Specification	Web page
NCBI	National Center for Biotechnology Information	http://www.ncbi.nlm.nih.gov
CoGePedia	Comparative genomics	http://genomevolution.org/wiki/index
Co-GNB	Co-expressed Gene Network in Barley	http://coexpression.psc.riken.jp/barley
dCAPS finder 2.0	Design of CAPS markers	http://helix.wustl.edu/dcaps/dcaps
DDBJ	DNA Data Bank of Japan	http://www.ddbj.nig.ac.jp
EMBL-EBI	European Bioinformatics Institute	http://www.ebi.ac.uk
Gbrowser	*Brachypodium distachyon* Gbrowser	http://gbrowse.brachypodium.org
Gramene	Comparative genomics	http://www.gramene.org
HarvEST	Assemblies of barley ESTs	http://harvest.ucr.edu
JGI	*Sorghum bicolor* Gbrowser	http://genome.jgi.doe.gov/Sorbi1/Sorbi1.home.html
Mips	Barley genome database	http://mips.helmholtz-muenchen.de/plant/barley/index
MSU	MSU-rice genome annotation	http://rice.plantbiology.msu.edu
NEB Cutter V2.0	Restriction enzyme sites	http://tools.neb.com/NEBcutter2
Pfam 25.0	Protein family database	http://pfam.sanger.ac.uk
Phytozome	Comparative genomics	http://www.phytozome.net
Plaza 2.0	Comparative genomics	http://bioinformatics.psb.ugent.be/plaza
RAP-DB	The Rice Annotation Project Database	http://rapdb.dna.affrc.go.jp
SMART	Simple Modular Architecture Research Tool	http://smart.embl-heidelberg.de
ViroBLAST	Barley BLAST IPK data	http://webblast.ipk-gatersleben.de/barley/viroblast

2.2 Methods

2.2.1 Plant and pathogen cultivation

2.2.1.1 Barley plants

Barley seedlings were grown in controlled environment growth chambers at 20°C, with 16 h light/8 h darkness at 60% relative humidity.

2.2.1.2 Barley powdery mildew fungus

Barley powdery mildew (*Bgh*) isolate K1 was propagated on seven-day-old barley seedlings line I10. Infected plants were kept under controlled conditions in a growth chamber (21°C, 70% relative humidity with 14 h light/10 h darkness).

2.2.1.3 Plant-Pathogen Infection

Barley seedlings were grown under pathogen-free conditions (Section 2.2.1.1) for seven days and transferred to a dedicated growth chamber for barley plants infected with powdery mildew fungus, *Bgh* (Section 2.2.1.2). Barley primary leaves were inoculated with *Bgh* spores and the infection phenotype was scored macroscopically 7 days after inoculation. In parallel secondary leaves were collected for DNA/RNA extraction.

2.2.2 Plant DNA extraction

Barley genomic DNA was isolated from leaves using a modified urea extraction protocol (Anja Reinstädler, personal communication). One piece of barley leaf (~3 cm long) was harvested in a 1.5 ml test tube and frozen in liquid nitrogen. The tissue was ground while still frozen and 500 µl of urea buffer was added. The samples were

vortexed briefly and 500 µl phenol/chloroform/isoamylalcohol was added. After centrifugation for 10 min at 13000 rpm, 500 µl of supernatant was transferred into a new test tube and the DNA was precipitated with 1 V of cold isopropanol and $^{1}/_{10}$ V of 4.4 M NH_4Ac pH 5.2. Subsequently, the samples were centrifuged for 10 min at 13000 rpm. The DNA pellet was washed with 70% ethanol, air dried and resuspended in 50 µl TE.

2.2.3 Screening of the YAC library

A total of 330 (96-well) microtiter plates containing a single unique YAC clone per well (~31.680 clones) were screened by PCR in a five step process:

1. YAC clones contained in each microtiter plate from the barley YAC library were grown in solid YPD media.
2. YAC DNA pools (containing a mix of all grown colonies of the microtiter plate) were prepared and screened by PCR.
3. Positive pools were confirmed again by PCR.
4. YAC clones from confirmed positive pools (microtiter plate) were re-grown in YPD solid medium. Pools of clones from each of the 12 columns and 8 rows were prepared. These rows and columns pools were screened by PCR with the same primers used in step 2. A combination of a positive row and a column provided the location of a single positive clone on the 96-well microtiter plate.
5. Single positive clones were confirmed by colony PCR. DNA from single clones was prepared using the same protocol for YAC DNA pools.

2.2.3.1 Preparation of YAC DNA for PCR

A protocol for the preparation of YAC DNA pools was carried out according to (Schmidt et al., 2001) with some modifications. For each YAC (96-well) microtiter plate, a 12 cm square petri dish with YPD solid medium was prepared. Using a 96-pin replicator each YAC microtiter plate was copied on the media and grown for 3 days at 30°C. From each plate the colonies were collected in 5 ml TE with 20% glycerol. From

this cell suspension (YAC-colonies/TE/glycerol solution) 1 ml was transferred to a 2.0 ml test tube and 250 µl of autoclaved glass beads (0.45 – 0.50 mm, Carl Roth GmbH, Karlsruhe, Germany) and 400 µl extraction buffer were added. The suspension was vortexed for 5 min and after sedimentation of the glass beads, the supernatant was transferred to a new tube. To precipitate the DNA, 1 V of cold isopropanol was added. After centrifugation (5 min at 13000 rpm) the DNA pellet was resuspended in 400 µl of sterile H_2O. An aliquot of 1µl was used for a 25 µl PCR reaction. The remaining of YAC-colonies/TE/glycerol solution was stored at -20°C for later use.

To prepare the YAC DNA for rows and columns pools the same protocol was used. However, in this case the colonies of each row and column were collected in a separate tube in the TE with 20% glycerol solution. For the single clones instead, solely the positive clone was diluted in the TE with 20% glycerol solution.

2.2.3.2 Polymerase Chain Reaction (PCR)

The PCR reactions were carried out in the thermal DNA Engine Tetrad 2 cycler (BIO-RAD, Hercules, USA). Homemade *Taq* DNA polymerase was used. To detect the target sequence with high sensitivity, PCR primer pairs for two consecutive rounds of PCR (Primary-Nested) were designed using the FastPCR software (Kalendar et al., 2009). The PCR reaction mix was prepared as mentioned in Table 2.5; general conditions for the PCR cycle programme are described in Table 2.6.

Table 2.5. PCR Reaction mix components

Reaction Mix	Volume in µl
dNTPs (10mM)	0.5
Forward primer (10 µM)	1.0
Reverse primer (10 µM)	1.0
Buffer SB (10 X)	2.5
Taq Polymerase	0.5
DNA Template	1.0
Sterile H_2O	18.5
Total Volume	25.0

Table 2.6. PCR cycle programme

Step	Time	Temperature in °C	
Denaturation I	5 min	95	
Denaturation II	30 sec	95	
Annealing	30 sec	55-62	35 cycles
Extension	1-3 min	72	
Final extension	10 min	72	
End	5 min	16	

Note: The annealing temperature varied according to primer melting temperature and extension time varied according to the amplicon length.

2.2.3.3 Agarose gel electrophoresis

PCR products were separated by gel electrophoresis. The samples were mixed with 6 µl of DNA loading dye (5X) and 15 µl were loaded on 1% agarose gels. Gels were run with TAE buffer (1X) at 5V/cm during 50 min. A 1 kb ladder was used as size reference (Catalogue No. 15615-016, Invitrogen, Karlsruhe, Germany).

2.2.3.4 DNA quantification

DNA quantification was carried out with the NANODrop 1000 (Thermo Scientific, Schwerte, Germany).

2.2.4 YAC insert size

Using pulse field gel electrophoresis (PFGE) the barley YAC insert size was determined.

2.2.4.1 Agarose-embedded YAC DNA plugs

To determine the barley insert size by PFGE, agarose-embedded YAC DNA plugs were prepared using the CHEF Yeast Genomic DNA Plug Kit, (BIO-RAD, Hercules, USA) according to manufacturer instructions. Therefore, from the isolated single YAC-clone

cell suspension in TE/glycerol solution (Section 2.2.3.1), 100 µl was streaked on a 12 cm square petri dish containing uracil-drop out solid medium. A total of 10 plates per clone were prepared and grown for 3 days at 30°C. From each grown plate, colonies were collected in 1ml of uracil- drop out liquid medium and collected together (suspension from the 10 plates) in a 50 ml test tube. This cell suspension was used for the preparation of agarose-embedded YAC DNA plugs and for YAC DNA extraction. 1 ml of the suspension was diluted with 1 ml of uracil-drop out liquid medium. From this 2 ml cell suspension, 10 µl was further diluted with 990 µl of sterile H_2O. This final suspension was used to determine the cell concentration using a Neubauer improved haemocytometer with 0.0025 mm^2 and 0.100 mm depth (Superior Marienfeld, Germany). In total 10 of the 25 centre squares, at 100X magnification (Zeiss Axiophot microscope, Carl Zeiss Jena, Jena, Germany) were counted.

The following equation was used to determine the cell concentration:

$$\frac{\text{Cells counted}}{\text{Number of squares}} = \text{Average cells per square}$$

$$\text{Average cells per square x 25 x dilution factor x } 10^4 = \text{cells per ml}$$

$$\frac{\text{Desired cell concentration}}{\text{actual cell concentration}} \text{ x ml of plugs to be made} = \text{ml of cell suspension to use}$$

For yeast 6 x 10^8 cells per ml was used for the desired cell concentration

The following steps were performed according to manufacturer instructions. Five to ten blocks per clone were prepared and were kept at 4°C in washing buffer until they were analysed by PFGE.

2.2.4.2 Pulse Field Gel Electrophoresis (PFGE)

The separation of yeast chromosomes by PFGE was carried out in collaboration with Dr. Pietro Spanu from Imperial College London, UK. The yeast chromosomes embedded in agarose plugs were separated on a CHEF-DR II PFGE system (BIO-RAD, Hercules, USA) in a 1% PFGE certified agarose in 0.5X TBE buffer at 4°C. The run was

24 hrs at 6V/cm (200V) with a 60-120s switch time ramp. The gel was stained post electrophoresis by adding Sybr Safe (S33102, Invitrogen, Karlsruhe, Germany) 0.1 µl/ml for 30 min and photographed under blue light with an orange filter. Yeast chromosomes from strain YNN295 (BIO-RAD, Hercules, USA) were used as a size marker. To calculate the approximate size of the YAC the migration distance of the artificial yeast chromosome was interpolated with the known size of the marker chromosomes.

2.2.4.3 Southern blot

Because not all the artificial yeast chromosomes were visualized using PFGE, Southern blot analysis was used to detect the presence and approximate size of the YACs. The DIG Application Manual for Filter Hybridization Roche (Mannheim, Germany) was used as a guide for generation, hybridization and detection of the YAC-specific probes.

DNA from the PFGE gel was blotted on a positively charged nylon membrane (Hybond-N+, Amersham pharmacia biotech, GE Healthcare Europe GmbH, Freiburg, Germany) and fixed with ultraviolet (UV) radiation (Stratalinker / 1200uJ).

Highly sensitive probes labelled with DIG-dUTP (alkali-labile) were generated by PCR using the PCR DIG probe synthesis kit from Roche (Mannheim, Germany) according to the manufacturer instructions. For the pre-hybridisation, 20 ml DIG easy hyb (Roche, Mannheim, Germany) solution was pre-heated in a hybridisation tube at 42°C in a hybridisation incubator (GFL-7601, Greater Hannover, Lower Saxony, Germany). Subsequently, the nylon membrane was rinsed with sterile H_2O and transferred into the hybridisation tube and incubated for 1 hour at 42°C. In parallel, the DIG-labelled probe was denatured at 100°C for 10 min, followed by a short incubation on ice and centrifugation at 13000 rpm for 5 min; 10 µl of the denatured probe were mixed with 10 ml of fresh DIG easy hyb solution (pre-heated at 42°C). This solution was added to the membrane after the pre-hybridisation solution was discarded followed by overnight hybridisation at 42°C. Hereafter, the washing of the membrane was performed twice in low stringency washing buffer for 5 min at room temperature

(RT) while shaking and twice with pre-heated high stringency washing buffer for 15 min at 68°C under constant shaking. Subsequently, the membrane was incubated in maleic acid buffer for 3 min at RT while shaking and then incubated for 1 hour in 1X blocking buffer at RT while shaking. The Anti-Digoxigenin-AP conjugate, Fab fragments (Roche, Mannheim, Germany) was centrifuged at 10000 rpm for 10 min at RT and diluted 1:20000 in 1X blocking buffer (1.25 µl: 25 ml). Afterwards, the membrane was incubated in the antibody solution for 30 min at RT, washed three times in washing buffer for 15 min and equilibrated in detection buffer for 5 min, at RT while shaking. Finally, the membrane with DNA side facing up was incubated in 1 ml CDP-*Star* (Roche, Mannheim, Germany) working solution (1:100 dilution with detection buffer) for 5 min at RT before it was heat-sealed in between two plastic foils. Two X-ray films were exposed to the membrane, one for 30 min and another one overnight. After exposure, the films were developed directly.

2.2.5 YAC DNA extraction

A protocol for YAC DNA extraction from Chaplin and Brownstein (2001a) with some modifications was followed. From the isolated single YAC clone-cell suspension in TE/glycerol solution (Section 2.2.3.1), 10 µl was inoculated in 20 ml of YPD liquid media and grown for 48 hours at 30 °C while shaking at 250 rpm. Hereafter, 1 ml of this culture was transferred into 100 ml of YPD liquid media and grown for 24 hours at 30 °C while shaking at 250 rpm. The liquid culture was transferred to 50-ml test tubes and centrifuged for 5 min at 2000 rpm at 4°C. The cell pellets were resuspended in 5 ml SCE buffer and collected in one tube. 1 ml of SCEM buffer was added to the suspension and incubated for 2 hours at 37°C while shaking at 100 rpm. Hereafter, the samples were centrifuged for 5 min at 2000 rpm at 4°C and the resulting cell pellet was resuspended in 5 ml lysis buffer and 0.5 ml of 10% SDS. The samples were incubated for 20 min, at 65°C. To isolate the nucleic acids 2 ml of ice-cold 5M potassium acetate was added and the tubes were incubated on ice during 60 min. After, the samples were centrifuged 10 min at 2000 rpm at RT and the supernatant was transferred to a new tube and mixed with 2 V 95% ethanol (RT). After a second centrifugation (5 min at 2000 rpm) the supernatant was discarded and

the pellet was dissolved overnight in 3 ml TE buffer at 4°C. Subsequently, the solution was treated with 0.1 ml of 1 mg/ml DNase-free RNase A for 1 hour at 37°C. After this, 6 ml RT isopropanol was added and DNA was spooled in a 2 ml test tube. The DNA was dissolved in 0.5 ml TE buffer, pH 8.0, 50 µl 5M NaCl and 2 ml RT 95% ethanol. The solution was mixed by inversion, the DNA was spooled again in a 2 ml test tube and dissolved in 0.5 ml TE buffer.

2.2.6 Recovering of YAC ends

To isolate the end fragments from the YAC inserts, the "bubble oligonucleotide" approach was used (Ogilvie and James, 1996; Chaplin and Brownstein, 2001a). This protocol provides a means to recover the end fragments from the YAC insert using PCR amplification. Figure 2.2 shows a scheme of this approach. The YAC DNA was digested with different restriction enzymes creating a collection of restriction fragments. Among these, one contains the distal portion of the YAC insert associated with part of the right vector arm and another contains the other end of the insert associated with part of the left vector arm (Figure 2.2B). A double-stranded DNA tag containing a "bubble" of non-complementary sequence, flanked by short complementary sequences, was prepared and ligated to the collection of restricted YAC DNA fragments (Figure 2.2C). Selective amplification of the two YAC end fragment sequences was achieved using one PCR primer derived from the YAC vector (the left arm or the right arm) and one primer containing the sequence of the non-complementary portion in the "bubble" (Figure 2.2D). Occasionally, non-specific DNA fragments can be amplified using the "bubble oligonucleotide" approach. In order to increase specificity, nested PCR was used (Figure 2.2D). Thereby, only fragments derived from the end of the YAC genomic insert, containing its associated YAC vector sequences, which were ligated to the "bubble", will be amplified (Figure 2.2E) (Chaplin and Brownstein, 2001a).

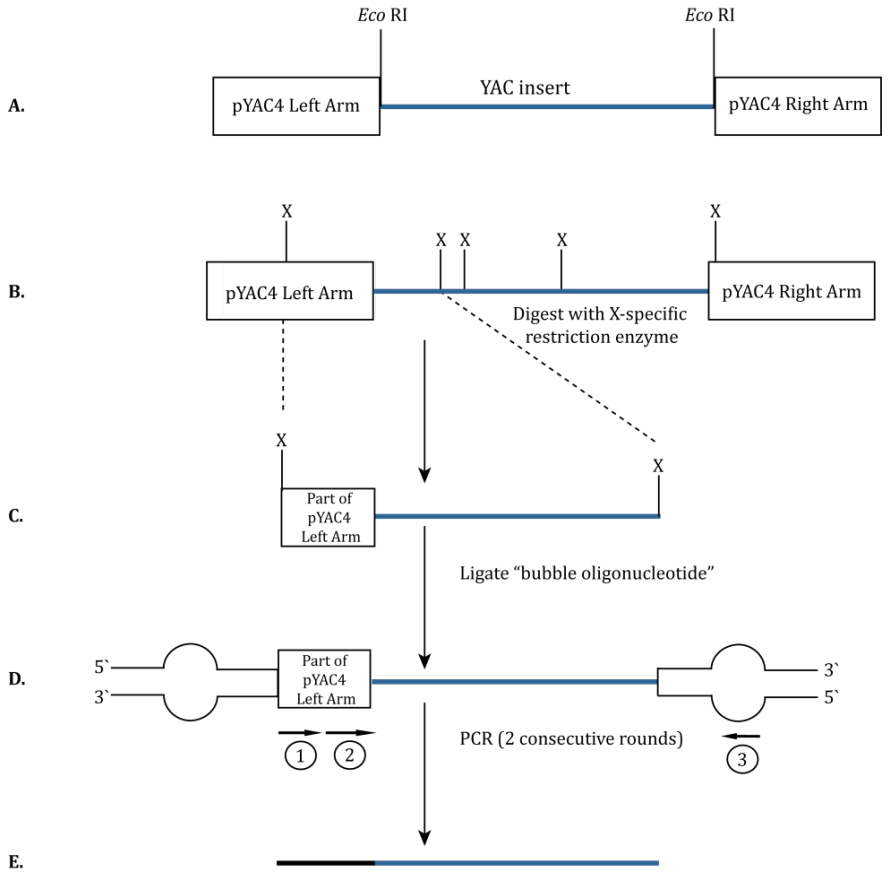

Figure 2.2. Schematic representation to recover the YAC ends using the PCR-based "bubble oligonucleotide" approach. **(A)** Linear representation of the YAC (pYAC4 vector + insert). **(B)** and **(C)** The yeast DNA was restricted with enzyme "X" to generate a collection of DNA fragments. One of the fragments contained the distal portion of the YAC insert still associated to the vector left arm, while another contained the other end of the YAC insert associated with a portion of the vector right arm. **(D)** The fragments obtained in B-C were ligated to the "bubble". **(E)** The YAC insert end fragments could be selectively amplified using one PCR primer derived from the vector arm (1) and one primer with the sequence of the "bubble" (3). To increase the amplification specificity it is advised to use nested PCR. Here a second internal primer from the vector arm (2) was used in combination with the "bubble" primer (3).

The "bubble" is generated by annealing of a bubble-top and a bubble bottom oligonucleotides (Chaplin and Brownstein, 2001a). In this case, the bubble-top and the bubble bottom oligonucleotides were adjusted to a concentration of 4 nmol/ml with H_2O. 1 nmol of each was mixed together, annealed by heating during 15 min at 68°C and naturally cooled down to room temperature during 60 min. Three different "bubbles" were generated: oligonucleotides JA80 + JA81 (bubble 1); oligonucleotides JA83 + JA81 (bubble 2); and oligonucleotides J108 + JA81 (bubble 3) (see oligonucleotides sequences in Table 2.2). 2.5 µg of YAC DNA was digested with the

following restriction enzymes in a final volume of 50 µl applying temperatures according to the manufacturer recommendation: *Rsa* I, *Hinf* I, *Alu* I (Fermentas GmbH, St. Leon-Rot, Germany), *Pvu* II, *Eco* RV (New England Biolabs GmbH, Frankfurt, Germany) and *Bgl* II (Roche, Mannheim, Germany). The enzymes were heat-inactivated if necessary.

The following reaction mix was carried out for overnight ligation at RT

X µl (250 ng)	digested DNA
1 µl (2 pmol)	"bubble 1, 2 or 3"
5 µl 10X	ligase buffer
2 µl (2 U)	T4 DNA ligase
X µl	Sterile H_2O
50 µl	Final volume

Bubble 1 and bubble 2 were ligated to the DNA fragments obtained after restriction with enzyme *Rsa* I and *Hinf* I, respectively. Bubble 3 was ligated to the DNA fragments obtained after restriction with the other enzymes. To amplify the fragments containing the YAC insert end the PCR conditions described in Table 2.7 were applied. Digested-bubble ligated YAC DNA (1ng) was used as template for the primary PCR reaction. For the nested PCR, 1 µl of the amplification product obtained in the primary PCR was used as template.

Table 2.7. PCR conditions used to amplify the DNA fragments containing the YAC end sequences

	Primary PCR			Nested PCR		
Step	**Time in min**	**Temperature in °C**		**Time in min**	**Temperature in °C**	
Denaturation I	5	92		5	92	
Denaturation II	1	92		1	92	
Annealing	2	62	20 cycles	2	65	30 cycles
Extension	2	72		2	72	
Final extension	10	72		10	72	
End	5	16		5	16	

The combination of primers according to the YAC end to be amplified and the restriction enzyme are shown in Table 2.8. Separation of PCR amplified fragments was as described on section 2.2.3.3. PCR fragments amplified with bubble 1 and bubble 2 were sequenced with primer JA88. PCR fragments amplified with bubble 3, for left side were sequenced with primer J107 and for right side were sequenced with primer J104 (see primer sequences in Table 2.2).

Table 2.8. PCR primers to amplify the DNA fragments containing the YAC end sequences

YAC End	Primary PCR	Nested PCR	Enzyme (s)
Right	JA82 and JA85	JA82 and JA86	*Rsa* I
Right	JA82 and J102	JA82 and J103	*Alu* I, *Pvu* II, *Eco* RV *Bgl* II
Left	JA82 and JA84	JA82 and JA87	*Hinf* I, *Rsa* I
Left	JA82 and J105	JA82 and J106	*Alu* I, *Pvu* II, *Eco* RV *Bgl* II

2.2.6.1 DNA sequencing and analysis

DNA sequencing was performed by the MPIPZ DNA core facility on Abi Prism 377 and 3700 sequencers (Applied Biosystems, Weiterstadt, Germany) using BigDye-terminator v3.1 chemistry. Premixed reagents were from Applied Biosystems. Sequence data were analysed using the BioEdit software.

2.2.7 Overlapping YAC clones

To find overlapping YACs from the isolated clones, the YAC library was re-screened by PCR. Sequences obtained from the YAC ends were used to design primers for two consecutive rounds of PCR (primary and nested) (FastPCR, Kalendar et al., 2009). Because of the presence of highly repetitive regions in the YAC ends, the nested PCR product was digested with restriction enzymes to identify unique (informative) copies of repetitive DNA present in the positive YAC clone. The sequence from the nested PCR product from the positive YAC clone (query sequence) was analysed using the BLAST tool (Altschul et al., 1990). The sub-sequences with similarity to repetitive regions were compared to the query sequence to identify SNPs between them. We used the software gene runner for clone 87A3 (right end) and the web tool NEB

cutter (New England Biolabs GmbH, Frankfurt, Germany) for clones 87A3 (left end), 82B11 (both ends), 305A11 (both ends) and 354G1 (right end) to find suitable restriction enzymes that distinguish the identified SNPs. Nested PCR products were restricted and separated by gel electrophoresis on a 3-4% agarose gel. Gels were run with TAE buffer (1X) at 4V/cm during 90 min. A low range DNA ladder was included to determine the fragment sizes (Fermentas GmbH, St. Leon-Rot, Germany).

2.2.8 Next Generation Sequencing (NGS) of isolated YAC clones

Illumina sequencing of the isolated YAC clones was carried out in collaboration with Dr. Peter Nürnberg and Dr. Janine Altmüller from Cologne Center for Genomics (CCG, University of Cologne, Germany). 5 µg of high-molecular-weight YAC-containing DNA was used to prepare the paired-end DNA libraries. A "short" sequencing run of paired-ends (2 x 36 bp) with one sample/lane was sequenced using the genome analyzer GAIIx (Illumina Inc., San Diego, California, USA). The obtained data was analysed in collaboration with Dr. Nahal Ahmadinejad (Computational Biology, University of Bonn, Germany). The 36 bp Illumina paired end reads were mapped to the yeast genome, received from the Comprehensive Yeast Genome Database (CYGD)[3] at the Munich information center for protein sequences (MIPS).[4] The mapping program bowtie (Langmead et al., 2009) was used in paired-end mode, with a maximum insert size of 500 nucleotides. All sequence reads, which did not map to the yeast genome, were mapped to different sources of barley sequence information: (1) HarvEST database (version 1.77, assembly No. 35); (2) FLcDNA library (Matsumoto et al., 2011): DDBJ (AK353559-AK377172) and the barley database[5]. Additionally, the reads which did not map to the yeast genome were partially assembled using the program ABySS (Simpson et al., 2009) parameters k=20, n=10 (k=kmer length; all possible substrings with length k, of the sequence read n=minimum number of pairs needed to consider joining two contigs) with subsequent blasting (Altschul et al., 1990) of the resulting scaffolds. The mapped data was visualized using the integrative

[3] ftp://ftpmips.gsf.de/yeast/sequences
[4] http://mips.helmholtz-muenchen.de
[5] http://barleyflc.dna.affrc.go.jp/hvdb/index.html

genomic viewer (IGV, Robinson et al, 2011, Broad Institute of Massachusetts Institute of Technology and Harvard Cambridge, MA, USA).

2.2.9 Fluorescence *In Situ* Hybridization (FISH)

The FISH experiments were carried out in collaboration with Dr. Andreas Houben and Dr. Lu Ma, chromosome structure and function group from the Leibniz Institute of Plant Genetics and Crop Plant Research (IPK, Gatersleben, Germany). Protocols from Dr. Lu Ma were followed.

2.2.9.1 Probe preparation

Unique sequences for *Cons*, *Pol*, *myosin-2* and *AK363338* were amplified by PCR from genomic DNA from barley cv. Ingrid or YAC DNA (clones 87A3, 82B11, 158C12 or 305A11) and the PCR products were used as template for probe labelling. Conditions for PCR were as described in section 2.2.3.2. PCR product extraction from the agarose gel was performed with the MinElute Gel Extraction Kit and the cleanup of PCR products with the QIAquick PCR purification kit both from Qiagen GmbH (Hilden, Germany). Spectrophotometrical quality parameters of the purified PCR products needed to be higher than 1.80 and higher than 1.30 for the A260/A280 and A260/A230 ratios, respectively. The probes were labelled with Texas red-dUTP (Perkin Elmer, Massachusetts, USA) or Alex-488-dUTP (Invitrogen, Karlsruhe, Germany) directly by nick translation (Table 2.9). Subsequently, the probes were incubated at 15°C for 2 hours and 3 µl were checked by 1% agarose gel. Afterwards, the probes were precipitated in 1.5 ml safe lock tubes at -20°C overnight in 1X TE (added up to 200 µl), 3 µl salmon sperm DNA, 20 µl sodium acetate (3M, pH 5.2) and 500 µl 96-100% ethanol (-20°C). On the following day the probes were centrifuged at 13000 rpm for 30 min at 4°C. Finally the pellet was rinsed with ice-cold 70% ethanol, air dried and dissolved in 7 µl 2X SSC by incubation at 37°C for 1 hour and subsequently at 4°C overnight.

Table 2.9. Nick translation for FISH probes labelling

Component	Amount
DNA 3 µg	X µl
10X Nick translation buffer	4.0 µl
Non-labelled dNTP	4 .0 µl
0.1 M MetOH	4 .0 µl
Labelled- dUTP (1mM)	0.8 µl
H_2O	X µl
Thoroughly mix by vortex	
DNA polymerase I	4.0 µl
DNase I (0.1U)	3.0 µl (1:10 dilution)
Mix by pipetting	
Final volume	40.0 µl

2.2.9.2 Preparation of chromosomes spreads

Barley seeds from cv. Ingrid were germinated for 2.5 days in the dark in a moist environment. The root tips were treated with ice-cold water and fixed in ethanol: acetic acid (3:1 ratio) for 1h and stored at 4°C until use. The roots were washed twice with ice-cold water for 5 min and then washed three times with citrate buffer for 5 min. The root meristems (whitish portion of the root tip, about 2 mm in length) were cut and treated with the enzyme mixture for 50 min at 37°C, washed twice with citrate buffer and twice with 96% ethanol. The ethanol was replaced with 15-30 µl of freshly prepared acetic acid: methanol (3:1 ratio) per one root tip. The root tips were broken with a dissecting needle in a tube and then tapped to resuspend the cells. The cell suspension (6-8 µl for one slide) was spread on a microscope slide (superfrost, Thermo Scientific, Schwerte, Germany) and stored in a humid chamber.

2.2.9.3 Single-copy FISH

Freshly prepared slides were used in all experiments. After quality selection, slides were treated on 2X SSC for 5 min, 45% acetic acid 10 min at RT, rinsed in 2X SSC for 10 min, treated with pepsin (0.1 mg ml^{-1}) in 10mM HCl for 10 min and rinsed twice in 2X SSC for 5 min each. The slides were fixed in 4% formaldehyde in 2X 2SSC for 10 min, rinsed three times in 2X SSC each for 4 min, dehydrated in an ethanol series (70%, 90% and 96%) each for 2 min and air-dried at RT for 20 min. 20 µl of

hybridization buffer was added to each slide covered with a cover slip, fixed with glue and denatured at 80°C for 2 min on a hot plate. The hybridization was carried out in a moist chamber at 37°C overnight. Subsequently, the slides were shortly washed in 2X SSC at RT to remove the cover slip. Afterwards, the slides were washed in 2X SSC at 60°C for 20 min. The slides were rinsed in 2X SSC, dehydrated in an ethanol series (70%, 90% and 96%) each for 2 min and air-dried before counterstaining with DAPI in Vectashield (4',6-diamidino-2-phenylindole) Vector Laboratories (Servion, Switzerland). Images were captured using a cooled CCD camera (Spot 2e; Diagnostic Instruments, Michigan, USA) attached to an epifluorescence microscope (Axioplan 2; Zeiss, Oberkochen, Germany) equipped with a Plan Apochromat 63×/numerical aperture 1.40. The monochromatic images were pseudo coloured and merged using the software Adobe Photoshop.

3. Results

3.1 Barley YAC library screening

The closest predicted *Ror1* gene flanking markers, a gene encoding a protein of unknown function (DUF1218 family member; Os10g0495900, RAP-DB nomenclature), named *Cons*, and the gene encoding a DNA-directed RNA polymerase I subunit 2 (Os10g0495600, RAP-DB nomenclature), named *Pol*, were considered the starting point to generate oligonucleotides for the barley YAC library screening. A four-genome-equivalent barley YAC library with an average insert size of 480 kb (Simons et al., 1997) was screened by PCR for the presence of clones containing either *Cons* or *Pol*. The library was constructed using barley genomic DNA of cv. Ingrid in the YAC vector pYAC4 and the *Saccharomyces cerevisiae* strain AB1380 (Simons et al., 1997).

3.1.1 Optimization of PCR-based library screening

To screen a YAC library by PCR it is advised to prepare pools of clones (Chinault and Sternberg, 2001). To detect with high sensitivity a positive PCR signal it is necessary to define the number of YAC clones that can be pooled. Therefore, we performed an initial optimization of PCR-based library screening. Different numbers of clones per pool combined with a *Mlo*-containing YAC clone (positive control) were used as template. Three experiments were carried out: (1) *Mlo*-YAC clone pooled with 96 library clones (plate 42); (2) *Mlo*-YAC clone pooled with 8 library clones (a column of the plate); (3) Single *Mlo*-YAC clone. Conditions of growth and YAC DNA preparation were as mentioned in section 2.2.3.1. We performed two consecutive rounds of PCR using the set of primers Mlo23/Mlo8 (primary PCR) with Mlo10/Mlo6 (nested PCR) and Mlo21/Mlo40 (primary PCR) with Mlo34/Mlo41 (nested PCR); conditions for PCR were as mentioned in section 2.2.3.2. After the primary PCR, detection of target

DNA was weak in the three experiments (Figure 3.1A and C). However, after the nested PCR, the positive PCR signal was detected in all the experiments (Figure 3.1B and D). Thus, we decided to perform the barley YAC library screening with pools of 96 clones (a complete microtiter plate) and two consecutive rounds of PCR using nested PCR primers.

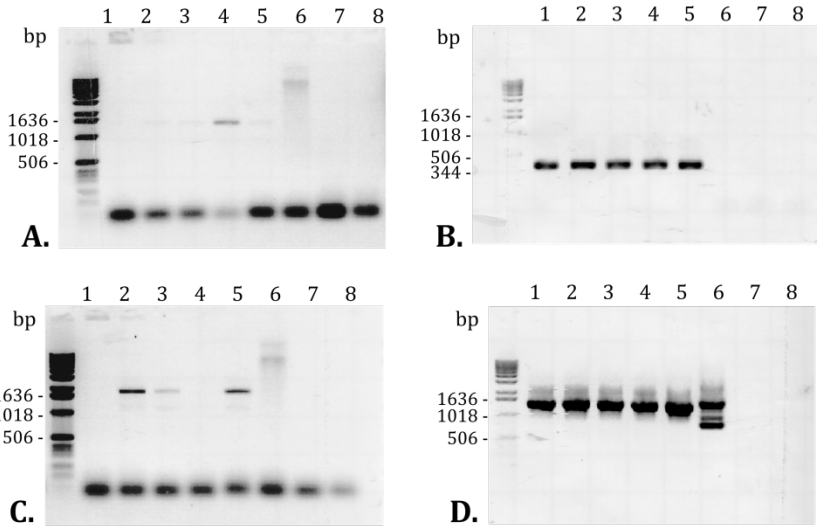

Figure 3.1. Optimization of PCR-based barley YAC library screening. Samples: (1) *Mlo*-YAC clone pooled with 96 library clones, growth in YPD; (2) *Mlo*-YAC clone pooled with 8 library clones, growth in YPD; (3) *Mlo*-YAC clone pooled with 8 library clones, growth in drop-out medium lacking uracil; (4) *Mlo*-YAC clone, growth in YPD; (5) *Mlo*-YAC clone, growth in drop-out medium lacking uracil; (6) cDNA clone pUbi-*Mlo*; (7) H_2O; (8) master mix. **(A)** Primary PCR with primers Mlo23/Mlo8 **(B)** Nested PCR with primers Mlo6/Mlo10 using as template the PCR product from A. **(C)** Primary PCR with primers Mlo21/Mlo40, **(D)** Nested PCR with primers Mlo34/Mlo41 using as template the PCR product from C. Numbers given on the left side of each gel refer to the size (in bp) of marker bands.

3.1.2 Isolation of YAC clones containing *Pol* and *Cons* genes

3.1.2.1 Screening for YAC pools

The barley DNA sequences for the *Pol* and *Cons* genes from cultivar Ingrid (*Mlo*) and Malteria Heda (*mlo*-3) were obtained from Nicholas Collins (unpublished data) (Supplement Material 7.1), and were used to design oligonucleotides for the barley YAC library screening (Table 3.1).

Table 3.1. Primer pairs used to amplify the *Pol* and *Cons* genes

Set No.	Primary PCR	Expected Size (bp)	Nested PCR	Expected Size (bp)
1	JA50-CONS1F / JA51-CONS1R	964	JA52-CONS2F / JA53-CONS2R	520
2	JA54-CONS3F / JA55-CONS3R	1020	JA56-CONS4F / JA57-CONS4R	617
3	JA58-CONS5F / JA59-CONS5R	1382	JA60-CONS6F / JA61-CONS6R	593
4	JA62-CONS7F / JA63-CONS7R	1020	JA64-CONS8F / JA65-CONS8R	641
5	JA66-POL1F / JA67-POL1R	1241	JA68-POL2F / JA69-POL2R	498
6	JA70-POL3F / JA71-POL3R	1001	JA72-POL4F / JA73-POL4R	610

Note: The annealing temperature used for all primers was 55°C

The initial barley YAC library contained 428 microtiter plates (96-well; ~41.088 clones) (Simons et al., 1997). However, in the context of the present study 98 plates were missing from the original collection. Therefore, only 330 microtiter plates (~31.680 clones) were screened by PCR. YAC DNA pools were prepared as mentioned in section 2.2.3.1. Two consecutive rounds of PCR (primary and nested) using a subset of primers specific for the *Cons* and *Pol* genes (Table 3.1) were performed (Section 2.2.3.2). As controls, genomic barley DNA from cv. Golden Promise (positive control) and the master mix without DNA (negative control) were used.

As a result of the PCR screening several positive pools were detected (Table 3.2 and Figure 3.2A). These pools were re-tested with the complete set of primers for the *Cons* and *Pol* genes primers (Table 3.1). Ultimately, pool 87 was confirmed as positive for the *Cons* gene (Figure 3.2B) and pools 82 and 158 were confirmed as positive for the *Pol* gene.

Table 3.2. Positive pools for the *Cons* and *Pol* genes after the PCR-based YAC library screening

Gene	Status	Set of primers (Table 3.1)	Positive Pools
Cons	First Screening	3	87, 294, 313, 319, 328, 342, 370, 363
	Second Screening	2	87, 101, 139, 253, 265, 392
	Confirmed Pools	1-4	87
Pol	First Screening	6	82, 158, 254, 274, 284, 285, 287, 288, 289, 303, 340, 346, 358, 368, 369, 377, 393, 394, 395, 409, 412
	Second Screening	5	82, 139, 158
	Confirmed Pools	5-6	82, 158

3.1.2.2 Isolation of single positive YAC clones

To determine the individual positive YAC within the pool of 96 clones, DNA pools representing the 8 rows and the 12 columns of the 96-well microtiter plate were prepared and screened to identify the coordinates of the positive clone for pools 87, 82 and 158. Using the set of primers No. 4 (Table 3.1), row A and column 3 were positive for pool 87 (Figure 3.2C). Using the set of primers No. 5 (Table 3.1) row B and column 11 were positive for pool 82; row C and column 12 were positive for pool 158. Single positive clones 87A3, 82B11 and 158C12 were confirmed by colony PCR. DNA from single clones was prepared following the protocol for YAC DNA pools mentioned in section 2.2.3.1.

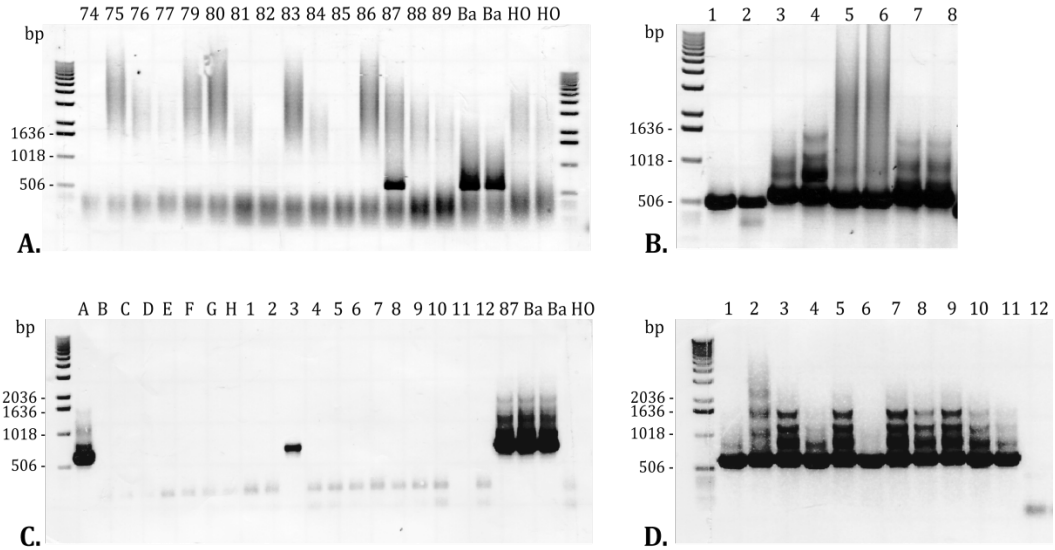

Figure 3.2. PCR screening of the barley YAC library. Ba, positive control with barley genomic DNA; HO, negative control with water. **(A)** Screening of the YAC pools (only part of the library is shown). Pool 87 shows the positive signal. **(B)** Confirmation of pool 87 with the complete set of primers designed for *Cons* gene. 1-2, set 1; 3-4, set 2; 5-6, set 3; 7-8, set 4. **(C)** Screening of rows and columns of the positive pool 87. Pool A of the rows and pool 3 of the columns show the positive signal. **(D)** Stability of the single clone 87A3. 92% of the tested colonies (eleven of twelve) carry the barley insert. Numbers given on the left side of each gel refer to the size (in bp) of marker bands.

3.1.2.3 Stability of single isolated YAC clones

To test the stability of the barley insert in the single isolated YAC clones, the respective clones were streaked on non-selective medium and 12 colonies each were

picked randomly to be evaluated by PCR. The percentage of colonies carrying the insert was (1) 92% for clone 87A3 (Figure 3.2D), (2) 58% for clone 82B11, and (3) 8% for clone 158C12. This suggests that some of the clones lose the YAC more frequently and faster than other ones.

3.2 Recovering of YAC ends for clones 87A3, 82B11 and 158C12

To isolate the ends from the YAC inserts, the "bubble oligonucleotide" approach was used (Ogilvie and James, 1996; Chaplin and Brownstein, 2001a) -Section 2.2.6-). YAC DNA from each clone was obtained using a protocol from (Chaplin and Brownstein, 2001a) (Section 2.2.5) and digested with different restriction enzymes (Section 2.2.6). Table 3.3 lists the best results for each end ("left" and "right") per clone. The longer the fragment, the more suitable it was to design new primers to seek for overlapping clones (the sequences obtained with this approach, which were used to design primers can be found as Supplemental Material 7.2).

Table 3.3. List of the best YAC end PCR products for clones 87A3, 82B11 and 158C12 obtained using the "bubble oligonucleotide" approach

Clone	End	Enzyme	Size (bp)
87A3	Right	*Alu* I	396
		Eco RV	1300
		Rsa I	820
	Left	*Bgl* II	1636
		Hinf I	332
		Pvu II	1020
82B11	Right	*Alu* I	344
		Eco RV	1318
		Rsa I	685
	Left	*Eco* RV	800
		Hinf I	292
		Pvu II	800
158C12	Right	*Eco* RV	1318
		Eco RV	396
		Rsa I	245
	Left	*Bgl* II	600
		Hinf I	547
		Pvu II	750

Note: The fourth column indicates the approximate size (bp) of the PCR product

3.3 Overlapping YACs for clones 87A3, 82B11 and 158C12

To find overlapping YACs for the isolated clones 87A3, 82B11 and 158C12 the sequences obtained from the corresponding YAC ends (Section 3.2) were used to design primer pairs for primary and nested PCR (Table 3.4). The YAC library was re-screened by PCR as mentioned in Section 2.2.3.2. Due to the frequent presence of highly repetitive regions in the YAC ends, in some cases all YAC pools showed a positive signal after the second PCR. To identify potentially unique (informative) copies of repetitive DNA, PCR products were cleaved using restriction enzymes (Section 2.2.7). In some instances this approach resulted in characteristic restriction patterns ("fingerprint") that could be used to identify overlapping YAC clones despite the presence of repetitive YAC ends (see below).

Table 3.4. Primer pairs designed to identify overlapping YACs for clones 87A3, 82B11 and 158C12

Set No.	End	Primary PCR	Nested PCR
7	87A3 Right	JA97-87RPF / JA98-87RPR	JA99-87RNF / J100-87RNR
8	87A3 Left	J117-87LPF / J118-87LPR	J119-87LNF / J120-87LNR
9	82B11 Right	J109-82R_2_PF / J110-82R_2_PR	J111-82R_2_NF / J112-82R_2_NR
10	82B11 Left	J113-82LPF / J114-82LPR	J115-82LNF / J116-82LNR
11	158C12 Left	J121-158L_2_PF / J122-158L_2_PR	J123-158L_2_NF / J125-158L_2_NR

3.3.1 Clone 87A3

Right end: We designed primer pairs No. 7 (Table 3.4) using the YAC end sequence obtained with restriction enzyme *Rsa* I. After PCR of seven random YAC pools and the control, pool 87, all products were positive (Figure 3.3A). Therefore, the nested product was restricted with enzymes *Hph* I and *Mnl* I. After restriction with enzyme *Hph* I, the nested product from pool 87 showed a unique restriction pattern, different from the other YAC pools (Figure 3.3B). Consequently, the barley YAC library was re-screened by PCR using the primer pairs No. 7 and the nested product was restricted with enzyme *Hph* I. The complete re-screening revealed several positive pools (Table 3.5). Subsequent screening of the rows and columns of the positive pools showed a

product of the expected size and restriction pattern in row A and column 11 of pool 305. The single clone 305A11 was isolated and confirmed by PCR as containing YAC end 87A3R, thus revealing physical overlap with YAC clone 87A3.

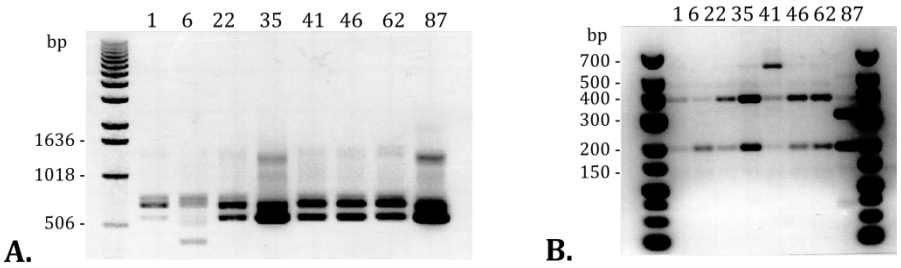

Figure 3.3. Optimization of conditions to find overlapping barley YAC clones. **(A)** PCR amplification with primer pairs No. 7. The product of seven random YAC pools and the positive pool 87, are undistinguishable. **(B)** Following restriction of the PCR products shown in (A) with enzyme *Hph* I, pool 87 showed a unique restriction pattern. Numbers given on the left side of each gel refer to the size (in bp) of marker bands

Left end: Primer pairs No. 8 (Table 3.4) were designed using the consensus YAC end sequences obtained with enzymes *Bgl* II and *Pvu* II. The nested amplification product was restricted with enzymes *Acc* I, *Eco* 24I (*Ban* II), *Hinf* I, *Taq* I, and *Xcm* I. However, none of these enzymes allowed differentiating potentially true positive pools from presumably false positive pools (Figure 3.4). Double digestion with enzymes *Acc* I and *Xcm* I or the use of dCAPs markers was not successful either. Therefore, no overlapping clones from 87A3L could be identified.

3.3.2 Clone 82B11

Right end: Primer pairs No. 9 (Table 3.4) were designed using the YAC end sequence obtained with restriction enzyme *Rsa* I. The nested product was digested with enzymes *Dpn* I, *Eco* RI, *Hinf* I, *Tsp* 509, *Xap* I (*Apo* I). No difference between potentially true and presumably false positives was evident (data not shown). Consequently, no overlapping clones could be identified for 82B11R.

Left end: Primer pairs No. 10 (Table 3.4) were designed based on the YAC end sequence obtained with restriction enzyme *Pvu* II. The nested product was digested

with enzymes *Dra* I, *Hinc* II and *Mnl* I. The nested amplification product from pool 82, digested with enzyme *Dra* I, showed a unique restriction pattern (data not shown). Therefore, the barley YAC library was re-screened by PCR using the primer pairs No. 10 and the nested amplification product was restricted with enzyme *Dra* I. The complete re-screen of the YAC library showed several positive pools (Table 3.5). Subsequent screening of the rows and columns of the confirmed positive pools led to the isolation of single clones 72C11, 313A6 and 354G1 and verified them as overlapping clones of 82B11L (data not shown).

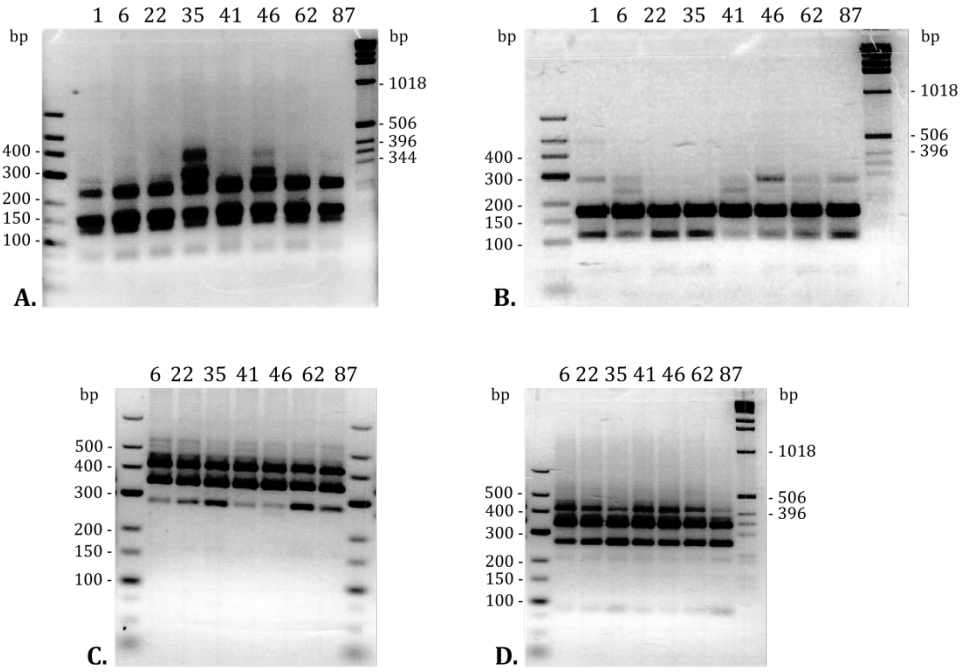

Figure 3.4. Restriction of nested PCR products for overlapping clones on 87A3L. Primer pairs No. 8. **(A)** *Taq* I **(B)** *Hinf* I **(C)** *Xcm* I **(D)** *Acc* I. A difference between the true positive, YAC pool 87, and the false positives (random YAC pools) was not possible to identify. Numbers given on the left and right side of each gel refer to the size (in bp) of marker bands.

3.3.3 Clone 158C12

Right end: using the "bubble oligonucleotide" approach with enzyme *Eco* RV a product of 1318 bp was obtained; however, the high quality DNA sequence of this product was not longer than 332 bp. None of the sequences for the right end of clone 158C12 were longer than 400 bp, making the design of primers for two consecutive rounds of PCR unfeasible.

Left end: Primer pairs No. 11 (Table 3.4) were designed using the consensus YAC end sequences obtained with enzymes *Bgl* II and *Pvu* II. After nested PCR the amplification was specific for the positive pool 158. Therefore, the barley YAC library was re-screened with these primer pairs. A high number of positive pools were obtained (Table 3.5). PCR analysis detected row F and column 4 from clone 415 as positive. Single clone 415F4 was isolated and confirmed as an overlapping clone of 158C12L (data not shown).

Taken together, these results indicate that the "bubble oligonucleotide" was a suitable approach to recover the ends of YAC clones and could be used to find overlapping YAC clones in a chromosome walking strategy. However, owing to the abundant presence of repetitive sequences, it required in most cases restriction of the PCR products to identify overlapping clones. The first walking step extended the contig around the two YACs positive for *Pol* in both directions and the contig (single YAC) positive for marker *Cons* in one direction (Figure 3.5).

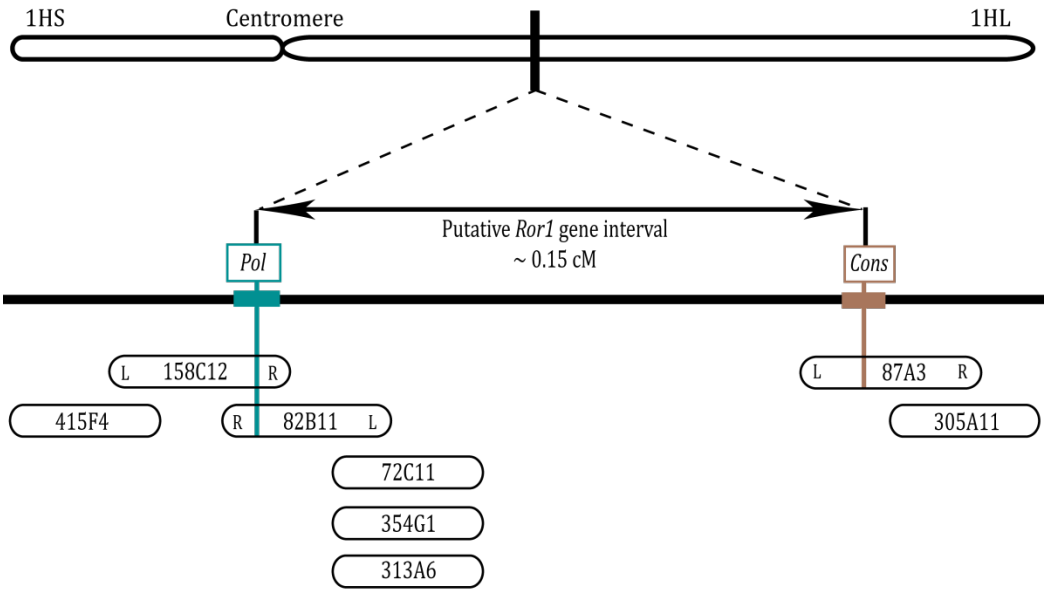

Figure 3.5. Schematic representation of the first walking step around the *Ror1* gene region on the long arm of barley chromosome 1H. The contig started with two YACs positive for *Pol* (82B11 and 158C12) and one YAC positive for *Cons* (87A3). Using the YAC ends the contig was extended in both directions around *Pol* and in one direction around *Cons*. L, Left end; R, Right end; 1HS, short arm of barley chromosome 1H; 1HL, long arm of barley chromosome 1H. The approximate position of the *Ror1* region on chromosome 1H was determined by FISH analysis (see below Section 3.9).

Table 3.5. Overlapping barley YAC for clones 87A3R, 82B11L and 158C12L

YAC end	Status	Set No.	Positive Pools
87A3R	Re-Screening	7	49, 142, 305 and 155
	Confirmed Clone (s)		305A11
82B11L	Re-Screening	10	72, 313, 354, 357 and 366
	Confirmed Clone (s)		72C11, 313A6 and 354G1
158C12L	Re-Screening	11	19, 59, 77, 89, 91, 105 and 415
	Confirmed Clone (s)		415F4

3.4 Recovering of YAC ends for clones 305A11, 72C11, 354G1 and 313A6

To isolate the YAC ends of clones 305A11, 72C11, 354G1 and 313A6 the same "bubble oligonucleotide" approach as described in section 3.2 and section 2.2.6 was used. YAC DNA from each clone was isolated using the Yeast DNA Isolation Kit E.Z.N.A., (Omega Bio-tek, Norcross, GA, USA) and digested with different restriction enzymes (Section 2.2.6). The best results are summarized in Table 3.6 and the sequences obtained with this approach, which were used to design primers, can be found as supplemental material 7.3. One of the disadvantages of working with YAC libraries is the instability that some clones can exhibit. Although YACs are usually stable in culture, deletions or other rearrangements of the insert may occur after the initial isolation of a clone (Chaplin and Brownstein, 2001b). In this case, clone 415F4, was unable to grow again in YPD or uracil-drop out liquid or solid media, suggesting pronounced instability of the YAC insert. Thus, we were not able to isolate enough DNA for further analysis. All attempts to rescue this YAC clone failed.

Table 3.6. List of best YAC end PCR products for clones 305A11, 72C11, 354G1 and 313A6 obtained using the "bubble oligonucleotide" approach

Clone	End	Enzyme	Size (bp)
305A11	Right	*Pvu* II	1300
		Rsa I	1600
	Left	*Eco* RV	1000
		Rsa I	700
72C11	Right	*Bgl* II	1100
		Eco RV	800
	Left	*Bgl* II	1800
		Rsa I	1600

Table 3.6. Continued

Clone	End	Enzyme	Size (bp)
354G1	Right	*Eco* RV	800
		Rsa I	1800
	Left	*Eco* RV	800
313A6	Right	*Bgl* II	1500
		Eco RV	2000
	Left	*Alu* I	600
		Pvu II	600

Note: The fourth column indicates the approximate size (bp) of the PCR product

3.5 Overlapping YACs for clones 305A11 and 354G1

To find overlapping YACs from the isolated clones 305A11 and 354G1, the sequences obtained from the corresponding YAC ends were used (Section 3.4). Primer pairs for primary and nested PCR were designed (Table 3.7) and the YAC library was re-screened (Section 2.2.3.2). Due to the presence of highly repetitive regions in the YAC ends, in some cases all YAC pools showed a positive signal after the nested PCR. Therefore, it was necessary to find suitable restriction enzymes to differentiate the potentially true positive from the presumably false positive YAC pools (Section 2.2.7)

Table 3.7. Primer pairs designed to find overlapping YACs for clones 305A and 354G1

Set No.	End	Primary PCR	Nested PCR
12	305A Right	221J-305RPF / 222J-305RPR	223J-305RNF / 224J-305RNR
13	305A Left	217J-305LPF / 218J-305LPR	219J-305LNF / 220J-305LNR
14	354G1 Right	229J-354RPF / 230-354RPR	231J-354RNF / 232J-354RNR
15	354G1 Left	225J-354LPF / 226J-354LPR	227J-354LNF / 228J-354LNR

3.5.1 Clone 305A11

Right end: Primer pairs No. 12 (Table 3.7) were designed using the YAC end sequence obtained with restriction enzyme *Pvu* II. The nested product was cleaved with enzymes *Dpn* I, *Mbo* II and *Pag* I (*Bsp* HI). Only restriction with enzyme *Pag* I, showed a unique pattern in the positive pool 305 (data not shown). After re-

screening of the barley YAC library under these conditions several positive pools were obtained; however, none of these could be confirmed as overlapping clones of 305A11R (data not shown).

Left end: Primer pairs No. 13 (Table 3.7) were designed using the YAC end sequence obtained with restriction enzyme *Eco* RV. The nested amplification product was restricted with enzymes *Mnl* I and *Xcm* I. No difference between potentially true and presumably false positive pools was evident (data not shown). Therefore, no overlapping clones could be identified for 305A11L.

3.5.2 Clone 354G1

Right end: Primer pairs No. 14 (Table 3.7) were designed based on the YAC end sequence obtained with restriction enzyme *Rsa* I. No suitable restriction enzymes were found to discriminate between the variant of the repetitive sequence present in 354G1R and other variants of this repetitive sequence that were identified by BLAST searches using the YAC end sequence as a query (data not shown). Consequently, the isolation of overlapping clones for 354G1R was not possible.

Left end: Using the YAC end sequence obtained with restriction enzyme *Eco* RV primer pairs No. 15 (Table 3.7) were designed. After nested PCR, only with DNA from clone 354G1 an amplification product was obtained. Therefore, the barley YAC library was re-screened using the primer pairs No. 15. A high number of preliminary positive pools were obtained; however, none of these pools could be confirmed as overlapping clones of 354G1L (data not shown).

In summary, further extension of the existing YAC contigs (Figure 3.5) *via* the isolation of overlapping YAC ends of clones 305A11 and 354G1 failed. However, at a later stage of the project the YAC contigs could be further expanded on the basis of DNA sequence data (see below section 3.8.1)

3.6 YAC insert size

To determine the approximate size of the barley insert of each isolated YAC clone, the yeast chromosomes of positive clones were separated by pulse field gel electrophoresis (PFGE). Agarose-embedded plugs for clones 87A3, 82B11, 158C12 and a strain lacking any YAC (JD53, as control) were prepared using the CHEF Yeast Genomic DNA Plug Kit (BIO-RAD, Hercules, USA) (Section 2.2.4.1). PFGE experiments were carried out in collaboration with Dr. Pietro Spanu from Imperial College London, UK (Section 2.2.4.2). Figure 3.6A shows the yeast chromosomes separated by PFGE; for clones 87A3 and 158C12 the artificial chromosome was readily detected as an extra band (compared to the control strain) in the Sybr safe-stained agarose gel. To calculate the approximate size of the barley insert in the artificial chromosome, the size of marker bands and the distance migrated by the artificial chromosomes was interpolated. We determined for clone 87A3 and 158C12 a size of 520 kb and 500 kb, respectively. Since no extra band was detectable for clone 82B11 we performed Southern blot analysis to detect the artificial chromosome of this clone.

To prepare the Southern blot the DIG Application Manual for Filter Hybridization Roche (Mannheim, Germany), with some modifications was followed (Section 2.2.4.3). A PCR probe with set of primers No. 6 (*Pol* gene) was generated (Table 3.1) using DNA from clone 82B11 as the template. The primary PCR was carried out under normal conditions (Section 2.2.3.2) and the nested PCR was performed using the PCR DIG probe synthesis kit from Roche (Mannheim, Germany) -Section 2.2.4.3-. Following detection of the DIG label, a strong signal for clone 82B11 was detected, which, after interpolation, was estimated to have a size of approximately 900 kb (Figure 3.6B). Because the probe was generated with specific primers for the *Pol* gene, the artificial chromosome from clone 158C12 was detected as well (Figure 3.6B).

Combination of PFGE and Southern blot were suitable to determine the barley YAC insert size in the isolated clones. These results verified an insert size larger than 480 kb as stated by (Simons et al., 1997).

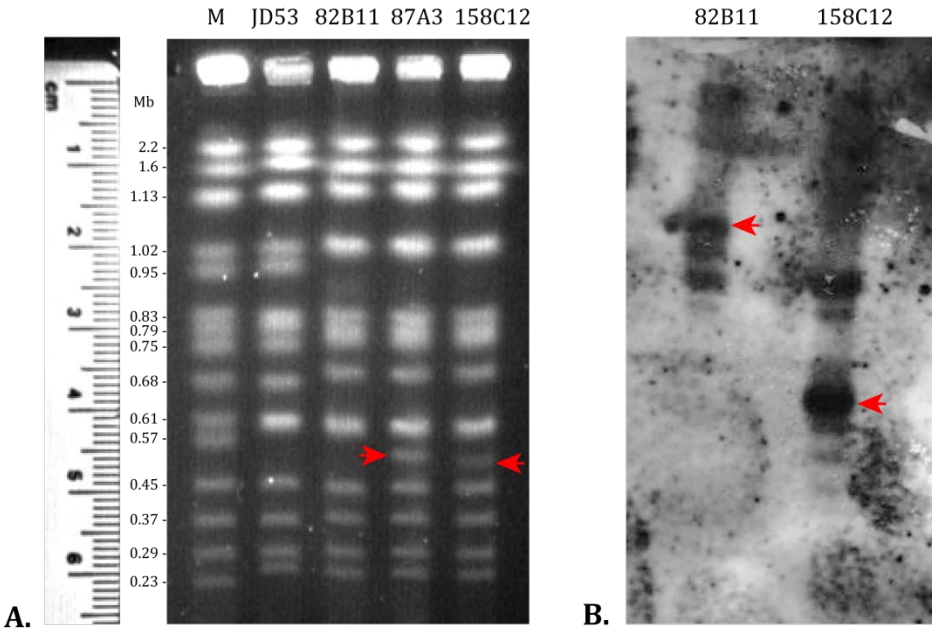

Figure 3.6. Barley YAC insert size determined by PFGE (60-120 s, 200V, 24h). Lane M, marker; lane JD53, yeast strain without YAC. **(A)** Sybr safe-stained gel showing natural yeast chromosomes and the YAC from clones 87A3 and 158C12 (red arrowheads). **(B)** The gel shown in A was blotted on a positively-charged nylon membrane and hybridized with the probe (DNA amplified with set of primers 6, for *Pol*). The red arrowheads point to strong signals detected for clones 82B11 and 158C12. By interpolation of the data (distance migrated by the YAC vs. size of the marker) we determined a size of 520 kb, 500 kb and 900 kb for clones 87A3, 158C12 and 82B11, respectively. Numbers given on the left side of the gel refer to the size (in Mb) of marker bands (lane M). A segment of a ruler is shown on the very left.

For clones 305A11, 72C11, 354G1 and 313A6, after separation of yeast chromosomes by PFGE, no extra chromosome was evident in any of the four clones (data not shown). Therefore, we performed Southern blot analysis (Section 2.2.4.3) in an attempt to detect the artificial chromosomes of these clones. Two independent experiments were carried out. The probes were obtained with primers No. 7 (Table 3.4) and primers No. 23 (Table 3.13) and DNA from clone 87A3 and 82B11 were used as the template, respectively. The primary PCR was carried out under normal conditions (Section 2.2.3.2) and the nested PCR was performed using the PCR DIG probe synthesis kit from Roche (Mannheim, Germany) -Section 2.2.4.3-. However, despite multiple attempts, we were unable to detect any signal and therefore the size of the barley YAC insert for clones 305A11, 72C11, 354G1 and 313A6 remained unknown (data not shown).

3.7 Next generation sequencing (NGS) of isolated YAC clones

Genomic DNA from clones 87A3, 82B11, 158C12, 305A11, 354G1 and 72C11 was isolated using the Yeast DNA Isolation Kit E.Z.N.A., (Omega Bio-tek, Norcross, GA, USA). Table 3.8 shows the quality parameters of the six samples prepared for sequencing as determined by spectrophotometric analysis.

Table 3.8. Quality of genomic DNA samples for Illumina sequencing

Clone	ng/µl	A260	A280	260/280	260/230
87A3	105,31	2,106	1,107	1,90	1,44
82B11	142,93	2,859	1,503	1,90	1,41
158C12	97,02	1,940	1,027	1,89	1,47
305A11	92,37	1,847	0,969	1,91	1,38
354G1	86,45	1,729	0,947	1,83	1,47
72C11	108,98	2,180	1,182	1,84	1,33

Illumina sequencing of the samples was carried out in collaboration with Dr. Peter Nürnberg and Dr. Janine Altmüller from the Cologne Center for Genomics (CCG, University of Cologne, Germany). The obtained data was analysed in collaboration with Dr. Nahal Ahmadinejad (Computational Biology, University of Bonn, Germany), (Section 2.2.8).

Paired-end sequencing using the genome analyzer GAIIx (Illumina Inc., San Diego, California, USA) resulted in 2 x 36 bp per read on average and >30 million reads per YAC clone. This resulted in an average coverage of approximately 130X. The data were filtered for reads mapping to the yeast (*Saccharomyces cerevisiae*) genome, which were excluded from further analysis. The remaining reads were mapped to the barley expressed sequence tag (EST) library (HarvEST database, version 1.77, assembly No. 35,) or the barley full-length cDNA (FLcDNA) library: DDBJ (AK353559-AK377172) (Matsumoto et al., 2011).

For the initial analysis of the data we used the paired-end reads. Table 3.9 depicts the number of total reads, the number of reads that mapped to yeast and barley, and the number of mapped barley ESTs. At a first glance the number of mapped barley ESTs seemed low, and we considered reducing the stringency of the analysis by using only

the single-pass reads (Table 3.10). This second type of analysis showed an increase in the number of reads mapping to barley ESTs and the number of mapped barley ESTs. However, the quality of the results decreased dramatically. Figure 3.7 illustrates a snapshot from the integrative genomics viewer (IGV, Broad Institute of Massachusetts Institute of Technology and Harvard Cambridge, MA, USA) with an example of the assembly of an EST for each analysis (1) paired-end reads for EST U35_5789 (Figure 3.7A) or (2) single-end forward reads for EST U35_337 (Figure 3.7B). In the case of the first approach, an even distribution of reads along the EST can be noticed. Conversely, in the case of the second method, the reads were confined to a single region and not distributed along the EST, likely reflecting mapping to a repetitive sequence. Therefore, the paired-end reads were used for the analysis of the data. Furthermore, the singleton ESTs were included, giving a considerably increase in the number of mapped barley ESTs (Table 3.11).

Table 3.9. Analysis of Illumina data using the paired-end reads

Clone	No. paired-end reads (36 bp)	No. reads mapped to yeast (%)	No. reads mapped to barley (%)	No. of mapped barley ESTs
87A3	34875716	31740075 (91.01%)	8924 (0.03%)	30
82B11	35516397	32155163 (90.54%)	9409 (0.03%)	69
158C12	35348764	32070610 (90.73%)	14296 (0.04%)	35

Table 3.10. Analysis of Illumina data using the single-end reads

Clone	No. reads mapped to barley (%)	No. mapped barley ESTs	No. reads mapped to barley (%)	No. of mapped barley ESTs
	Forward reads		Reverse reads	
87A3	42937 (0.12%)	1099	52980 (0.15%)	1600
82B11	51961 (0.15%)	1366	64600 (0.18%)	2166
158C12	59991 (0.17%)	1398	74014 (0.21%)	2342

Table 3.11. Analysis of Illumina data using the paired-end reads, including singleton ESTs

Clone	No. paired-end reads (36 bp)	No. reads mapped to yeast (%)	No. reads mapped to barley (%)	No. of mapped barley ESTs
87A3	34875716	31740075 (91.01%)	13580 (0.04%)	90
82B11	35516397	32155163 (90.54%)	17801 (0.05%)	184
158C12	35348764	32070610 (90.73%)	25151 (0.07%)	101
305A11	46297475	42262182 (91.28%)	7660 (0.02%)	60
354G1	43979498	39948281 (90.83%)	13003 (0.03%)	120
72C11	44350602	39506510 (89.07%)	26293 (0.06%)	184

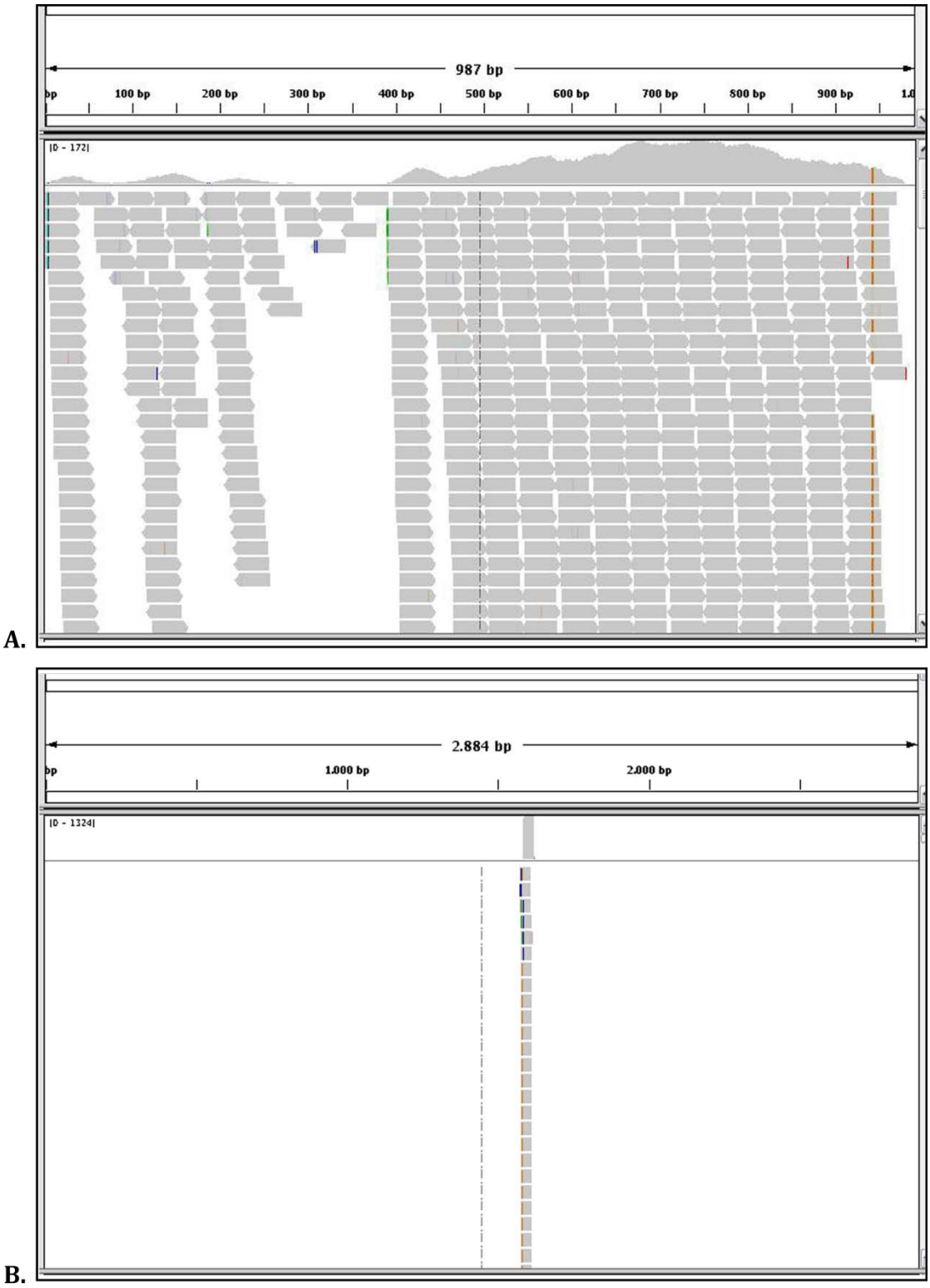

Figure 3.7. Snapshot of the integrative genomics viewer (IGV) representation of mapped sequencing data for clone 87A3. **(A)** Alignment of paired-end reads for EST U35_5789. Note that the reads (grey boxes) are evenly distributed along the EST. **(B)** Alignment of single-end-forward reads for EST U35_337. The reads are confined to a single region making it unsuitable for further analysis.

The total number of mapped barley ESTs was divided into three categories: (1) annotated genes that are sequence-related to genes in rice and/or wheat; (2) ESTs with less than 40 reads in the alignment (likely false positives); (3) "ESTs" corresponding to repetitive sequences e.g. transposons (Figure 3.8). This analysis revealed that most hits to ESTs are based on less than 40 reads, which are likely false positives.

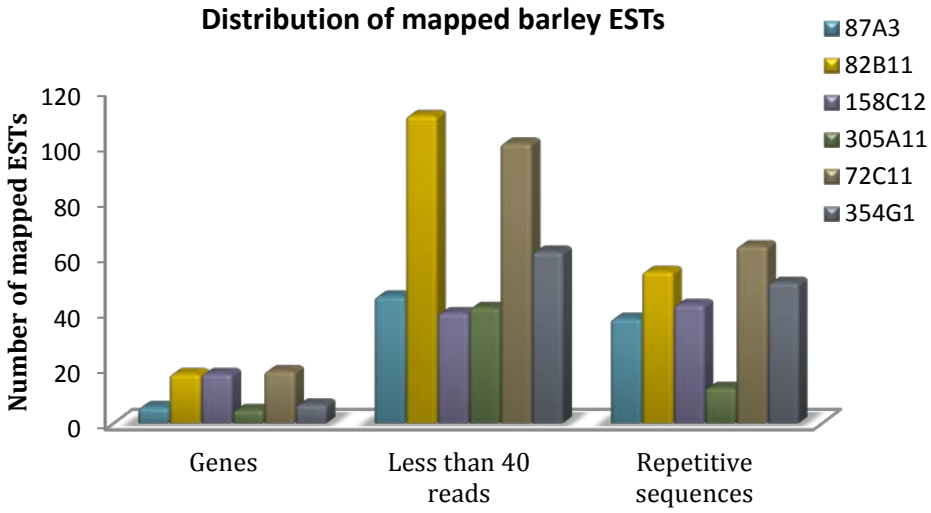

Figure 3.8. Distribution of mapped barley ESTs in barley YAC clones 87A3, 82B11, 158C12, 305A11, 72C11 and 354G1.

3.7.1 Presence of *Cons* and *Pol* genes in the sequencing data

Analysis of data from paired-end reads following mapping to contigs and singleton barley ESTs confirmed the presence of the marker genes *Cons* and *Pol*. For clone 87A3, 859 reads were mapped to EST U35_5789 (best BLASTX, *Cons*, Os10g0495900 [RAP-DB nomenclature]. For clone 82B11: 767, 44, 62, 55 reads and for clone 158C12: 1880, 120, 132, 138 reads were mapped to ESTs U35_7164, U35_32424, U35_35390 and U35_43139, respectively, which represent different regions of the *Pol* gene (best BLASTX, *Pol*, Os10g0495600 [RAP-DB nomenclature]). For both *Cons* and *Pol*, the integrative genomic viewer (IGV, Broad Institute of Massachusetts Institute of Technology and Harvard Cambridge, MA, USA) showed an even distribution of the mapped reads to the matching ESTs. –Illumina sequencing data is summarized in Supplemental Material 7.4 and 7.5-.

3.7.2 Sequenced isolated YAC clones do not close the gap between genes *Cons* and *Pol*

Notably, a few ESTs were mapped by reads from all sequenced YAC clones. Figure 3.9 shows the example of EST U35_2897; for this EST, 361, 498, 1068, 357, 160 and 104 reads were aligned to clones 87A3, 82B11, 158C12, 305A11, 354G1 and 72C11, respectively. On the first glance, the presence of shared ESTs in the hit list of all YAC clones (Supplemental Material 7.4 and 7.5) could be interpreted as evidence for an overlap between clone 87A3 (containing *Cons*) and its overlapping YAC 305A11 on the one side and clone 82B11 and clone 158C12 (containing *Pol*) and its overlapping YACs 72C11 and 354G1 on the other side. However, closer inspection and visualization of sequence details in the IGV revealed the presence of single nucleotide polymorphisms (SNPs) in the reads that mapped to these barley ESTs. For example, in the case of EST U35_2897 the SNPs present for clone 87A3 and 305A11 differed from the ones in clone 82B11 and 158C11 and the ones in clones 354G1 and 72C11, suggesting three highly related, yet non-identical, sequence variants that are present in the YACs. Additionally, the respective ESTs lack any significant BLAST hits to known genes, suggesting that they represent transcripts that derive from repetitive barley genomic regions. Thus, the sequence analysis does not provide any evidence for closure of the gap between the *Cons*- and *Pol*-containing YAC contigs.

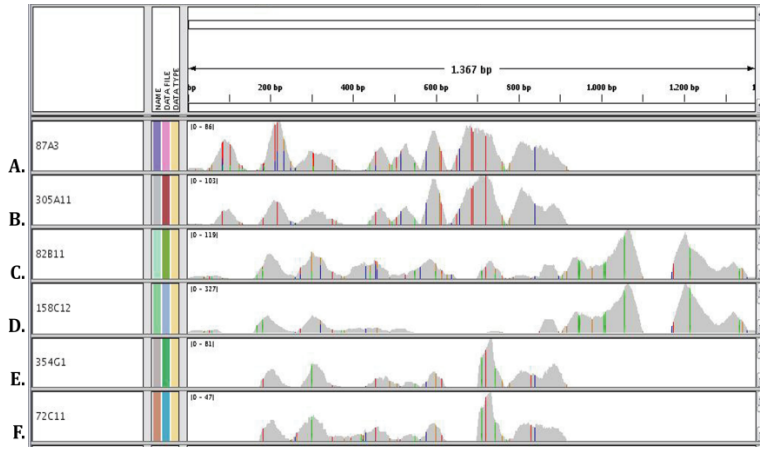

Figure 3.9. IGV visualization of single nucleotide polymorphisms (SNPs) in barley EST U35_2897 mapped to the six sequenced YAC clones. **(A)** 87A3. **(B)** 305A11. **(C)** 82B11. **(D)** 158C12. **(E)** 354G1. **(F)** 72C11. The SNPs (vertical coloured lines in the grey regions) present for clone 87A3-305A11 differed from the ones in clones 82B11-158C11 and the ones in clones 354G1-72C11, suggesting three related, yet non-identical, sequence variants.

3.7.3 YAC clone 72C11 is chimeric

Chimerism, the presence of non-contiguous DNA fragments in the same clone, is one of the common problems encountered when working with YACs (Banfi and Zoghbi, 1996). Analysis of the mapped barley ESTs in clone 72C11 (via ViroBLAST[6] analysis of pyrosequencing data derived from flow-sorted barley chromosomes; Leibniz Institute of Plant Genetics and Crop Plant Research, IPK, Gatersleben, Germany), revealed that this clone contains DNA fragments from our region of interest, barley chromosome 1H, but also DNA fragments that have primary BLAST hits to other regions of the barley genome (chromosome 5H and 7H). From 19 ESTs that map to barley, ten belong to the mentioned chimeric group, suggesting that clone 72C11 is a chimera that besides DNA from barley chromosome 1H harbours a significant proportion of genomic DNA from chromosome 5H and/or 7H. Consequently, no further analysis of these ESTs was carried out.

3.8 Analysis of *Ror1* candidate genes

Selected annotated genes contained in the sequenced YAC clones were analysed in more detail (Table 3.12). Several parameters were used as selection criteria: (1) expressed tissue, leaf or epidermis, especially after inoculation with *Blumeria graminis*; (2) gene length, due to the presence of seven alleles of the *Ror1* gene a long gene rather than a short one is expected; (3) number of reads and distribution, which is a criterion for quality. In clone 87A3 apart from the *Cons* gene, no other gene was found. In clone 82B11 genes encoding (1) a meprin and TRAF homology (MATH) domain-containing protein (Os10g0478500, RAP-DB); (2) a far-red-impaired response 1 (Far1) transcription factor with an orthologous in wheat (*Triticum aestivum*); and (3) a structural maintenance of chromosomes (SMC) N-terminal domain-containing protein (Os05g0596600, RAP-DB) were chosen. In clone 158C12 genes encoding (1) a myosin-2 heavy chain family protein (Os10g0488800, RAP-DB); (2) a protease inhibitor/seed storage/lipid transfer protein (LTP) family

[6] http://webblast.ipk-gatersleben.de/barley/viroblast

(Os10g0148000, RAP-DB); and (3) a pentatricopeptide (PPR) repeat-containing protein (Os10g0488900) were selected. In clone 305A11 a gene encoding an expressed protein of unknown function (Os10g0497000, RAP-DB) was selected. Finally, in clone 354G1, a gene encoding a nucleolar complex protein 2 -NOC2- (Os10g0495500, RAP-DB) was chosen.

Table 3.12. *Ror1* candidate genes from clones 82B11, 158C12, 305A11 and 354G1 selected for further analysis

Clone	HarvEST/ FLcDNA	No. Reads	Size (bp)	Gene product	Best BLAST X (*Oryza sativa*)
82B11	U35_2581	954	1462	MATH domain-containing protein	Os10g0478500
	U35_2582	76	658		
	U35_26899	383	674	Far1, Transcription factor, *Triticum aestivum*	None
	U35_6091	261	1653	SMC N terminal domain-containing protein	Os05g0596600
158C12	U35_19977	1551	1490	myosin-2 heavy chain family protein	Os10g0488800
	U35_28313	259	677		
	U35_42973	250	712		
	U35_540	163	708	LTP, protease inhibitor/seed storage family protein	Os10g0148000
	U35_39431	110	627		
	U35_39189	79	559		
	U35_34977	975	618	PPR, Pentatricopeptide repeat-containing protein	Os10g0488900
305A11	U35_3986	2620	1599	Unknown protein (AK363338)	Os10g0497000
	U35_7604	1119	1200		
	AK363338	2736	3169		
354G1	U35_25890	163	681	NOC2, nucleolar complex protein 2	Os10g0495500

Note: FlcDNA AK363338 in clone 305A11 contains ESTs U35_3986 and U35_7604

To confirm the data deduced from the Illumina sequencing analysis, primer pairs for two consecutive rounds of PCR (Table 3.13) were designed based on the mapped candidate gene ESTs (Table 3.12). The presence of each gene in the respective isolated YAC clones was confirmed. Additionally, the DNA from the YAC clones 313A6 and 415F4 (which were not sequenced), was included in the PCR analysis. As a result, the gene encoding the transcription factor Far1 (*Triticum aestivum*) was detected in YAC clone 82B11 and 72C11; the gene encoding the MATH domain-containing protein was found in YAC clones 82B11, 72C11 and 354G1; the genes encoding the myosin-2

protein, the pentatricopeptide protein and the LTP protein were present in YAC clones 158C12 and 415F4; while the gene encoding the NOC2 protein was only present in clone 354G1, the gene encoding the protein SMCN protein was only present in clone 82B11 and the gene encoding for the unknown protein (AK363338) could only be detected in clone 305A11. Figure 3.10 shows the YAC contig generated with the available information and marks the deduced approximate location of the *Ror1* candidate genes.

Table 3.13. Primer pairs designed to investigate the *Ror1* candidate genes

Set No.	Gene	Primary PCR	Nested PCR
16	*myosin-2*	J135-42973-FP1 J136-19977-RP1	J137-42973-FN2 J138-19977-RN2
17		J139-19977-FP3 J140-19977-RP3	J141-19977-FN4 J142-19977-RN4
18		J135-42973-FP1 148J-42973-RP5	149J-42973-FN6 150J-42973-RN6
19		151J-42973-FP7 152J-42973-RP7	153J-42973-FN8 154J-42973-RN8
20	*PPR*	155J-34977-FP9 156J-34977-RP9	157J-34977-FN10 158J-34977-RN10
21	*Far1*	159J-26899-FP11 160J-26899-RP11	161J-26899-FN12 162J-26899-RN12
22		167J-26899-FP15 168J-26899-RP15	No nested primers
23	*MATH*	163J-2581-FP13 164J-2581-RP13	165J-2581-FN14 166J-2581-RN14
24		169J-2581-FP16 170J-2581-RP16	No nested primers
25	*SMCN*	171J-6091-FP17 172J-6091-RP17	173J-6091-FN18 174J-6091-RN18
26	*LTP*	269J-540-FP 270J-540-FR	271J-540-NF 272J-540-NR
27	*NOC2*	244J-25890-PF 245J-25890-PR	254J-25890-NF 255J-25890-NR
28	*AK363338*	252J-AK363338.3PF 253J-AK363338.3PR	259J-AK363338-PF 260J-AK363338-PR
29		257J-AK363338-PF 247J-AK363338.1PR	No nested primers
30		265J-AK363338.2PF 266J-AK363338.2PR	No nested primers
31		267J-AK363338-PF 268J-AK363338-PR	No nested primers

Note: The annealing temperature used for all primers was 55°C except (J135/J136 and J139/J140: 60°C) and (J137/ J138 and J141/J142: 62°C)

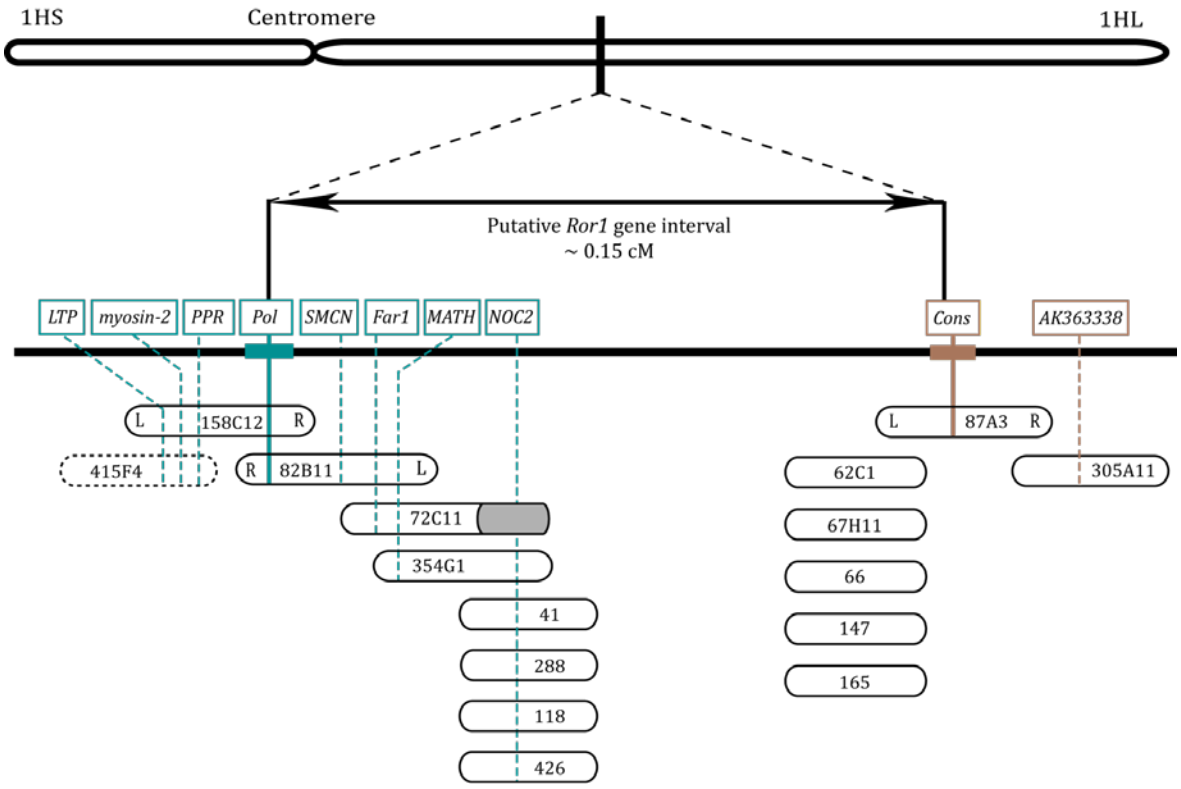

Figure 3.10. Schematic representation of the YAC contigs around the *Ror1* locus. The *Ror1* flanking genes, *Cons* and *Pol*, are indicated by vertical solid lines. Candidate genes are indicated by vertical dashed lines. Chimeric parts are displayed in grey. The unstable YAC clone 415F4 is drawn in dashed lines. The YAC clones are not displayed to scale. The orientation of the YAC clones is the most likely one (see below), but not confirmed. Note that the spaces between the genes do not represent physical distances and that the order of the genes around *Pol* is arbitrary. L, Left end; R, Right end; 1HS, short arm of barley chromosome 1H; 1HL, long arm of barley chromosome 1H. The approximate position of the *Ror1* region on chromosome 1H was determined by FISH analysis (see below section 3.9).

To discard or confirm the *Ror1* candidate genes, progeny of a set of recombinant lines from the mapping population A89 (*ror 1*-2; *mlo*-5, in the background of cv Ingrid) x Malteria Heda (*mlo*-3), (Collins et al., unpublished data) was used to "pseudo map" the candidate genes; from here named *Ror1* recombinants. These recombinant lines (F_4 or F_5 generation of the original cross used to generate the mapping population) are homozygous for the region surrounding the *Ror1* gene. The infection phenotype of the recombinants at seven days after pathogen inoculation (Section 2.2.1.3) was confirmed in comparison with the control lines Malteria Heda (genotype *mlo*-3 *Ror1*; resistant) and Ingrid (genotype *Mlo Ror1*; susceptible) (Figure 3.11). As expected, recombinants carrying the wild type *Ror1* allele (from Malteria Heda) were resistant and the ones carrying the mutated *ror1* allele (from line A89, *ror1* BCIngrid *mlo*-5;

(Freialdenhoven et al., 1996)) were partially susceptible (note the *mlo* genetic background for the recombinants). For each of the candidate genes, the primary PCR product, amplified from Malteria Heda and Ingrid genomic DNA, was sequenced and compared to identify DNA sequence polymorphisms between the two barley parental lines. If a polymorphism was identified (Figure 3.12A) amplification was carried out on genomic DNA of the recombinants and the respective gene "pseudo mapped" in relation to the known genetic constellation in each recombinant (Figure 3.12B).

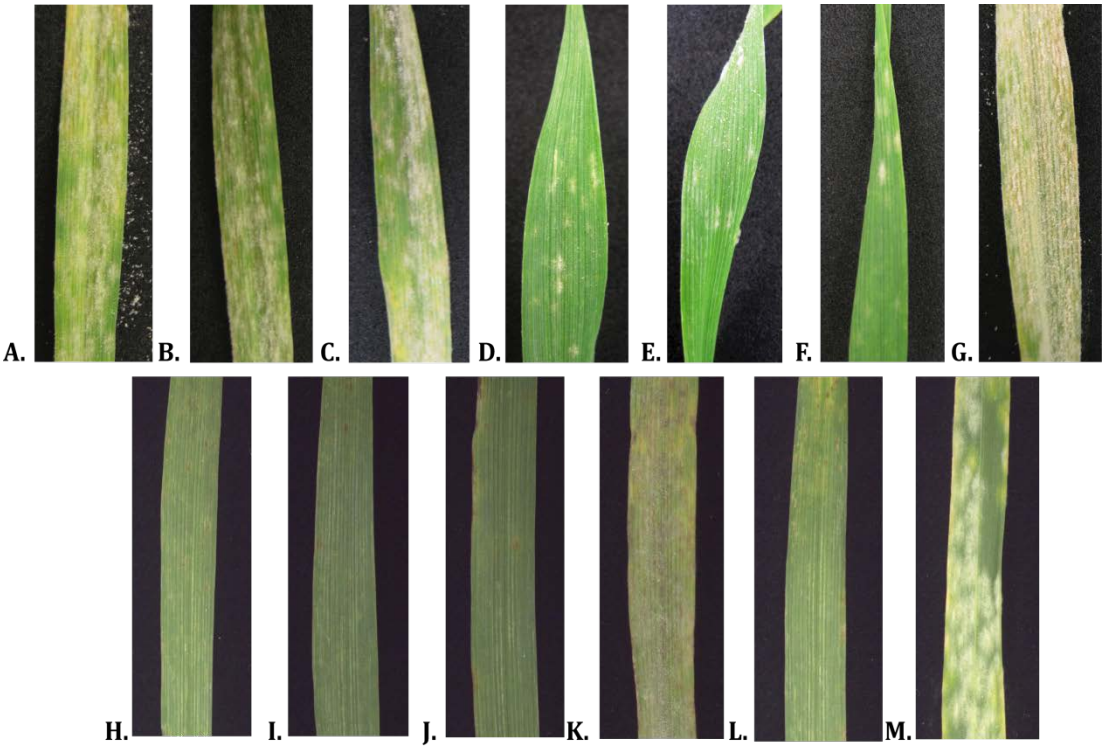

Figure 3.11. Powdery mildew infection phenotype of nine lines with recombination events in the *Ror1* region (progeny of the cross A89 x Malteria Heda), Ingrid and Malteria Heda seedlings at seven days after inoculation with *Blumeria graminis* f.sp. *hordei* (*Bgh*) isolate K1. **(A)** 77-5, partially susceptible. **(B)** 74-2, partially susceptible. **(C)** 51, partially susceptible. **(D)** 111, resistant. **(E)** C473, resistant. **(F)** Malteria Heda (*mlo*-3), resistant. **(G)** Ingrid, fully susceptible. **(H)** 26-3, resistant. **(I)** 21-2, resistant. **(J)** C487, resistant. **(K)** 102-1, partially susceptible. **(L)** Malteria Heda (*mlo*-3), resistant. **(M)** Ingrid, fully susceptible.

First, the sequenced *Cons* and *Pol* PCR products (primers JA52-CONS2F/JA53-CONS2R for *Cons* gene and JA70-POL3F/JA71-POL3R for *Pol* gene) from the parental lines Malteria Heda and Ingrid and the recombinants C473, 74-2, 51, 77-5 and 111 were compared to confirm the genetic constellation around the *Ror1* gene. This analysis revealed the expected allele pattern in all tested lines. Next, the YAC

candidate genes identified by Illumina sequencing were tested. The genes encoding the LTP protein (primary PCR primers No. 26 -Table 3.13-), the myosin-2 protein (primary PCR primers No. 17 -Table 3.13-), the MATH-domain containing protein (primary PCR primers No. 24 -Table 3.13-) and the nucleolar complex protein 2 -NOC2- (primary PCR primers No. 27 -Table 3.13-) showed an allele pattern that was identical to *Pol* (Figure 3.12B and Figure 3.12A for MATH domain-containing protein). None of the candidate genes showed the genetic constellation expected for the *Ror1* gene (Figure 3.12B). These findings discarded these four candidates as possible *Ror1* genes. No DNA sequence polymorphisms between Malteria Heda and Ingrid were found for the genes encoding the pentatricopeptide (PPR) protein (primary PCR primers No. 20 -Table 3.13-), the transcription factor Far1 (primary PCR primers No. 21-22, -Table 3.13-) and the SMC N-terminal domain-containing protein (primary PCR primers No. 25 -Table 3.13-). Thus, these candidates could not be pseudo mapped using the barley recombinants. The gene encoding the unknown protein -AK363338- (primary PCR primers No. 28 -Table 3.13- showed an allele pattern that was indistinguishable from *Cons*, suggesting that this gene is genetically closely linked to *Cons*, but presumably different from *Ror1* (Figure 3.12B). However, since only a single recombination event (in barley line 111) separates *Cons* from *Ror1* and because AK363338 is a rather large gene the formal possibility remained that AK363338 is *Ror1* and that an intragenic recombination event resulted in a situation where the part of AK363338 used for "pseudo mapping" resides proximal to *Cons* while the mutational *ror1* event in line 111 resides distal to *Cons* with regard to the actual recombination site. To test for this possibility and to correctly locate the candidate gene, four more recombinant barley lines (21-2, 26-3, C487, 102-1) were included in the analysis (Figure 3.11H-K). In this set of lines the recombination events are next to *Cons* (Collins et al., unpublished results). The allele pattern for the gene encoding the unknown protein -AK363338- was in each of the four lines distinct from the shared pattern for *Cons* and *Ror1*, thereby placing the gene unequivocally telomeric to *Cons* (Figure 3.12C). (Sequences of the candidate genes with DNA polymorphisms between Malteria Heda and Ingrid can be found as Supplemental Material 7.6).

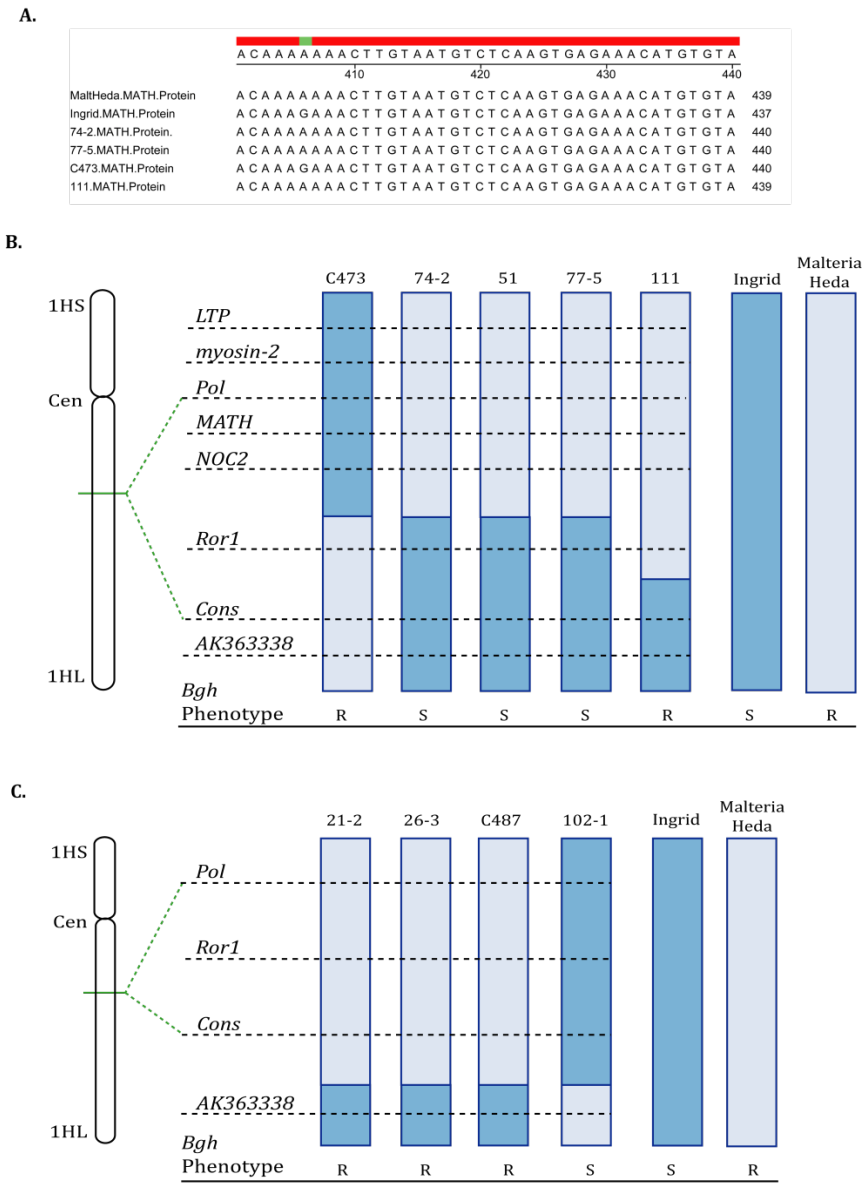

Figure 3.12. "Pseudo mapping" of *Ror1* candidate genes using a set of barley lines with recombination events in the *Ror1* region (A89 x Malteria Heda). (A) Detection of a SNP for the gene encoding a MATH-domain containing protein, which is useful to "map" the candidate gene using the *Ror1* recombinants. **(B)** Genetic constellation (allele pattern) of recombinants C473, 74-2, 51, 77-5, 111 and the parental lines Ingrid and Malteria Heda. The gene encoding the unknown protein, AK3633838 (Os10g0497000) mapped to the *Cons* region. The genes encoding the LTP protein (Os10g0148000), the myosin-2 protein (Os10g0488800), the MATH domain-containing protein (Os10g0478500) and the nucleolar complex 2 (NOC2) protein (Os10g0495500) "mapped" to the *Pol* gene region. None of the candidates "mapped" to the *Ror1* gene region. **(C)** Genetic constellation (allele pattern) of recombinants 21-2, 26-3, C487, 102-1 and the parental lines Ingrid and Malteria Heda. AK363338 encoding the unknown protein (Os10g049700) "maps" telomeric to the recombination event within the *Cons* region. Note that all recombination events are indicated with their approximate position and that the order of the genes around *Pol* is arbitrary. At the very left in B and C it is represented barley chromosome 1H. 1HS, short arm; 1HL, long arm; Cen, centromere. Green dashed lines denote the putative region between *Pol* and *Cons*.

3.8.1 Finding new overlapping clones using the NGS data

3.8.1.1 Clone 87A3

Using the "bubble oligonucleotide" approach the clone 305A11 was isolated for the right end of clone 87A3 (Section 3.3.1). However, for the left end it was not possible to find an overlapping clone with this technique. Additionally, in this clone no other predicted gene was found that could be used as a probe for re-screening of the barley YAC library. Thus, we proposed to (partially) assemble the non-yeast Illumina reads obtained from the sequencing of clone 87A3 with the goal to seek for scaffolds with low similarity to repetitive elements and to use them to design primers for re-screening of the barley YAC library. In collaboration with Dr. Nahal Ahmadinejad (Computational Biology, University of Bonn, Germany) several scaffolds were obtained and two of them, 141239 and 141664 (Supplemental Material 7.7), were selected for further analysis. Table 3.14 shows the primer pairs designed based on the scaffolds sequences. Following PCR with the two sets of primers in five random YAC pools, clone 87A3, clone 305A11 and barley genomic DNA showed an amplification product only in clone 87A3. Meaning this scaffold is specific for clone 87A3 and is not contained in the overlapping clone 305A11. Re-screening of the YAC library was carried out with these oligonucleotides. Using the primer pairs No. 33 (Table 3.14) several YAC pools (>10) showed a positive signal. However, none of them could be confirmed by secondary PCR analysis. Using the primer pairs No. 32 (Table 3.14) numerous YAC pools (>24) showed a positive signal. Secondary PCR analysis revealed a strong band in the case of YAC pools 62 and 67 and a weak band in the case of pools 66, 147 and 165 (data not shown). PCR analysis to unravel the positive rows and columns of plates 62 and 67 indicated as coordinates the single YAC clones 62C1 and 67H11. Subsequent colony PCR of the single clones confirmed 62C1 and 67H11 as overlapping clones of 87A3L (Figure 3.10). Owing to time constraints, the exact identity of the clones in pools 66, 147 and 165 could not be determined within the context of this thesis.

These results showed that scaffolds of assembled reads were suitable to design primers and could be used as probes for re-screening of the YAC library. This approach can be used as an alternative method to find overlapping clones and continue the barley YAC chromosome walking.

Table 3.14. Primer pairs designed using two scaffolds sequences from clone 87A3

Set No.	Scaffold ID	Primary PCR	Nested PCR
32	141239	209J-141239-FP / 210J-141239-RP	211J-141239-FN / 212J-141239-RN
33	141664	213J-141664-FP / 214J-141664-RP	215J-141664-FN / 216J-141664-RN

Note: The annealing temperature for the primary PCR was 61.8°C and for the nested PCR was 59.8°C

3.8.1.2 Clone 305A11

As mentioned in section 3.5.1, no overlapping YACs for clone 305A11 were isolated. As an alternative to find them, a re-screening of the YAC library with the primer pairs designed for the predicted unknown protein -AK363338- (Set No. 28, Table 3.13) was carried out. After re-screening of the YAC library only pools 305 and 87 (likely representing the already known clones 30511 and 87A3) were positive for this gene, indicating that AK363338 is unsuitable as a probe to uncover further overlapping YAC clones in this direction.

3.8.1.3 Clone 158C12

The "bubble oligonucleotide" was a useful approach to find YAC 415F4, which overlaps with clone 158C12 (Section 3.3.3). However, because of clone instability problems, it was impossible to obtain enough DNA for further analysis, e.g. Illumina sequencing. As an alternative to find a different overlapping clone, re-screening of the YAC library using the primer pairs to amplify the gene encoding the myosin-2 protein (set No. 17, Table 3.13) was performed. Solely pool 428 showed a positive signal after re-screening of the library. However, following PCR reactions from rows and columns from plate 428, no clone could be identified. In the context of this thesis further walking in the direction of YAC 415F4 was abandoned.

3.8.1.4 Clone 354G1

As mentioned in section 3.5.2, no overlapping YACs for clone 354G1 were isolated. As an alternative to find them, a re-screening of the YAC library with the primer pairs designed for the gene encoding a nucleolar protein complex 2 (NOC2) (Set No. 27, Table 3.13) was carried out. After re-screening of the YAC library pools 41 and 288 (strong positive signal) as well as pools 118 and 426 (weak positive signal) were positive for this gene (Figure 3.10). Owing to time constraints, the exact identity of the clones in these pools could not be determined within the context of this thesis.

3.9 Fluorescent *In Situ* Hybridization (FISH) analysis

We investigated the physical distance between the *Cons* and *Pol* genes flanking *Ror1* and the putative order of the YAC clones by performing single-copy FISH of suitable probes on barley metaphase chromosomes from root tip cells (Section 2.2.9). These experiments were performed in collaboration with the group of Dr. Andreas Houben: chromosome structure and function at the Leibniz Institute of Plant Genetics and Crop Plant Research (IPK, Gatersleben, Germany) under the supervision of Dr. Lu Ma.
In total eight unique sequences were amplified by PCR and used as probes in the FISH experiments (Table 3.15). To evaluate each probe for its quality and suitability for FISH, the PCR fragments were labelled with the red fluorescent dye Texas red-dUTP (Perkin Elmer, Massachusetts, USA). As control, a probe for the long arm of barley chromosome 1H, pHV-1112 (Kato, 2011) labelled with the green fluorescent dye Alex-488-dUTP (Invitrogen, Karlsruhe, Germany) (Section 2.2.9.1) was used. In independent experiments each red probe was combined with the green probe. The probes yielded clear and unique signals on the long arm of barley chromosome 1H (Figure 3.13). All the probes located to the same chromosomal region at roughly 1/3 distance from the centromere towards the telomere of the long arm of chromosome 1H in a subregion known to be a “cold spot” of meiotic recombination (Künzel et al., 2000). Subsequently, the probes were labelled in different colours to investigate the physical distance between the genes and to verify the orientation of the YAC clones.

Table 3.15. Primer pairs used to prepare unique probes for barley single-copy FISH.

Target	ID	Set No.	Primers	PCR product length (bp)	Total probe length (bp)
Cons	Cons 1	34	JA50-CONS1F JA51-CONS1R JA52-CONS2F JA53-CONS2R	600	2600
	Cons 2	35	261J-AK371545-PF JA55-CONS3R	2000	
Pol	Pol 1	36	JA66-POL1F JA67-POL1R	1500	3300
	Pol 2	37	JA72-POL4F 243J-POL-PR2	1800	
AK363338	AK 1	38	252J-AK363338.3PF 253J-AK363338.3PR	2100	2600
	AK 2	39	265J-AK363338.2PF 266J-AK363338.2PR	500	
myosin-2	My 1	40	J135-42973-FP1 148J-42973-RP5	1950	2950
	My 2	41	J139-19977-FP3 J140-19977-RP3	1000	

Note: The annealing temperature for all sets of primers was 55°C except for set No. 41, which was 60°C

Three different combinations of probes were used: (1) *Cons* (red) + *Pol* (green) + pHV-1112 (far red); (2) *Cons* (red) +*AK363338* (green) + pHV-1112 (far red); (3) *Pol* (green) + *myosin-2* (red) +pHV-1112 (far red). The probes labelled in red yielded a clear signal; however, the signal of the probes labelled in green was not as strong, making it difficult to determine the distance between the studied genes (Figure 3.14). If different genes can be distinguished on barley mitotic chromosomes as separate signals, there should be a megabase-sized distance between them (Ma et al., 2010). FISH with probes derived from *Cons*, *Pol* and pHV-1112 showed separate signals on both sister chromatids (Figure 3.14A) suggesting a more than one megabase-sized distance between them. Additionally, in three of the four chromatids in Figure 3.14A the FISH signals are adjacent and in one chromatid the red signal (*Cons*) is located more distal from the centromere than the green signal (*Pol*). FISH with probes derived from *Cons*, *AK363338* and pHV-1112 showed separate signals on both sister chromatids (Figure 3.14B). Moreover, the green signal (*AK363338*) is located more proximal to the centromere than the red signal (*Cons*), suggesting, in terms of our YAC contig, that *AK363338* could be located inside the *Cons-Pol* interval. However, this finding disagrees with our results from "pseudo mapping" of *AK363338* in the *Ror1* recombinant population (Section 3.8 and Figure 3.12C) where *AK363338* was located outside of the *Cons-Pol* interval. On the other hand, FISH signals with probes derived

from *Pol* and *myosin-2* were visible in one chromosome and the control probe, pHV-1112 was not visible (Figure 3.14C); in one of the chromatids the signal was overlapping and in the other chromatid the signals looked separated, revealing contradictory data with regard to the location of *myosin-2* in the *Cons-Pol* interval. Taken together, these results suggest that our proposed YAC contig around the *Ror1* gene (Figure 3.10) is likely to be correct with respect to the presence of the suggested genes. However, more images would be required to analyse the physical order of the studied genes with higher resolution and to position the genes unequivocally in regard to the reference genes, *Cons* and *Pol*. In addition, it would be advisable to generate longer probes for usage in future FISH experiments, because the length of the actual probes was between 2.6 kb and 3.3 kb, which is at the edge of sensitivity (Dr. Lu Ma, personal communication).

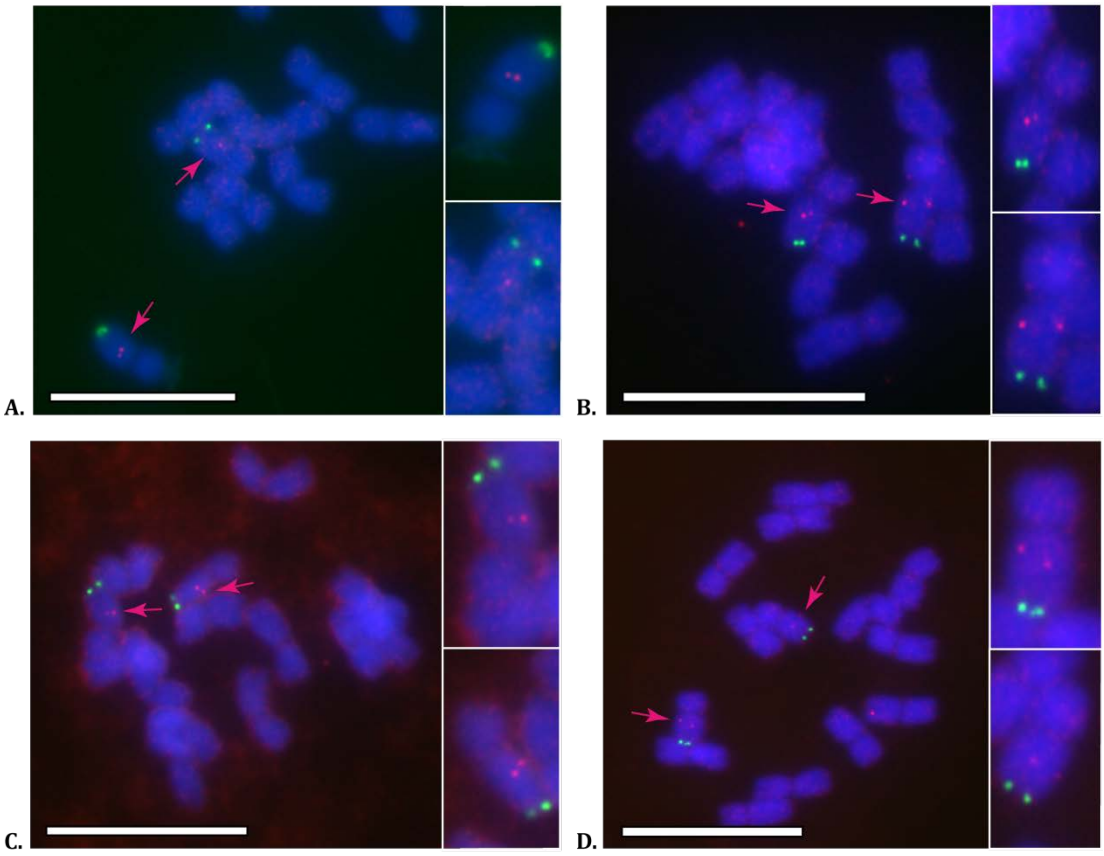

Figure 3.13. Single-copy FISH on barley root tip metaphase chromosomes of cv. Ingrid. Individual probes. Shown in green is the signal of the probe for the long arm of chromosome 1H (pHV-1112; Kato, 2011); shown in red and highlighted by arrows are the signals for the repeat-free probes of interest; the *insets* show a magnification of the chromosomes with the FISH signals. *Scale bar* = 20 µm. **(A)** Probe for *Pol.* **(B)** Probe for *Cons*. **(C)** Probe for *AK363338*. **(D)** Probe for *myosin-2*.

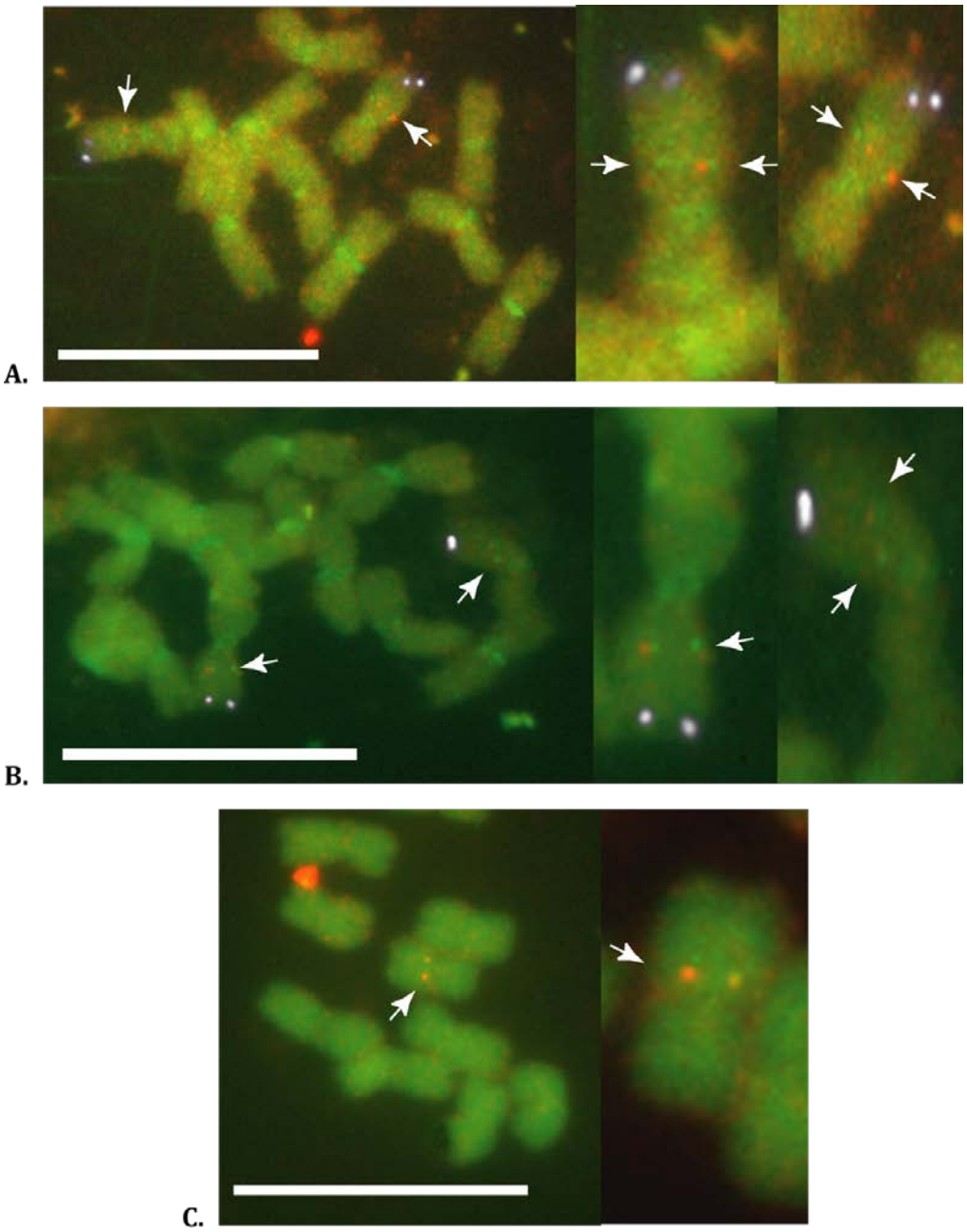

Figure 3.14. Single-copy FISH on barley root tip metaphase chromosomes of cv. Ingrid. Combined probes. Shown in white is the signal of the probe for the long arm of chromosome 1H (pHV-1112; Kato, 2011); the arrows indicate the position of the signals for green and red probes; the *insets* show a magnification of the chromosomes with the FISH signals. *Scale bar* = 20 µm. **(A)** Probes for *Cons* (red) + *Pol* (green) + pHV-1112. **(B)** *Cons* (red) + *AK363338* (green) + pHV-1112. **(C)** *Pol* (green) + *myosin-2* (red) + pHV-1112.

3.10 Comparative genomics between various monocot species

The rapid progress in the comparative analysis of Poaceae genomes revealed that they are composed of similar genomic blocks (Moore et al., 1995), nowadays denoted

as “synteny”. This term refers to gene loci in different taxa located on a chromosomal region of common evolutionary ancestry (Passarge et al., 1999; Keller and Feuillet, 2000). Synteny is typically recognizable by a conserved gene order (collinearity) that fades away with evolutionary distance between taxa, owing to small- or large scale-genomic re-arrangements such as insertions, deletions and inversions (Keller and Feuillet, 2000). Mayer et al, (2009; 2011) have identified syntenic chromosomal regions between chromosome 1H in barley (*Hordeum vulgare*), chromosome 5 and 10 in rice (*Oryza sativa*), chromosome 2 and 3 in *Brachypodium distachyon* and chromosome 1 and 9 in *Sorghum bicolor*. Using web-based resources for synteny analysis (CoGePedia, Gramene, Phytozome and Plaza 2.0, Table 2.4) and the genome browsers (MSU, Gbrowse, JGI and RAP-DB, Table 2.4) we determined that our region of interest (YAC contig in Figure 3.10) is syntenic with chromosome 10L of rice, chromosome 3L of *B. distachyon* and chromosome 1S of *S. bicolor* (Figure 3.15A). Comparison of the syntenic region revealed substantial re-arrangements between the four monocot species that perturb gene collinearity (Figure 3.15B). For all genes located in our barley YAC contig except the gene encoding the transcription factor Far1, the synteny analysis showed orthologs genes in at least one of the other three grass species (Table 3.16). While six of the genes are present in the syntenic regions of all four grass species investigated, the gene encoding the LTP protein is not present in *B. distachyon* and *S. bicolor* and the *Pol* gene is not present in *S. bicolor* (Table 3.16).

Table 3.16. Genes located in the *Ror1* YAC contig and their orthologs genes in rice (*O. sativa*), *B. distachyon* and *S. bicolor*

Hordeum vulgare	***Oryza sativa***	***Brachypodium distachyon***	***Sorghum bicolor***
LTP	Os10g0148000	None	None
myosin-2	Os10g0488800	Bradi3g29440	Sb01g018770
PPR	Os10g0488900	Bradi3g29450	Sb01g018760
Pol	Os10g0495600	Bradi3g29920	None
Far1	None	None	None
MATH	Os10g0478500	Bradi3g28880	Sb01g019200/210
NOC2	Os10g0495500	Bradi3g29890	Sb01g018260
Cons	Os10g0495900	Bradi3g29930	Sb01g018250
AK363338	Os10g0497000	Bradi3g29910	Sb01g018220

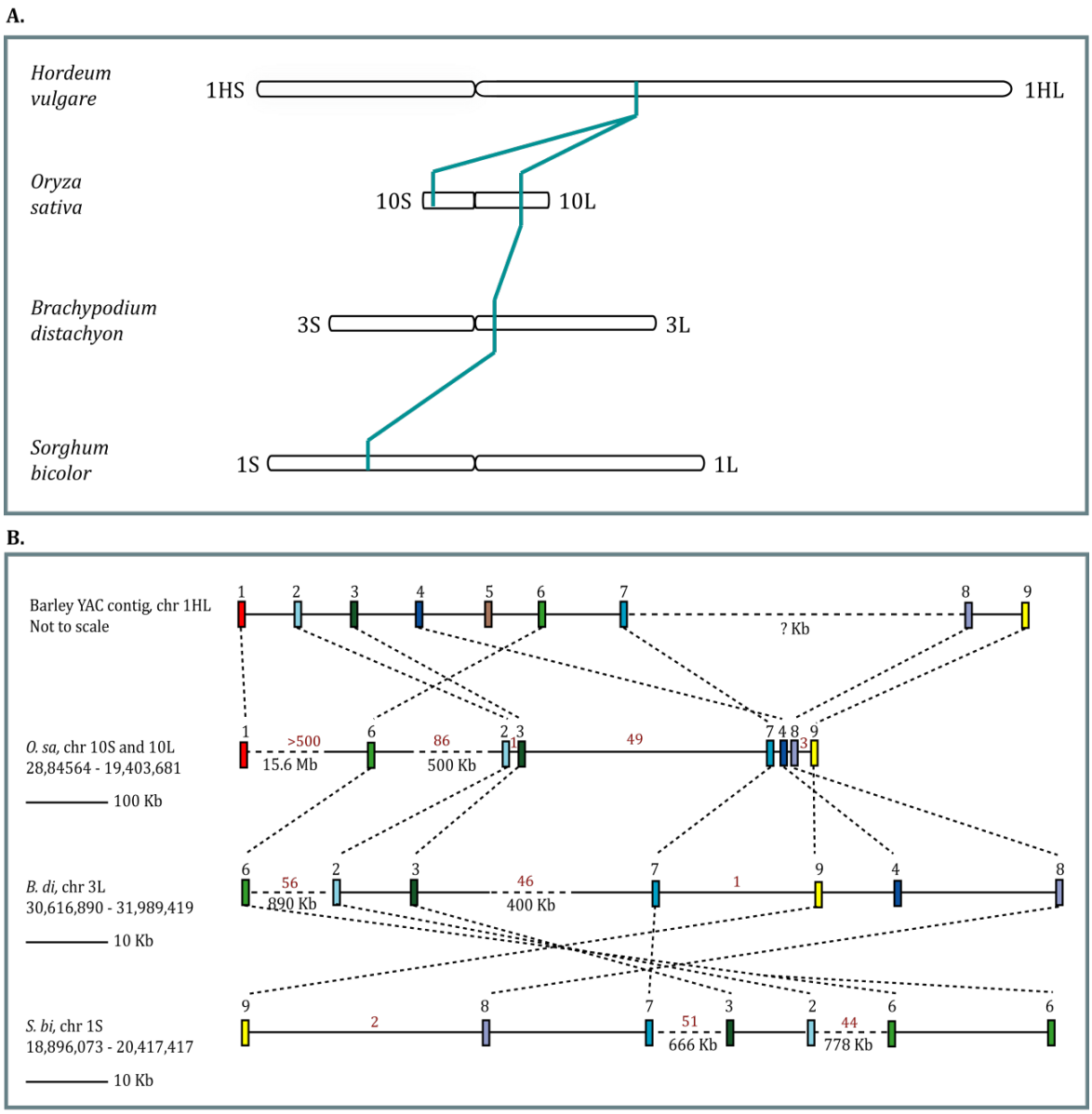

Figure 3.15. Comparative view of the barley *Ror1*-YAC contig in rice, *B. distachyon* and *S. bicolor*. **(A)** General overview of the syntenic region in the chromosomes of the four grass species. S: short arm; L: long arm. **(B)** Schematic representation of the re-arrangements at the gene level for the syntenic region in the four grass species. From 1 to 9, genes found in the *Ror1*-YAC contigs, connected with dash lines between the chromosomes of the four monocot species studied 1, *LTP*; 2, *myosin-2*; 3, *PPR*; 4, *Pol*; 5, *Far1*; 6, *MATH*; 7, *NOC2*; 8, *Cons*; 9, *AK363338*. Note that the position of the genes 1-3 and 5-7 is the most likely but not confirmed. In red is given the number of additional genes that are present in the genomes of *O. sativa, B. distachyon* and *S. bicolor* in between the detected genes in the *Ror1*-YAC contigs of this study.

3.11 A conserved regulon in plant resistance against powdery mildew: an alternative approach to find the *Ror1* gene

Recently, Humphry et al., (2010) showed on the basis of gene expression meta-analysis that a common set of genes is co-expressed with genetically defined core components of antifungal defence in the monocot barley and the dicot *A. thaliana*. These genes code amongst other functions for proteins involved in secondary metabolite biosynthesis and exocytosis/extrusion. Notably, genes known to represent in its mutant form suppressors of *mlo* resistance in *Arabidopsis* (e.g. *PEN1*, *PEN2* and *PEN3* (Consonni et al., 2006) are prominent members of the list of co-expressed genes. We therefore reasoned that genes that function as suppressors of barley *mlo* resistance (e.g. *Ror1*) might be likewise members of the list of co-expressed barley genes. We focussed on 356 unique barley ESTs assemblies that were found to be co-expressed with the gene encoding the seven-transmembrane domain-containing Mlo protein, the gene encoding the syntaxin Ror2 (identified from the same EMS mutagenesis screen as *Ror1*, (Freialdenhoven et al., 1996)) and the gene encoding the SNARE protein, SNAP34. BLAST analysis was performed with the 356 barley ESTs and the results were filtered for the best hits to chromosome 10 from rice (syntenic chromosomal region with the barley chromosome 1H, Section 3.10). We selected six genes as candidates for *Ror1* (Table 3.17) and analysed them using the same "pseudo mapping" approach as we did for the candidate genes found in our YAC contig (Section 3.8). Based on polymorphisms between the two parental lines of the *Ror1* recombinants, Malteria Heda and Ingrid, the gene encoding a glutaredoxin domain-containing protein (U35_22190; Os10g0482900) and the gene encoding a receptor-like protein-hcrVf2 (U35_21139; Os10g0469700) showed an allele pattern that is identical to the *Pol* gene in the *Ror1* recombinants (Figure 3.16) (sequences of the candidate genes with DNA polymorphisms between Malteria Heda and Ingrid can be found as Supplemental Material 7.8). No DNA sequence polymorphisms between the parental lines were found for the genes encoding the MAPK protein, glutathione S-transferase protein, glycosyl transferase 8 domain-containing protein and UDP-glucoronosyl domain-containing protein. Thus, these candidates could not be examined using the *Ror1* recombinants. Furthermore, none of these candidate genes

was identified in the isolated YAC clones present in the YAC contigs depicted in Figure 3.10 (data not shown). Taken together, by this approach only two of the six candidate genes could be discarded as the possible *Ror1* gene. However, after the recent publication of the barley FLcDNA library by (Matsumoto et al., 2011), there is still the possibility to obtain other regions of the candidate genes (not covered by the EST contigs in the HarvEST database used in the Humphry et al, (2010) study) to design new sets of primers and test them in the *Ror1* recombinant population. Moreover, of the 356 co-expressed barley ESTs we so far selected candidates with best BLAST hits to chromosome 10. Nevertheless, because of the synteny that chromosome 5 of rice also has with chromosome 1H of barley, it could be interesting to evaluate some additional ESTs (U35_960, U35_1807 and U35_4602) that have best BLAST hits on rice chromosome 5.

Table 3.17. *Ror1* candidate genes selected from 356 barley ESTs co-expressed with *Mlo*, *Ror2* and *SNAP34*

HarvEST	Gene Product	Best BLAST (*Oryza sativa*)	Primers
U35_2346	Putative MAPK based on amino acid sequence homology	Os10g0533600	197J-2346-FP 198J-2346-RP
U35_16367	Protein glutathione S-transferase	Os10g0530900	189J-16367-FP 190J-16367-RP
U35_18727	Protein glycosyl transferase 8 domain-containing protein	Os10g0555100	175J-18727-FP 187J-18727-2RP
U35_20658	Protein UDP-glucoronosyl/UDP-glucosyl transferase domain-containing protein	Os10g0322200	237J-20658-PF 238J-20658-PR
U35_21139	Receptor-like protein, similar to hcrVf2 protein	Os10g0469700	193J-21139-FP 194J-21139-RP
U35_22190	Protein glutaredoxin domain-containing protein	Os10g0482900	179J-22190-FP 180J-22190-RP

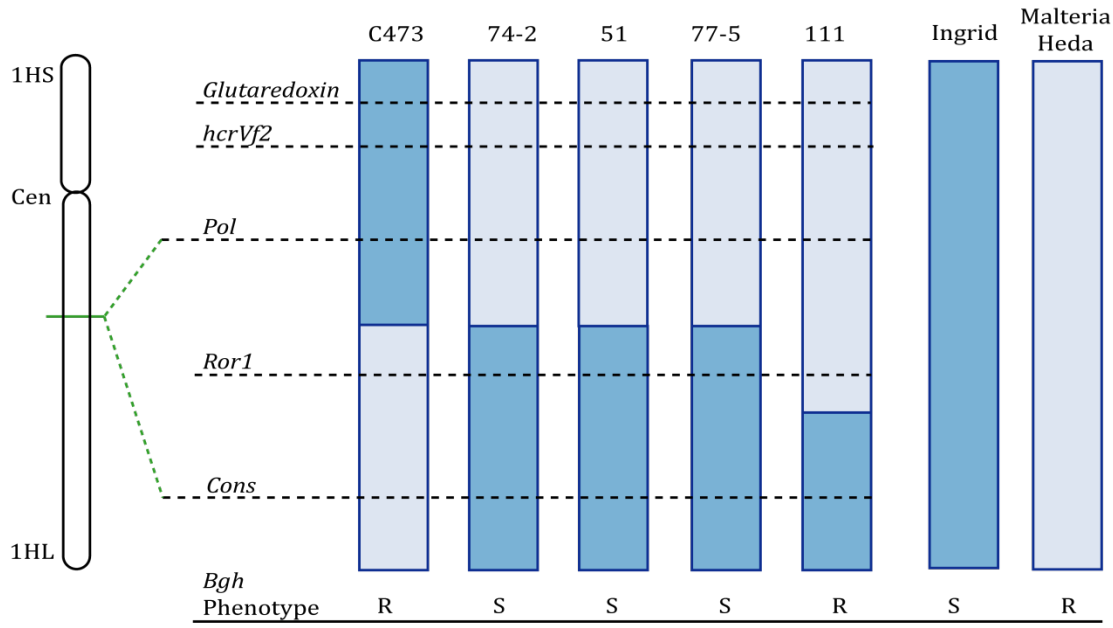

Figure 3.16. "Pseudo mapping" of a second group of *Ror1* candidate genes using a set of barley lines with recombination events in the *Ror1* region (A89 x Malteria Heda). Genetic constellation (allele pattern) of recombinants C473, 74-2, 51, 77-5, 111 and the parental lines Ingrid and Malteria Heda. The gene encoding the glutaredoxin protein (Os10g0482900) and the gene encoding the receptor-like protein-hcrVf2 (Os10g0469700) "mapped" to the *Pol* gene region. None of the candidates "mapped" to the *Ror1* gene region. Note that all recombination events are indicated with their approximate position and that the order of the genes around *Pol* is arbitrary. At the very left it is represented barley chromosome 1H. 1HS, short arm; 1HL, long arm; Cen, centromere. Green dashed lines denote the putative region between *Pol* and *Cons*.

4. Discussion

4.1 Chromosome walking towards the *Ror1* locus using YAC libraries and Illumina sequencing: *the approach*

The pursue of cloning the *Ror1* gene has been of remarkable interest since its identification as a suppressor of *ml*o-resistance in barley to the powdery mildew pathogen, *Bgh* (Freialdenhoven et al., 1996). In previous years, three approaches were followed to isolate the gene, (1) fine mapping using barley sequence-tagged site (STS) markers (2) synteny-based marker saturation using rice BACs and (3) synteny-based gene isolation using *B. sylvaticum* BAC libraries. The first approach mapped the *Ror1* gene to the long arm of barley chromosome 1H and resulted in the isolation of a valuable collection of *Ror1* recombinants. In addition, *Ror1* was located to a 0.2- to 0.5- cM marker interval (Collins et al., 2001). Taking advantage of synteny among three monocot species, the second approach revealed that the barley *Ror1* region is syntenic with a region on chromosome 10 in rice. Comparison of gene order between barley and rice with rice BACs as a reference plus analysis of the recombinant population, delimited the region containing *Ror1* to an interval of ~0.15 cM between the marker genes *Cons* and a cosegregating group of markers containing *Pol* as the closest predicted gene (Collins et al., unpublished data). However, due to a lack of recombination events and more markers, the *Ror1* gene could not be identified. The distance in rice between *Cons* and *Pol* was found to be ~2 kb and no further coding genes were recognized in this interval. The third approach used the information generated by Collins et al., (unpublished data) and focussed on the *Ror1* region in the monocot *B. sylvaticum*. Screening of *B. sylvaticum* BAC libraries resulted in the identification of two BACs containing *Cons* and *Pol* with a distance of ~4.5 kb and no coding genes between them. Thus, also by this approach the *Ror1* gene could not be identified (Benjdia et al., unpublished data).

In this thesis, a chromosome walking towards the *Ror1* locus is described using a barley YAC library. The capacity of YAC vectors for cloning long DNA inserts makes them especially suitable to study large eukaryotic genomes (Larin et al., 1996). The closest predicted flanking *Ror1* genes identified by Collins et al., (unpublished data) were used for the initial isolation of YAC clones by PCR. Subsequently, recovery of end fragments from the YAC inserts was carried out by using the "bubble oligonucleotide" approach. Three out of six ends provided sufficient information to design primers which then could be used to re-screen the YAC library, to isolate overlapping clones and to continue the chromosome walking. However, due to the highly repetitive sequences in the other three ends, the PCR method failed to generate sufficient information after re-screening of the YAC libraries. Nevertheless, as reported before, the "bubble oligonucleotide" approach provided a rapid and versatile method to be used in chromosome walking (Riley et al., 1990; Gibson and Somerville, 1992; Schmidt et al., 2001). Genomic DNA from six YAC clones was paired-end sequenced by second generation sequencing (Illumina®). The application of this new technology demonstrated a time-efficient way to obtain an adequate coverage of the insert sequence of a YAC in contrast to the classical approach, which involves subcloning into plasmid vectors followed by Sanger sequencing. To our knowledge this is the first report of using Illumina sequencing in a chromosome walking procedure with YAC libraries.

The analysis of the sequencing data revealed that we have two separated YAC contigs around *Ror1*, one each on the *Pol* and the *Cons* side, with a gap of unknown size in between. Earlier studies revealed an estimated genetic distance between the two flanking genes of around 0.15 cM (Collins et al., unpublished data). Initially, based on the genome-wide average, we assumed a physical/genetic distance ratio of approximately 3 Mb/cM (Büschges et al., 1997). However, the physical distance between the two flanking *Ror1* genes seems to be greater than the estimated ~450 kb since the two YAC contigs did not overlap, despite considerable extension to both sides of the *Cons* and *Pol* flanking markers. Furthermore, our FISH experiments on barley metaphase chromosomes, located the *Ror1* region roughly at 1/3 distance from the centromere towards the telomere of the long arm of chromosome 1H (Figure 3.13) Künzel and co-workers (2000) subdivided the barley genome into

regions with a high (less than 1Mb/cM), medium (1-4 Mb/cM), and low (greater than 4 Mb/cM) recombination frequency. Their studies were based on a physical map developed using translocation breakpoints and PCR mapping of low-copy number probes on isolated chromosomes. According to this subdivision, our region of interest exhibits a suppressed recombination rate and has an expected physical/genetic distance ratio of >4.4 Mb/cM to ≤47 Mb/cM (Künzel et al., 2000). This suggests that the *Ror1* flanking markers, *Pol* and *Cons*, can be separated by a physical distance between 0.6 Mb and 7 Mb. In addition, the FISH analysis (Figure 3.14) showed separate hybridization signals for the *Cons* and *Pol* probes, which indicates a greater than a megabase-sized distance between them (Ma et al., 2010).

The analysis of the sequencing data revealed a chimeric YAC clone (72C11; Figure 3.10). In YAC libraries the frequency of chimerism can vary between 5% and 50%, and this issue is one of the major disadvantages of working with YACs (Banfi and Zoghbi, 1996; Chaplin and Brownstein, 2001b). The library screened in this project was previously used to find the *Mlo* gene on chromosome 4H in barley (Simons et al., 1997) and the *Rar1* gene on chromosome 2H in barley (Lahaye et al., 1998). In these studies, respectively, two out of four and three out of five YAC clones were found to be chimeric. Although the mechanism(s) is not fully understood, chimeric YAC clones likely arise at the stage of DNA cloning into the YAC vector or by homologous recombination between two different YACs introduced into one yeast cell (Green et al., 1991; Roosen et al., 2001). The impact of the chimeric clone for our studies was minimized, since a second non-chimeric overlapping YAC clone on the same side (354G1; Figure 3.10) was isolated.

Thorough analysis of the distribution of the Illumina sequence reads that mapped on barley ESTs revealed that ~ 40% of the mapped barley ESTs comprised repetitive DNA. In comparison to the rice genome (400 Mb) and the *B. distachyon* genome (280 Mb), the barley genome (5.1 Gb) is of extreme size and contains at least 80% of repetitive DNA (Mayer et al., 2009; Wicker et al., 2009). The repetitive fraction of the Triticeae genomes consists primarily of transposable elements (TEs). The TEs affect the genome by their ability to move and replicate, thereby generating plasticity (Wicker et al., 2007). TEs display extreme diversity and they are classified into two

main classes on the basis of the presence or absence of RNA as a transposition intermediate, (a) class I, retrotransposons and (b) class II, DNA-transposons (Wicker et al., 2007). The TEs discovered in our YAC sequences mainly represented members of class I of the long terminal repeat (LTR) order and the *Gypsy* and *Copia* superfamily. In low numbers, TEs from class II of the terminal inverted repeat (TIR) order and the *CACTA* superfamily were present. For the remaining 60% of the mapped barley ESTs, 50% were covered by less than 40 reads in the alignment. These ESTs most likely represent false positives, e.g. owing to the presence of short stretches of repetitive DNA in the EST sequence. The remaining 10% mapped to annotated genes that are sequence-related to genes in rice and/or wheat. Based on various criteria (e.g. expression pattern, gene length, read coverage and function), eight genes were selected as *Ror1* candidates. Five out of the eight candidates (*LTP*, *myosin-2*, *MATH*, *NOC2* and *AK363338*) were "pseudo mapped" in a set of set of *Ror1* recombinant from the mapping population A89 (*ror 1*-2; BCIngrid *mlo*-5) x Malteria Heda (*mlo*-3) generated by Collins et al., (unpublished data) (Figure 3.12) and based on the "mapping" results could be discarded as candidates. The three remaining candidate genes (*Far1*, *SMCN5* and *PRR*) could not be "pseudo mapped" to the *Ror1* recombinants owing to a lack of DNA polymorphisms between the parental lines. However, the three candidates could be positioned in the *Pol*-YAC contig (Figure 3.10). We indirectly discarded *Far1* and *SMCN5* due to its position with respect to *MATH* and *NOC2*, which showed the same allele pattern as *Pol*. The position of *PRR* is still arbitrary with respect to *LTP* and *myosin-2* (which also showed an allele pattern as *Pol*) and it could not be discarded. Finally, it is important to consider that, although unlikely, it is still possible that we have not found the *Ror1* gene since its ESTs are not represented in the current HarvEST collection. However, the overall analysis of candidate genes regarding the genetic constellation of the *Ror1* recombinants showed the allele pattern expected for *Pol* or *Cons*, but not the one expected for *Ror1*, suggesting that the *Ror1* region has not been reached yet.

The sequencing data from clone 87A3 (with a size of 520 kb), and clone 305A11 (unknown size) in the *Cons*-YAC contig revealed the presence of large blocks of transposable elements with evidence for a single gene per YAC clone. In this case, the *Cons* gene (in clone 87A3) and the gene coding for the unknown protein AK363338

(in clone 305A11) were identified. These results are in agreement with previous studies from Rostoks et al., (2002) suggesting that this arrangement of single isolated genes may be a common feature of some regions of the barley genome. It has also been shown that barley genes are sometimes organized as "islands" separated by blocks of TEs (Rostoks et al., 2002). For these "gene islands" (Panstruga et al., 1998) and (Rostoks et al., 2002) reported an average of one gene per 20 kb with a variation in density ranging from 1 gene per 12 kb to 1 gene per 103 kb (Rostoks et al., 2002). For clone 82B11 (900 kb), and for clone 158C12 (500 kb) six and four genes, respectively, were identified; suggesting an average of ca. 1 gene per 130 kb. However, due to a lack of knowledge about the exact organization of genes and repetitive elements in the mentioned YAC clones the proposed average is just speculative. The observed low density of genes in the YACs supports the theory that in gene-poor regions recombination is suppressed as can be expected for the centromeric and subcentromeric chromosomal regions (Künzel et al., 2000).

Our FISH analysis confirmed that with respect to the presence of the suggested genes the proposed YAC contigs around the *Ror*1 locus are correct (Figure 3.13). However, it was not possible to clarify the positioning of the candidate genes (*myosin-2* and *AK363338*) relative to *Pol* and *Cons* (Figure 3.14B and C). Therefore, the orientation of the YAC clones with respect to the *Ror1* locus is still arbitrary (Figure 3.10). In this case, the *Pol*-YAC contig should be extended in both directions. In contrast, the candidate gene *AK363338* was "mapped" telomeric to *Cons* (Figure 3.12B and C), suggesting the *Cons*-YAC contig should be extended in the direction opposite to *AK363338*.

To continue the chromosome walking towards the *Ror1* locus, additional overlapping clones/pools were identified using the Illumina sequencing data. For the left end of clone 87A3 it was not possible to find an overlapping clone using the "bubble oligonucleotide" approach. In addition, in this clone no other predicted gene was found that could be used as a probe for re-screening of the barley YAC library. Thus, a *de novo* (partial) assembly was carried out using the software ABySS (assembly by short sequencing) (Simpson et al., 2009). In this case the paired-end short Illumina reads were assembled in contigs (a contiguous sequence without gaps, generated

from determining the non-redundant path along an order set of component sequences[7]). Contigs with coherent and unambiguous distances were joined to build scaffolds. A scaffold will contain gaps, but there is typically some evidence to support the contig order, orientation and gap size estimates[8]. This approach enabled us to find suitable scaffolds with low similarity to TEs. The selected scaffolds were used to design primers for a YAC library re-screening and to isolate the new overlapping clones 62C1, 67H11 and pools 66, 147, 165 on this side of the *Cons*-YAC contig (Figure 3.10). Even though long repeat regions are a significant barrier to contig growth (Simpson et al., 2009) this approach proved to be a helpful method in chromosome walking when the recovery of end fragments of the YAC inserts did not provide useful information.

To extend the *Pol*-YAC contig in both directions, the *NOC2* gene (in clone 354G1) was used to design new primers for re-screening of the YAC library and the identification of new overlapping pools 41, 288, 118 and 426 (Figure 3.10). In the other direction, clone 415F4 proved to be an inherently instable clone and could not be re-isolated. Analysis of YACs from the human genome demonstrated that instability may correlate with the abundant occurrence of repeat sequences (Neil et al., 1990; Dunford et al., 1993; Michalek et al., 1997). In yeast, copies of the endogenous *Ty* retro-element are common substrates for recombination. Thus, recombination may also occur between copies of plant retro-elements cloned as part of large inserts in YACs (Dunford et al., 1993). Therefore, in a YAC library constructed with a genome that carries more than 80% of repeated sequences, it is not surprising that frequently recombination occurs. Furthermore, deletion or other rearrangements of the insert may occur months after the initial isolation of a clone (Chaplin and Brownstein, 2001b). In general, this type of problem is solved isolating (a) new overlapping clone(s) from the same side. However, multiple re-screenings of the YAC library with primers for some of the genes located in clone 415F4 and 158C12 were unsuccessful. The lack of additional overlapping clones can be in part attributed to the ~10.000 clones missing from the original library (Simons et al., 1997). However, for large parts of the two contigs we

[7] http://www.ncbi.nlm.nih.gov/projects/genome/assembly/grc/info/definitions.shtml
[8] http://www.ncbi.nlm.nih.gov/projects/genome/assembly/grc/info/definitions.shtml

isolated less than the 3-4 clones that should, on average, cover each locus in the genome given that the library represents 4X coverage of the barley genome. There is still the possibility to continue the chromosome walking in this side of the *Pol*-YAC contig: (1) using the EST sequences of *LTP* to design primers and to perform a new barley YAC library re-screening; (2) using the NGS data from clone 158C12 to find scaffolds and to use them to design primers for re-screening of the barley YAC library, as shown for clone 87A3 in section 3.8.11; (3) considering another strategy like chromosome walking with BAC clones.

In sum, the identification of genes flanking *Cons* and *Pol* proved that the combination of YAC library screening and next generation DNA sequencing technology had the theoretical potential to clone *Ror1*, as exemplified by multiple *Cons*- and *Pol*-flanking genes identified by this approach. However, an unexpected large gap size between *Cons* and *Pol* in combination with low coverage of the region, YAC clone chimerism and instability hampered the identification of *Ror1* to date.

4.2 Comparative genomics: syntenic models for the barley YAC contigs at the *Ror1* region

Smaller genomes of grass species like rice, *B. distachyon* and *S. bicolor* are models for molecular genomics and positional cloning in cereals with large genomes (Mayer et al., 2009; Thiel et al., 2009; Mayer et al., 2011). Use of the genome information of the grass species as support for gene cloning is aided by a significant level of synteny among Poaceae genomes (Moore et al., 1995; Murat et al., 2010). Moreover, some high quality reference genome sequences are available (IRGSP, 2005; Paterson et al., 2009; TIBI, 2010) and provide a vehicle for such an approach. Taking advantage of this information we analysed the selected genes in the non-bridged YAC contigs around the *Ror1* region. The vast majority of the genes (six out of nine) defined a syntenic region on chromosome 10L, 3L and 1S in *O. sativa*, *B. distachyon* and *S. bicolor*, respectively (Figure 3.15A). Comparative genomic analysis of the *Ror1* region in barley revealed a syntenic physical unit of 950, 1370 and 1520 kb, which harbour

178, 142 and 138 putative genes in the three grass model genomes of *O. sativa*, *B. distachyon* and *S .bicolor*, respectively (Figure 3.15B). This comparison does not include the insertion of the orthologous gene encoding the LTP protein in rice. In this case *LTP* is located on the short arm of chromosome 10 in rice and is 15 Mb apart from the core syntenic region on the long arm where the section equivalent to the *Ror1* locus is located. Closer inspection of the syntenic regions showed a disruption in collinearity between the four grass species, manifested by small to medium-sized inversions, duplications, gene insertions and deletions. These findings indicated that the re-arrangements in the region is one of the reasons why the synteny-based cloning strategy started by Collins et al., and Benjdia et al., (unpublished data), which proved successful to clone *Ror2* (Collins et al., 2003), was not suitable to isolate *Ror1*. In addition, it is known that only 50% of the barley genes remain collinear compared to rice (Stein, 2007b).

Based on different map-based gene isolation reports in barley three different scenarios can be envisioned for *Ror1* in the interval between *Cons* and *Pol* (Figure 4.1): (1) the *Ror1* gene has an orthologous in rice which is out of synteny. This situation would be similar to the gene *Rar1* located on barley chromosome 2H, which is syntenic with chromosomes 4 and 7 in rice, but its orthologous is present on rice chromosome 2 (Lahaye et al., 1998; Shirasu et al., 1999); (2) there is no *Ror1* orthologous in the other grass species used in this study. An example of this scenario is *Rpg1*, which is located on barley chromosome 7H, but does not have an orthologous in the rice genome (Brueggeman et al., 2002); (3) owing to the scrambled collinearity in the syntenic region, *Ror1* became an insertion between *Cons* and *Pol*, but it is still syntenic with respect to other grasses, e.g its orthologous is present in chromosome 10 or 5 in rice. This situation was reported for the *Vrs1* gene located on barley chromosome 2H. This region is syntenic with rice chromosome 4 and 7. The region around *Vrs1* is collinear with chromosome 4, but the gene is an insertion from chromosome 7 (Pourkheirandish et al., 2007).

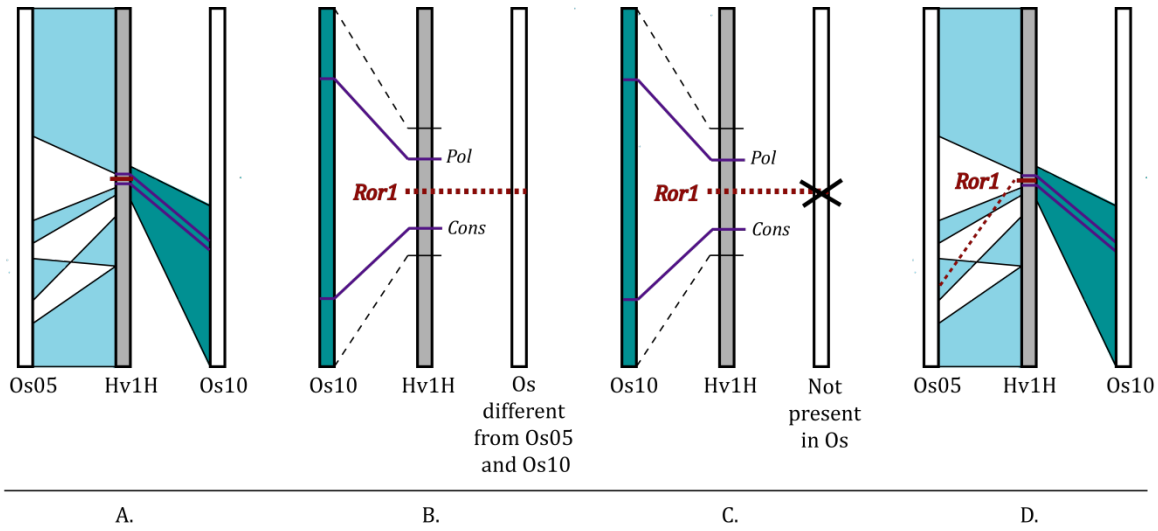

Figure 4.1. Schematic representation of three different scenarios for the ancestry of *Ror1* in the interval between *Cons* and *Pol*. Bars in white: rice chromosomes. Bars in grey: barley chromosome 1H. Regions of synteny are indicated as shadings between rice/barley chromosomes. In red, the location of *Ror1* and in purple the position of *Cons* and *Pol* is represented. Os: *Oryza sativa*; Hv: *Hordeum vulgare*. **(A)** Schematic visualization of synteny between barley and rice, modified from (Stein et al., 2007a). **(B)** Scenario 1: The *Ror1* gene has an orthologous gene in rice, but is out of synteny. In this case, in a chromosome different from Os05 and Os10. **(C)** Scenario 2: there is no *Ror1* orthologous in rice. **(D)** Scenario 3: *Ror1* became and insertion but is still syntenic to chromosome Os05 or Os10

4.2.1 Unlocking the barley genome: The International Barley Genome Sequencing Consortium (IBSC)

Access to a genome sequence is considered pivotal to unravel key questions in crop plant biology and to interrogate the molecular mechanisms that underpin trait formation (Mayer et al., 2011). Initiated in 2006 and with a time line for completion at the end of 2011[9], the IBSC aims at developing a complete DNA sequence of the barley genome and a genetically anchored physical map (Schulte et al., 2009). However, due to its size and complexity, deciphering this genome sequence has proven more challenging than expected (Mayer et al., 2011). A first draft of the putative linear gene order, the so-called "genome zipper", has been compiled by the IBSC for the seven barley pseudo chromosomes. This approach incorporates 454

[9] http://mips.helmholtz-muenchen.de/plant/triticeae/barley

pyrosequencing data of flow-sorted chromosomes, barley ESTs and full length-cDNAs, DNA hybridization microarray data, barley gene-based markers (Close et al., 2009) and systematic exploitation of conserved synteny with model grasses (*O. sativa, B. distachyon and S. bicolor*) (Mayer et al., 2009; Mayer et al., 2011). By this procedure, 86% of the estimated 32.000 barley genes were tentatively positioned along each of the individual barley chromosomes (Mayer et al., 2011). Furthermore, for barley chromosome 1H, the entire chromosome could be sorted, without clear positioning of the centromere. The genetic centromere of barley chromosomes is characterized by large clusters of genes/markers whose order cannot be genetically resolved due to insufficient recombination in relatively small mapping populations. These regions around the centromere may extend in barley over as much as half of a chromosome (Mayer et al., 2011). Unfortunately, this places severe constraints on positional gene cloning for as many as one-third of the barley genes. Although, the "genome zippers" provide a rich source of information for candidate gene identification, in the context of this thesis it has not aided in finding the *Ror1* gene. The *Ror1* gene is positioned in a subcentromeric region of the long arm of chromosome 1H where the recombination rate is suppressed and where the collinearity with the model grass species is disturbed. Personal communication with Dr. Nils Stein (Leibniz Institute of Plant Genetics and Crop Plant Research, IPK, Germany) confirmed the difficulties in assembling contigs around the centromere of all barley chromosomes. In addition, owing to the unfavourable situation in these regions, at this moment, there are no barley BAC contigs available containing the marker genes *Cons* and *Pol*.

4.3 Co-expressed gene network in monocot (*Arabidopsis*) and dicot (barley) plants and its application to discover the *Ror1* gene

Comprehensive and high-throughput analysis of gene expression has become a significant approach for screening candidate genes, predicting gene function, identifying genes that are functionally related to query genes and characterizing transcriptional regulatory networks (Obayashi and Kinoshita, 2010; Mochida et al., 2011). Web-based tools such as CressExpress (Srinivasasainagendra et al., 2008) and ATTED-II (Obayashi et al., 2009) have been employed for various approaches in the

discovery of genes and their function (Okazaki et al., 2009; Humphry et al., 2010). For example, the ATTED-II database was used to identify novel genes involved in lipid metabolism in *Arabidopsis*. This approach resulted in the identification of a novel gene, *UDP-glucose pyrophosphorylase 3* (*UGP3*), required for sulfolipid biosynthesis (Okazaki et al., 2009). Co-expression analysis with the CressExpress database was used to identify components that modulate plant resistance against the fungal powdery mildew disease in barley and *Arabidopsis* (Humphry et al., 2010). Based on this study, in this thesis, we followed a secondary approach to identify *Ror1* candidate genes in barley that are co-expressed with the encoding genes of Mlo, Ror2 and SNAP34 proteins. Two out of six candidates could be discarded as the *Ror1* gene, based on "pseudo mapping" in a population of *Ror1* recombinants (Figure 3.16). However, due to a lack of polymorphisms between the parental lines of the recombinant population, the remaining four candidate genes could not be discarded. Nevertheless, they can be further studied using the available barley FlcDNA data to design new primers for the discovery of polymorphisms between the parental lines. Taking into account that the selection of candidates was based on the synteny between the barley chromosome 1H and the rice chromosomes 5 and 10, this approach is a suitable strategy to discover the *Ror1* gene. However, if the scenario for *Ror1* is as described in section 4.2, in which the gene is out of synteny or does not have and orthologous in rice, this approach will not provide further information.

4.4 The question remains open: what could possibly be the role of the *Ror1* gene?

Mutagenesis of the powdery mildew resistant BCIngrid *mlo*-5 mutant resulted in the identification of two partially susceptible suppressor mutants. The respective genes were designated *Ror1* and *Ror2* (Freialdenhoven et al., 1996). In the presence of wild-type *Mlo,* mutations in either *ror1* or *ror2* confer supersusceptibility to *Bgh*, suggesting that both *Ror* genes are positive regulators of basal defence towards *Bgh* (Collins et al., 2003). *Ror1*, but not *Ror2*, also limits the entry of *M. grisea* into barley epidermal cells, which is most evident in *Mlo* genotypes. In the presence of this

pathogen, the *ror1* (A89) mutation causes an increase in lesion number and a reduced formation of effective papillae (Jarosch et al., 2005). This finding indicates that *Ror1* has a broader impact on plant immunity than *Ror2*. Furthermore, the *ror1 ror2* double mutant (in *mlo*-5) permits higher penetration levels of *Bgh* than either the single mutant (Collins et al., 2003), suggesting *Ror1* and *Ror2* control two parallel resistance pathways.

Since the genes are cloned and the biochemical activity of the gene products is known, the role of *Ror2* and its *Arabidopsis* orthologous *PEN1* in penetration resistance is well known. About the role of *Ror1* in defence signalling/execution we can only hypothesize, but based on the available phenotypic data we might make guesses about the potential role of *Ror1* in penetration resistance.

Penetration of the cell wall is an early step in the infection of plants by some fungi or oomycetes. In response to attempted pathogen ingress, the plant cytosol is rearranged and the endoplasmic reticulum (ER), Golgi bodies and peroxisomes accumulate around the penetration site (Takemoto et al., 2003). This process coincides with the formation of the CWA, also called papilla. The papilla forms regardless of the final outcome of the interaction. CWAs have a heterogeneous appearance and typically contain cellulose, lignin, pectin, lipids, phytoalexins, phenolics, silicon, callose (β-1,3 glucan), H_2O_2 and proteins including peroxidases and enzyme inhibitors. These changes in cytoplasmic dynamics correlate with major reorganization of the cytoskeleton (Schmelzer, 2002; Zeyen et al., 2002; An et al., 2006; Hardham et al., 2007). Hydrogen peroxide (H_2O_2) is a versatile molecule that participates in normal plant physiological processes and in resistance mechanisms, such as the reinforcement of plant cell walls (e.g. lignification) or phytoalexin production. H_2O_2 can be produced at the apoplast as well as in mitochondria, chloroplasts and peroxisomes (Quan et al., 2008). In barley, it has been shown that H_2O_2 accumulation is influenced by the function of *Ror1* and *Ror2* genes. After infection with *Bgh*, the BCIngrid *mlo*-5 *ror1* mutant exhibited higher rates of HR and whole cell H_2O_2 accumulation in comparison with the visible cytoplasmic aggregates of H_2O_2 beneath the appressorium in BCIngrid *mlo*-5 *Ror1* (Hückelhoven et al., 2000). Whole cell accumulation of H_2O_2 instead of localized H_2O_2 generation as in wild-type

plants, would suggest the *ror1* mutant is impaired in cellular targeting of enzymes and organelles, like peroxisomes, controlling localized H_2O_2 accumulation. At the same time, signalling cascades controlling the formation of H_2O_2 apparently are left intact. This would suggest Ror1 might control movement of components along the cytoskeleton (Figure 4.2).

The plant cytoskeleton is an intracellular scaffold composed of microtubules and actin microfilaments and plays a major role in many plant responses including stomatal closure, responses to hormones, pathogens or abiotic environmental stimuli, as well as in cell growth and development. Moreover, it is an important factor in the transport of vesicles and organelles mediated by motor proteins and cytoplasmic streaming (Takemoto and Hardham, 2004; Hardham et al., 2007; Day et al., 2011; Mucha et al., 2011). Thus, it is not surprising that plants also employ the cytoskeleton network as a platform for defence signalling and pathogens may have found equally clever ways to hijack or usurp this platform for their own purpose. The actin cytoskeleton has not been documented as a direct virulence target of plant-pathogenic fungi and oomycetes. However, it has been reported that the actin-depolymerizing factor 4 (*ADF4*) mediates defence signal transduction in *A. thaliana,* which is triggered by the *Pseudomonas syringae* effector AvrPphB, but does not affect pathogen entry (Tian et al., 2009). In humans instead, the modulation of the cytoskeleton by bacterial effectors has been well characterized, for example in the pathogenic genus *Yersinia* (Aepfelbacher and Heesemann, 2001). In plants, microtubules and actin microfilaments become radially arranged in the cortical cytoplasm underneath the attempted entry site of a host or nonhost powdery mildew sporelings (Kobayashi et al., 1992; Kobayashi et al., 1997a; Kobayashi et al., 1997b). Actin filaments are believed to control the trafficking of secretory vesicles that deliver new wall materials during diffuse growth, similar to the well-established principles of tip growth in pollen tube (Day et al., 2011). Pharmacological studies with actin and tubulin inhibitors have revealed that the cytoskeleton is involved in polarization of defence-related reactions at fungal penetration sites (cytoplasmic aggregation, papillae formation and accumulation of autofluorescent compounds) (Kobayashi et al., 1997b).

Using an actin polymerization inhibitor (cytochalasin E) and the ectopic expression of actin-depolymerizing factor 3 (*ADF3*) in barley leaf epidermis cells, prior to infection with *Bgh*, Miklis and associates (2007) observed enhanced fungal entry (supersusceptibility) in the *Mlo* genotype and a partial break down of *mlo* resistance. These data demonstrated that barley requires an intact actin cytoskeleton for basal defence to *Bgh* and for *mlo*-mediated resistance. By contrast, pharmacological disruption of microtubules with oryzalin and propyzamide did not affect *mlo*-mediated resistance. Pharmacological interference with cytochalasin E and ectopic expression of *ADF3* also demonstrated that host actin cytoskeleton compromises nonhost resistance but does not affect race-specific immune responses to *Bgh* (Miklis et al., 2007).

These observations are reminiscent of those observed in *ror1* mutants and it is therefore tempting to speculate that Ror1 might be involved in an actin-mediated penetration resistance pathway. Interference of the actin microfilaments or microtubules with pharmacological inhibitors in the *ror1* and *ror2* mutants has not been analysed so far. Nevertheless, in barley, actin depolymerisation by expression of *ADF3* was shown to not inhibit the focal accumulation of GFP-Ror2 at attempted *Bgh* penetration sites (Bhat et al., 2005). Similarly, in *Arabidopsis* GFP-PEN1 accumulation at penetration sites is not affected by treatment with cytochalasin E (Underwood and Somerville, 2008). Furthermore, the *pen1-1* mutation does not interfere with cytoplasmic aggregation, recruitment of actin filaments and the ER to the penetration site (Takemoto et al., 2006). These data suggested that Ror2/PEN1 and Mlo/MLO are governed to penetration sites through actin-independent mechanisms, most likely involving lipid raft-like plasma membrane microdomains. However, this assumption conflicts with the hypothesis of exosome biogenesis proposed by (Meyer et al., 2009) and (Böhlenius et al., 2010) in which the plasma membrane-resident binary SNARE complex comprising PEN1 and SNAP33 is internalized by endocytosis, fused to sorting endosomes to generate an intraluminal vesicle (ILV) within a multivesicular body (MVB), which later is fused to the plasma membrane to release the ILVs in the paramural space as exosomes. Indirectly, this mechanism would imply actin-dependent movement, while endosome and MVB movement require an intact cytoskeleton. In addition, the mechanism transporting VAMP721 or VAMP722

towards the penetration site to form ternary SNARE complexes with Ror2/PEN1 and SNAP34/SNAP33 is still unknown.

By contrast, in *Arabidopsis* a parallel actin-dependent defence pathway involves the atypical myrosinase PEN2 and the ABC transporter PEN3. Fluorescent labelling of the proteins revealed an association of the PEN2 protein with the periphery of peroxisomes, which are subject to pathogen-induced cellular polarization (Lipka et al., 2005). Furthermore, contrary to animals, intracellular transport of plant peroxisomes was shown to occur along actin filaments and not microtubules (Mathur et al., 2002). After pharmacological interference with actin dynamics the peroxisomes aggregated and cessated their motility (Mathur et al., 2002) and the PEN3-GFP focal accumulation at sites of penetration was disrupted (Underwood and Somerville, 2008). The myrosinase activity of PEN2 and its localization to peroxisomes suggests a localized synthesis and concentration of glucosinolate-derived secondary antimicrobial metabolites to be discharged at fungal entry sites by PEN-3 (Hardham et al., 2007; Bednarek et al., 2009).

The first thought would be to consider barley *Ror1* as a homolog/orthologous of *Arabidopsis PEN2* or *PEN3*. However, phylogenetic analysis suggests that the *PEN2* and *PEN3* genes represent an evolutionarily recent acquisition of *Arabidopsis* (Xu et al., 2004; Consonni et al., 2006). Nevertheless, it is likely that there exists an actin-dependent mechanism that is conserved between monocots and dicots by which secondary metabolites with antimicrobial activity (phytoalexins) or other defence compounds and the enzymes required for their biosynthesis are mobilized to the infection site. This might involve peroxisomes or likely a secretory pathway independent of the action of Ror2. Thus, it is also possible to envisage Ror1 as a biosynthetic enzyme involved in the synthesis of phytoalexins/secondary metabolites or as a transporter in the plasma membrane to facilitate the delivery of anti-fungal compounds to the site of attempted pathogen ingress (Figure 4.2).

As an example of secondary antifungal metabolites in barley we find the hordatines, derivatives of coumarylagmatine (Stoessl, 1967; Smith and Best, 1978). A soluble phenolic coumarylagmatine conjugate, *p*-coumaroyl-hydroxyagmatine (*p*-CHA) has

been identified (von Röpenack et al., 1998). In this study, the metabolite accumulated differentially in a *mlo*-mediated resistance response in comparison to the susceptible *Mlo* genotype and showed a delayed and reduced accumulation in the *ror2* (A44) mutant. However, in this study, in the *ror1* mutant there were no changes in the levels of the phenolic compounds. The latter findings support the hypothesis of the deployment of an actin-dependent mechanism by which antimicrobial compounds are synthesized and mobilized to the infection site.

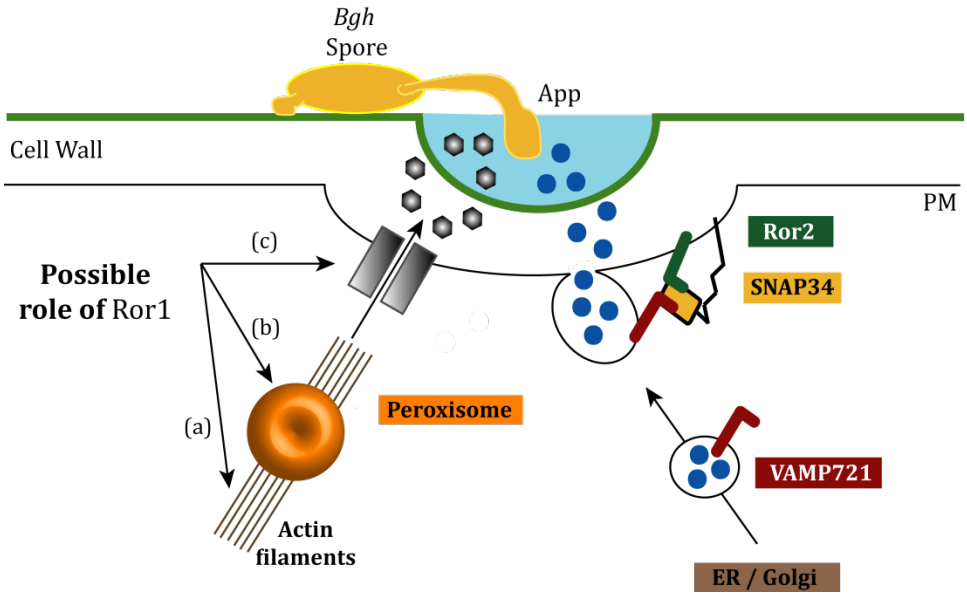

Figure 4.2. A hypothetical model for the role of Ror1 in basal defence towards the powdery mildew pathogen, *Bgh*. PM: Plasma membrane. App: Appressorium. Right side: The Ror2 defence pathway. The syntaxin Ror2 (green) forms a binary t-SNARE complex with the SNAP34 protein (yellow), which interacts with the VAMP721 protein (red). The vesicles are thought to be loaded with anti-fungal compounds and cell wall components (blue) derived from the ER/Golgi (brown). The protein complex facilitates the secretion of the cargo (blue circles) at the site of pathogen ingress. Left side: The possible role of Ror1. It is tempting to speculate that Ror1 might be involved in an actin-mediated penetration resistance pathway in which antimicrobial compounds (black hexagons) are synthesized and mobilized to the infection site. Ror1 could: **(a)** control the movement of anti-fungal components along the cytoskeleton; **(b)** be a biosynthetic enzyme involved in the synthesis of phytoalexins/secondary metabolites, likely by peroxisomes or a secretory pathway independent of the action of Ror2; or **(c)** act as a transporter at the plasma membrane to deliver anti-fungal compounds (black hexagons).

5. Concluding remarks and perspectives

We have shown in this thesis the usage of chromosome walking in a barley YAC library combined with second generation sequencing (Illumina®) as an approach to find the *Ror1* gene. We have obtained two non-overlapping YAC contigs around the *Ror1* locus (Figure 3.10). Comparative genomics with model grasses revealed a substantial disruption in gene collinearity in this region (Figure 3.15B). Furthermore, "pseudo mapping" in a *Ror1* recombinant population (Figure 3.12) and positioning in the YAC contigs (Figure 3.10) excluded seven of the eight selected candidates to encode *Ror1*. FISH experiments suggested that the gap between the predicted closest *Ror1* markers is greater than 1Mb (Figure 3.14A). In addition, for the first time we could physically locate the *Ror1* region in a subcentromeric, recombination-suppressed area on the long arm of chromosome 1H (Figure 3.13). Future chromosome walking is required to complete the *Ror1* YAC contig. Therefore, we have isolated new overlapping clones/pools for further sequencing and analysis. In the *Cons*-YAC contig we have isolated clones 62C1, 67H11 and pools 66, 147, 165 (Figure 3.10). However, in the *Pol*-YAC contig the orientation is still arbitrary and the walking should follow both directions. For one side (direction of *NOC2*, Figure 3.10) the walking can continue with the YAC library using the pools 41, 288, 118 and 426. For the other side (direction *myosin-2*, Figure 3.10) we have shown that clone 415F4 is instable and so far we have not found another overlapping YAC to replace it. Thus, to continue in that direction, it would be necessary to re-screen the library using the ESTs for *LTP* or scaffolds from clone 158C12 to design primers or to consider another strategy like chromosome walking with BAC clones. Our approach combining classical genetics and next generation sequencing technologies has opened a door that possibly can lead us to finally isolate our enigmatic gene of interest, *Ror1*.

In the future, to facilitate the cloning of the *Ror1* gene, two different approaches could be considered using the *ror1* mutants, the mutant BCIngrid *mlo*-5 and the wild type Ingrid: (1) transcriptome analysis (RNA-seq); and (2) deep sequencing. In brief we

describe here these possibilities. For the transcriptome approach we propose a RNA analysis of the barley mutants and cultivar mentioned above, after infection with the powdery mildew fungi (*Bgh*), through cDNA next-generation sequencing (RNA-seq). In this case, in the absence of the barley reference genome, different methods for *de novo* assembly could be used (Robertson et al., 2010; Grabherr et al., 2011). Furthermore, the available barley FlcDNA and EST resources[10],[11] (Matsumoto et al., 2011) provide a useful platform for the analysis of data and the selection of candidate genes. Considering the alignment of the transcriptome sequences to the genome of a related species like rice or *B. distachyon* is a second strategy for identifying candidate genes (Morozova et al., 2009). The last approach refers to the high coverage sequencing of genomes of the barley mutants and cultivar mentioned above. For the success of this approach, a collaborative effort with the IBSC is necessary to make use of the last information regarding contigs and sequencing data from chromosome 1H in barley (Dr. Nils Stein, personal communication).

[10] http://pgrc.ipk-gatersleben.de/cr-est
[11] http://harvest.ucr.edu

6. References

Adam L, Somerville SC (1996) Genetic characterization of five powdery mildew disease resistance loci in Arabidopsis thaliana. The Plant Journal **9:** 341-356

Aepfelbacher M, Heesemann J (2001) Modulation of Rho GTPases and the actin cytoskeleton by Yersinia outer proteins (Yops). International Journal of Medical Microbiology **291:** 269-276

Agrios GN, ed (2005) Plant Pathology, Ed Fifth. Elsevier Academic Press, Burlington

Altschul S, Gish W, Miller W, Myers E, Lipman D (1990) Basic local alignment search tool. J Mol Biol **215:** 403 - 410

An Q, Hückelhoven R, Kogel K-H, Van Bel AJE (2006) Multivesicular bodies participate in a cell wall-associated defence response in barley leaves attacked by the pathogenic powdery mildew fungus. Cellular Microbiology **8:** 1009-1019

Aslam SN, Erbs G, Morrissey KL, Newman M-A, Chinchilla D, Boller T, Molinaro A, Jackson RW, Cooper RM (2009) Microbe-associated molecular pattern (MAMP) signatures, synergy, size and charge: influences on perception or mobility and host defence responses. Molecular Plant Pathology **10:** 375-387

Bai Y, Pavan S, Zheng Z, Zappel NF, Reinstädler A, Lotti C, De Giovanni C, Ricciardi L, Lindhout P, Visser R, Theres K, Panstruga R (2008) Naturally Occurring Broad-Spectrum Powdery Mildew Resistance in a Central American Tomato Accession Is Caused by Loss of Mlo Function. Molecular Plant-Microbe Interactions **21:** 30-39

Banfi S, Zoghbi HY (1996) Detection of Chimerism in YAC Clones. *In* D Marki, ed, YAC Protocols, Vol 54. Humana Press, pp 115-121

Bednarek P, Piślewska-Bednarek M, Svatoš A, Schneider B, Doubský J, Mansurova M, Humphry M, Consonni C, Panstruga R, Sanchez-Vallet A, Molina A, Schulze-Lefert P (2009) A Glucosinolate Metabolism Pathway in Living Plant Cells Mediates Broad-Spectrum Antifungal Defense. Science **323:** 101-106

Bhat RA, Miklis M, Schmelzer E, Schulze-Lefert P, Panstruga R (2005) Recruitment and interaction dynamics of plant penetration resistance components in a plasma membrane microdomain. Proceedings of the National Academy of Sciences of the United States of America **102:** 3135-3140

Bittel P, Robatzek S (2007) Microbe-associated molecular patterns (MAMPs) probe plant immunity. Current Opinion in Plant Biology **10:** 335-341

Bockus WW, Bowden RL, Hunger RM, Morrill WL, Murray TD, Smiley RW, eds (2010) Compendium of Wheat Diseases and Pests, Ed Third. APS Press

Böhlenius H, Mørch SM, Godfrey D, Nielsen ME, Thordal-Christensen H (2010) The Multivesicular Body-Localized GTPase ARFA1b/1c Is Important for Callose Deposition and ROR2 Syntaxin-Dependent Preinvasive Basal Defense in Barley. The Plant Cell Online **22:** 3831-3844

Brueggeman R, Rostoks N, Kudrna D, Kilian A, Han F, Chen J, Druka A, Steffenson B, Kleinhofs A (2002) The barley stem rust-resistance gene Rpg1 is a novel disease-resistance gene with homology to receptor kinases. Proceedings of the National Academy of Sciences **99:** 9328-9333

Burke D, Carle G, Olson M (1987) Cloning of large segments of exogenous DNA into yeast by means of artificial chromosome vectors. Science **236:** 806-812

Büschges R, Hollricher K, Panstruga R, Simons G, Wolter M, Frijters A, van Daelen R, van der Lee T, Diergaarde P, Groenendijk J, Töpsch S, Vos P, Salamini F, Schulze-

Lefert P (1997) The Barley Mlo Gene: A Novel Control Element of Plant Pathogen Resistance. Cell **88:** 695-705

Chaplin DD, Brownstein BH (2001a) Analysis of Isolated YAC Clones. *In* Current Protocols in Molecular Biology. John Wiley & Sons, Inc.

Chaplin DD, Brownstein BH (2001b) Overview of Strategies for Screening YAC Libraries and Analyzing YAC Clones. *In* Current Protocols in Molecular Biology. John Wiley & Sons, Inc.

Cheng H, Kun W, Liu D, Su Y, He Q (2011) Molecular cloning and expression analysis of *CmMlo1* in melon. Molecular Biology Reports**:** 1-5

Chinault AC, Sternberg NL (2001) Screening Large-Insert Libraries by PCR. *In* Current Protocols in Human Genetics. John Wiley & Sons, Inc.

Close T, Bhat P, Lonardi S, Wu Y, Rostoks N, Ramsay L, Druka A, Stein N, Svensson J, Wanamaker S, Bozdag S, Roose M, Moscou M, Chao S, Varshney R, Szucs P, Sato K, Hayes P, Matthews D, Kleinhofs A, Muehlbauer G, DeYoung J, Marshall D, Madishetty K, Fenton R, Condamine P, Graner A, Waugh R (2009) Development and implementation of high-throughput SNP genotyping in barley. BMC Genomics **10:** 582

Collins NC, Lahaye T, Peterhänsel C, Freialdenhoven A, Corbitt M, Schulze-Lefert P (2001) Sequence Haplotypes Revealed by Sequence-Tagged Site Fine Mapping of the Ror1 Gene in the Centromeric Region of Barley Chromosome 1H. Plant Physiology **125:** 1236-1247

Collins NC, Thordal-Christensen H, Lipka V, Bau S, Kombrink E, Qiu J-L, Hückelhoven R, Stein M, Freialdenhoven A, Somerville SC, Schulze-Lefert P (2003) SNARE-protein-mediated disease resistance at the plant cell wall. Nature **425:** 973-977

Consonni C, Humphry ME, Hartmann HA, Livaja M, Durner J, Westphal L, Vogel J, Lipka V, Kemmerling B, Schulze-Lefert P, Somerville SC, Panstruga R (2006) Conserved requirement for a plant host cell protein in powdery mildew pathogenesis. Nat Genet **38:** 716-720

Dangl JL, Jones JDG (2001) Plant pathogens and integrated defence responses to infection. Nature **411:** 826-833

Day B, Henty JL, Porter KJ, Staiger CJ (2011) The Pathogen-Actin Connection: A Platform for Defense Signaling in Plants. Annual Review of Phytopathology **49:** 483-506

Devoto A, Hartmann HA, Piffanelli P, Elliott C, Simmons C, Taramino G, Goh C-S, Cohen FE, Emerson BC, Schulze-Lefert P, Panstruga R (2003) Molecular Phylogeny and Evolution of the Plant-Specific Seven-Transmembrane MLO Family. Journal of Molecular Evolution **56:** 77-88

Devoto A, Piffanelli P, Nilsson I, Wallin E, Panstruga R, von Heijne G, Schulze-Lefert P (1999) Topology, subcellular localization, and sequence diversity of the Mlo family in plants. J Biol Chem **274:** 34993 - 35004

Dodds PN, Rathjen JP (2010) Plant immunity: towards an integrated view of plant-pathogen interactions. Nat Rev Genet **11:** 539-548

Dunford R, Vilageliu L, Graham M (1993) Stabilisation of a yeast artificial chromosome containing plant DNA using a recombination-deficient host. Plant Molecular Biology **21:** 1187-1189

Eichmann R, Hückelhoven R (2008) Accommodation of powdery mildew fungi in intact plant cells. Journal of Plant Physiology **165:** 5-18

Elliott C, Müller J, Miklis M, Bhat RA, Schulze-Lefert P, Panstruga R (2005) Conserved extracellular cysteine residues and cytoplasmic loop-loop interplay are required for functionality of the heptahelical MLO protein. Biochem. J. **385:** 243-254

Favret EA (1965) Induced mutations in breeding for disease resistance. *In* FaAOotU Nations, ed, The use of Induced Mutations in Plant Breeding. Pergamon Press, London, p 832

Feechan A, Jermakow AM, Torregrosa L, Panstruga R, Dry IB (2008) Identification of grapevine MLO gene candidates involved in susceptibility to powdery mildew. Functional Plant Biology **35:** 1255-1266

Foote S, Denny C (2001) Construction of YAC Libraries with Large Inserts. *In* Current Protocols in Human Genetics. John Wiley & Sons, Inc.

Freialdenhoven A, Peterhansel C, Kurth J, Kreuzaler F, Schulze-Lefert P (1996) Identification of Genes Required for the Function of Non-Race-Specific mlo Resistance to Powdery Mildew in Barley. Plant Cell **8:** 5-14

Gadoury DM, Cadle-Davidson L, Wilcox WF, Dry IB, Seem RC, Milgroom MG (2011) Grapevine powdery mildew (Erysiphe necator): a fascinating system for the study of the biology, ecology and epidemiology of an obligate biotroph. Molecular Plant Pathology**:** no-no

Gibson SI, Somerville C (1992) Chromosome walking in Arabidopsis thaliana using Yeast Artificial Chromosomes. *In* C Koncz, N-H Chua, J Schell, eds, Methods in Arabidopsis research. World Scientific Co. Pte. Ltd, Singapore, p 482

Glawe DA (2008) The Powdery Mildews: A Review of the World's Most Familiar (Yet Poorly Known) Plant Pathogens. Annual Review of Phytopathology **46:** 27-51

Görg R, Hollricher K, Schulze-Lefert P (1993) Functional analysis and RFLP-mediated mapping of the Mlg resistance locus in barley. The Plant Journal **3:** 857-866

Grabherr MG, Haas BJ, Yassour M, Levin JZ, Thompson DA, Amit I, Adiconis X, Fan L, Raychowdhury R, Zeng Q, Chen Z, Mauceli E, Hacohen N, Gnirke A, Rhind N, di Palma F, Birren BW, Nusbaum C, Lindblad-Toh K, Friedman N, Regev A (2011) Full-length transcriptome assembly from RNA-Seq data without a reference genome. Nat Biotech **29:** 644-652

Green ED, Riethman HC, Dutchik JE, Olson MV (1991) Detection and characterization of chimeric yeast artificial-chromosome clones. Genomics **11:** 658-669

Hall TA (1999) BioEdit: a user-friendly biological sequence alignment editor and analysis program for Windows 95/98/NT. Nucleic Acids Symposium Series **41:** 95-98

Hardham AR, Jones DA, Takemoto D (2007) Cytoskeleton and cell wall function in penetration resistance. Current Opinion in Plant Biology **10:** 342-348

Horst RK, Cloyd R, eds (2007) Compendium of Rose Diseases and Pests, Ed Second. APS Press

Hückelhoven R, Trujillo M, Kogel K-H (2000) Mutations in Ror1 and Ror2 genes cause modification of hydrogen peroxide accumulation in mlo-barley under attack from the powdery mildew fungus. Molecular Plant Pathology **1:** 287-292

Humphry M, Bednarek P, Kemmerling B, Koh S, Stein M, Göbel U, Stüber K, Piślewska-Bednarek M, Loraine A, Schulze-Lefert P, Somerville S, Panstruga R (2010) A regulon conserved in monocot and dicot plants defines a functional module in antifungal plant immunity. Proceedings of the National Academy of Sciences **107:** 21896-21901

Humphry M, ReinstÄDler A, Ivanov S, Bisseling TON, Panstruga R (2011) Durable broad-spectrum powdery mildew resistance in pea er1 plants is conferred by natural loss-of-function mutations in PsMLO1. Molecular Plant Pathology **12:** 866-878

IRGSP (2005) The map-based sequence of the rice genome. Nature **436:** 793 - 800

Jarosch B, Collins NC, Zellerhoff N, Schaffrath U (2005) RAR1, ROR1, and the Actin Cytoskeleton Contribute to Basal Resistance to Magnaporthe grisea in Barley. Molecular Plant-Microbe Interactions **18:** 397-404

Jarosch B, Kogel K-H, Schaffrath U (1999) The Ambivalence of the Barley Mlo Locus: Mutations Conferring Resistance Against Powdery Mildew (Blumeria graminis f. sp. hordei) Enhance Susceptibility to the Rice Blast Fungus Magnaporthe grisea. Molecular Plant-Microbe Interactions **12:** 508-514

Jones H, Whipps JM, Gurr SJ (2001) The tomato powdery mildew fungus Oidium neolycopersici. Molecular Plant Pathology **2:** 303-309

Jones JDG, Dangl JL (2006) The plant immune system. Nature **444:** 323-329

Jørgensen IH (1992b) Discovery, characterization and exploitation of Mlo powdery mildew resistance in barley. Euphytica **63:** 141-152

Jørgensen J (1994) Genetics of powdery mildew resistance in barley. Critical Reviews in Plant Sciences **13:** 97-119

Jørgensen JH (1992a) Sources and Genetics of Resistance to Fungal Pathogens. *In* PR Shewry, ed, Barley: Genetics, Biochemestry, Molecular Biology and Biotechnology, Vol Biotechnology in Agriculture CAB International

Kalendar R, Lee D, Schulman A (2009) FastPCR Software for PCR Primer and Probe Design and Repeat Search. Genes, Genomes and Genomics **3:** 1-14

Kato A (2011) High-density fluorescence in situ hybridization signal detection on barley (Hordeum vulgare L.) chromosomes with improved probe screening and reprobing procedures. Genome **54:** 151-159

Keller B, Feuillet C (2000) Colinearity and gene density in grass genomes. Trends in Plant Science **5:** 246-251

Kim MC, Panstruga R, Elliott C, Muller J, Devoto A, Yoon HW, Park HC, Cho MJ, Schulze-Lefert P (2002) Calmodulin interacts with MLO protein to regulate defence against mildew in barley. Nature **416:** 447-451

Kobayashi I, Kobayashi Y, Yamaoka N, Kunoh H (1992) Recognition of a pathogen and a nonpathogen by barley coleoptile cells. III. Responses of microtubules and actin filaments in barley coleoptile cells to penetration attempts. Canadian Journal of Botany **70:** 1815-1823

Kobayashi Y, Kobayashi I, Funaki Y, Fujimoto S, Takemoto T, Kunoh H (1997b) Dynamic reorganization of microfilaments and microtubules is necessary for the expression of non-host resistance in barley coleoptile cells. The Plant Journal **11:** 525-537

Kobayashi Y, Yamada M, Kobayashi I, Kunoh H (1997a) Actin Microfilaments are Required for the Expression of Nonhost Resistance in Higher Plants. Plant and Cell Physiology **38:** 725-733

Konishi S, Sasakuma T, Sasanuma T (2010) Identification of novel Mlo family members in wheat and their genetic characterization. Genes & Genetic Systems **85:** 167-175

Kraft JM, Pfleger FL, eds (2001) Compendium of Pead Diseases and Pests, Ed Second. APS Press

Kumar J, Hückelhoven R, Beckhove U, Nagarajan S, Kogel K-H (2001) A Compromised Mlo Pathway Affects the Response of Barley to the Necrotrophic Fungus Bipolaris sorokiniana (Teleomorph: Cochliobolus sativus) and Its Toxins. Phytopathology **91:** 127-133

Künzel G, Korzun L, Meister A (2000) Cytologically Integrated Physical Restriction Fragment Length Polymorphism Maps for the Barley Genome Based on Translocation Breakpoints. Genetics **154:** 397-412

Kwaaitaal M, Keinath NF, Pajonk S, Biskup C, Panstruga R (2010) Combined Bimolecular Fluorescence Complementation and Förster Resonance Energy Transfer Reveals Ternary SNARE Complex Formation in Living Plant Cells. Plant Physiology **152:** 1135-1147

Kwon C, Neu C, Pajonk S, Yun HS, Lipka U, Humphry M, Bau S, Straus M, Kwaaitaal M, Rampelt H, Kasmi FE, Jurgens G, Parker J, Panstruga R, Lipka V, Schulze-Lefert P (2008) Co-option of a default secretory pathway for plant immune responses. Nature **451:** 835-840

Lahaye T, Hartmann S, Töpsch S, Freialdenhoven A, Yano M, Schulze-Lefert P (1998) High-resolution genetic and physical mapping of the Rar1 locus in barley. TAG Theoretical and Applied Genetics **97:** 526-534

Langmead B, Trapnell C, Pop M, Salzberg S (2009) Ultrafast and memory-efficient alignment of short DNA sequences to the human genome. Genome Biology **10:** R25

Larin Z, Monaco AP, Lehrach H (1996) Generation of Large Insert YAC Libraries. *In* D Marki, ed, YAC Protocols, Vol 54. Humana Press, pp 1-11

Lipka U, Fuchs R, Kuhns C, Petutschnig E, Lipka V (2010) Live and let die - Arabidopsis nonhost resistance to powdery mildews. European Journal of Cell Biology **89:** 194-199

Lipka V, Dittgen J, Bednarek P, Bhat R, Wiermer M, Stein M, Landtag J, Brandt W, Rosahl S, Scheel D, Llorente F, Molina A, Parker J, Somerville S, Schulze-Lefert P (2005) Pre- and Postinvasion Defenses Both Contribute to Nonhost Resistance in Arabidopsis. Science **310:** 1180-1183

Liu Q, Zhu H (2008) Molecular evolution of the MLO gene family in Oryza sativa and their functional divergence. Gene **409:** 1-10

Ma L, Vu G, Schubert V, Watanabe K, Stein N, Houben A, Schubert I (2010) Synteny between Brachypodium distachyon and Hordeum vulgare as revealed by FISH. Chromosome Research **18:** 841-850

Mathre DE, ed (1997) Compendium of Barley Diseases, Ed Second. APS Press

Mathur J, Mathur N, Hülskamp M (2002) Simultaneous Visualization of Peroxisomes and Cytoskeletal Elements Reveals Actin and Not Microtubule-Based Peroxisome Motility in Plants. Plant Physiology **128:** 1031-1045

Matsumoto T, Tanaka T, Sakai H, Amano N, Kanamori H, Kurita K, Kikuta A, Kamiya K, Yamamoto M, Ikawa H, Fujii N, Hori K, Itoh T, Sato K (2011) Comprehensive Sequence Analysis of 24,783 Barley Full-Length cDNAs Derived from 12 Clone Libraries. Plant Physiology **156:** 20-28

Mayer KFX, Martis M, Hedley PE, Simková H, Liu H, Morris JA, Steuernagel B, Taudien S, Roessner S, Gundlach H, Kubaláková M, Suchánková P, Murat F, Felder M, Nussbaumer T, Graner A, Salse J, Endo T, Sakai H, Tanaka T, Itoh T, Sato K, Platzer M, Matsumoto T, Scholz U, Dolezel J, Waugh R, Stein N (2011) Unlocking the Barley Genome by Chromosomal and Comparative Genomics. Plant Cell **23:** 1249-1263

Mayer KFX, Taudien S, Martis M, Simková H, Suchánková P, Gundlach H, Wicker T, Petzold A, Felder M, Steuernagel B, Scholz U, Graner A, Platzer M, Dolezel J, Stein N (2009) Gene Content and Virtual Gene Order of Barley Chromosome 1H. Plant Physiology **151:** 496-505

Meyer D, Pajonk S, Micali C, O'Connell R, Schulze-Lefert P (2009) Extracellular transport and integration of plant secretory proteins into pathogen-induced cell wall compartments. The Plant Journal **57:** 986-999

Micali CO, Neumann U, Grunewald D, Panstruga R, O'Connell R (2011) Biogenesis of a specialized plant–fungal interface during host cell internalization of Golovinomyces orontii haustoria. Cellular Microbiology **13:** 210-226

Michalek W, Kleine M, Dargatz H, Wenzel G, Jahoor A (1997) Stability of Hor1-specific YAC-clones and physical mapping of Hor1-loci in barley. TAG Theoretical and Applied Genetics **95:** 369-374

Miklis M, Consonni C, Bhat RA, Lipka V, Schulze-Lefert P, Panstruga R (2007) Barley MLO Modulates Actin-Dependent and Actin-Independent Antifungal Defense Pathways at the Cell Periphery. Plant Physiology **144:** 1132-1143

Mochida K, Uehara-Yamaguchi Y, Yoshida T, Sakurai T, Shinozaki K (2011) Global Landscape of a Co-Expressed Gene Network in Barley and its Application to Gene Discovery in Triticeae Crops. Plant and Cell Physiology **52:** 785-803

Moore G, Devos K, Wang Z, Gale M (1995) Cereal genome evolution. Grasses, line up and form a circle. Curr Biol **5:** 737 - 739

Morozova O, Hirst M, Marra MA (2009) Applications of New Sequencing Technologies for Transcriptome Analysis. Annual Review of Genomics and Human Genetics **10:** 135-151

Mucha E, Fricke I, Schaefer A, Wittinghofer A, Berken A (2011) Rho proteins of plants – Functional cycle and regulation of cytoskeletal dynamics. European Journal of Cell Biology **90:** 934-943

Murat F, Xu J-H, Tannier E, Abrouk M, Guilhot N, Pont C, Messing J, Salse J (2010) Ancestral grass karyotype reconstruction unravels new mechanisms of genome shuffling as a source of plant evolution. Genome Research **20:** 1545-1557

Neil DL, Villasante A, Fisher RB, Vetrie D, Cox B, Tyler-Smit C (1990) Structural instability of human tandemly repeated DNA sequences cloned in yeast artificial chromosome vectors. Nucleic Acids Research **18:** 1421-1428

Nürnberger T, Brunner F, Kemmerling B, Piater L (2004) Innate immunity in plants and animals: striking similarities and obvious differences. Immunological Reviews **198:** 249-266

Nürnberger T, Lipka V (2005) Non-host resistance in plants: new insights into an old phenomenon. Molecular Plant Pathology **6:** 335-345

Obayashi T, Hayashi S, Saeki M, Ohta H, Kinoshita K (2009) ATTED-II provides coexpressed gene networks for Arabidopsis. Nucleic Acids Research **37:** D987-D991

Obayashi T, Kinoshita K (2010) Coexpression landscape in ATTED-II: usage of gene list and gene network for various types of pathways. Journal of Plant Research **123:** 311-319

Ogilvie DJ, James LA (1996) End Rescue from YACs Using the Vectorette. *In* D Markie, ed, YAC Protocols, Vol 54. Humana Press, pp 131-138

Okazaki Y, Shimojima M, Sawada Y, Toyooka K, Narisawa T, Mochida K, Tanaka H, Matsuda F, Hirai A, Hirai MY, Ohta H, Saito K (2009) A Chloroplastic UDP-Glucose Pyrophosphorylase from Arabidopsis Is the Committed Enzyme for the First Step of Sulfolipid Biosynthesis. The Plant Cell Online **21:** 892-909

Panstruga R (2005) Discovery of Novel Conserved Peptide Domains by Ortholog Comparison within Plant Multi-Protein Families. Plant Molecular Biology **59:** 485-500

Panstruga R, Büschges R, Piffanelli P, Schulze-Lefert P (1998) A contiguous 60 kb genomic stretch from barley reveals molecular evidence for gene islands in a monocot genome. Nucleic Acids Research **26:** 1056-1062

Passarge E, Horsthemke B, Farber2 RA (1999) Incorrect use of the term synteny. Nature Genetics **23:** 387

Paterson AH, Bowers JE, Bruggmann R, Dubchak I, Grimwood J, Gundlach H, Haberer G, Hellsten U, Mitros T, Poliakov A, Schmutz J, Spannagl M, Tang H, Wang X, Wicker T, Bharti AK, Chapman J, Feltus FA, Gowik U, Grigoriev IV, Lyons E, Maher CA, Martis M, Narechania A, Otillar RP, Penning BW, Salamov AA, Wang Y, Zhang L, Carpita NC, Freeling M, Gingle AR, Hash CT, Keller B, Klein P, Kresovich S, McCann MC, Ming R, Peterson DG, Mehboob ur R, Ware D, Westhoff P, Mayer KFX, Messing J, Rokhsar DS (2009) The Sorghum bicolor genome and the diversification of grasses. Nature **457:** 551-556

Pavan S, Schiavulli A, Appiano M, Marcotrigiano A, Cillo F, Visser R, Bai Y, Lotti C, Ricciardi L (2011) Pea powdery mildew resistance is associated to loss-of-function mutations at a MLO homologous locus. TAG Theoretical and Applied Genetics **123:** 1425-1431

Peterhänsel C, Freialdenhoven A, Kurth J, Kolsch R, Schulze-Lefert P (1997) Interaction Analyses of Genes Required for Resistance Responses to Powdery Mildew in Barley Reveal Distinct Pathways Leading to Leaf Cell Death. The Plant Cell Online **9:** 1397-1409

Piffanelli P, Zhou F, Casais C, Orme J, Jarosch B, Schaffrath U, Collins NC, Panstruga R, Schulze-Lefert P (2002) The Barley MLO Modulator of Defense and Cell Death Is Responsive to Biotic and Abiotic Stress Stimuli. Plant Physiology **129:** 1076-1085

Pourkheirandish M, Wicker T, Stein N, Fujimura T, Komatsuda T (2007) Analysis of the barley chromosome 2 region containing the six-rowed spike gene reveals a

breakdown of rice–barley micro collinearity by a transposition. TAG Theoretical and Applied Genetics **114:** 1357-1365

Quan L-J, Zhang B, Shi W-W, Li H-Y (2008) Hydrogen Peroxide in Plants: a Versatile Molecule of the Reactive Oxygen Species Network. Journal of Integrative Plant Biology **50:** 2-18

Riley J, Butler R, Ogilvie D, Finniear R, Jenner D, Powell S, Anand R, Smith JC, Markham AF (1990) A novel, rapid method for the isolation of terminal sequences from yeast artificial chromosome (YAC) clones. Nucleic Acids Research **18:** 2887-2890

Robertson G, Schein J, Chiu R, Corbett R, Field M, Jackman SD, Mungall K, Lee S, Okada HM, Qian JQ, Griffith M, Raymond A, Thiessen N, Cezard T, Butterfield YS, Newsome R, Chan SK, She R, Varhol R, Kamoh B, Prabhu A-L, Tam A, Zhao Y, Moore RA, Hirst M, Marra MA, Jones SJM, Hoodless PA, Birol I (2010) De novo assembly and analysis of RNA-seq data. Nat Meth **7:** 909-912

Robinson JT, Thorvaldsdóttir H, Winckler W, Guttman M, Lander ES, Getz G, Mesirov JP (2011) Integrative genomics viewer. Nature Biotechnology **29:** 24-26

Roosen G, Velten FW, Vos J-MH (2001) Artificial Chromosomes. *In* Encyclopedia of Life Sciences. John Wiley & Sons, Ltd

Rostoks N, Park Y-J, Ramakrishna W, Ma J, Druka A, Shiloff B, SanMiguel P, Jiang Z, Brueggeman R, Sandhu D, Gill K, Bennetzen J, Kleinhofs A (2002) Genomic sequencing reveals gene content, genomic organization, and recombination relationships in barley. Functional & Integrative Genomics **2:** 51-59

Salamini F, Ozkan H, Brandolini A, Schafer-Pregl R, Martin W (2002) Genetics and geography of wild cereal domestication in the near east. Nat Rev Genet **3:** 429-441

Schmelzer E (2002) Cell polarization, a crucial process in fungal defence. Trends in Plant Science **7:** 411-415

Schmidt D, Röder M, Dargatz H, Wolf N, Schweizer G, Tekauz A, Ganal M (2001) Construction of a YAC library from barley cultivar Franka and identification of YAC-derived markers linked to the *Rh2* gene conferring resistance to scald (*Rhynchosporium secalis*). Genome **44:** 1031-1040

Schulte D, Close TJ, Graner A, Langridge P, Matsumoto T, Muehlbauer G, Sato K, Schulman AH, Waugh R, Wise RP, Stein N (2009) The International Barley Sequencing Consortium—At the Threshold of Efficient Access to the Barley Genome. Plant Physiology **149:** 142-147

Shen Q-H (2004) Functional Analysis of Barley *MLA*-triggered Disease Resistance to the Powdery Mildew Pathogen. Universität zu Köln, Köln

Shirasu K, Lahaye T, Tan M-W, Zhou F, Azevedo C, Schulze-Lefert P (1999) A Novel Class of Eukaryotic Zinc-Binding Proteins Is Required for Disease Resistance Signaling in Barley and Development in C. elegans. Cell **99:** 355-366

Simons G, van der Lee T, Diergaarde P, van Daelen R, Groenendijk J, Frijters A, Büschges R, Hollricher K, Töpsch S, Schulze-Lefert P, Salamini F, Zabeau M, Vos P (1997) AFLP-Based Fine Mapping of the Mlo Gene to a 30-kb DNA Segment of the Barley Genome. Genomics **44:** 61-70

Simpson JT, Wong K, Jackman SD, Schein JE, Jones SJM, Birol İ (2009) ABySS: A parallel assembler for short read sequence data. Genome Research **19:** 1117-1123

Smith TA, Best GR (1978) Distribution of the hordatines in barley. Phytochemistry **17:** 1093-1098

Spanu PD, Abbott JC, Amselem J, Burgis TA, Soanes DM, Stüber K, Loren van Themaat EV, Brown JKM, Butcher SA, Gurr SJ, Lebrun M-H, Ridout CJ, Schulze-Lefert P, Talbot NJ, Ahmadinejad N, Ametz C, Barton GR, Benjdia M, Bidzinski P, Bindschedler LV, Both M, Brewer MT, Cadle-Davidson L, Cadle-Davidson MM, Collemare J, Cramer R, Frenkel O, Godfrey D, Harriman J, Hoede C, King BC, Klages S, Kleemann J, Knoll D, Koti PS, Kreplak J, López-Ruiz FJ, Lu X, Maekawa T, Mahanil S, Micali C, Milgroom MG, Montana G, Noir S, O'Connell RJ, Oberhaensli S,

Parlange F, Pedersen C, Quesneville H, Reinhardt R, Rott M, Sacristán S, Schmidt SM, Schön M, Skamnioti P, Sommer H, Stephens A, Takahara H, Thordal-Christensen H, Vigouroux M, Weßling R, Wicker T, Panstruga R (2010) Genome Expansion and Gene Loss in Powdery Mildew Fungi Reveal Tradeoffs in Extreme Parasitism. Science **330:** 1543-1546

Sreenivasulu N, Graner A, Wobus U (2008) Barley Genomics: An Overview. International Journal of Plant Genomics **2008**

Srinivasasainagendra V, Page GP, Mehta T, Coulibaly I, Loraine AE (2008) CressExpress: A Tool For Large-Scale Mining of Expression Data from Arabidopsis. Plant Physiology **147:** 1004-1016

Stein M, Dittgen J, Sánchez-Rodríguez C, Hou B-H, Molina A, Schulze-Lefert P, Lipka V, Somerville S (2006) Arabidopsis PEN3/PDR8, an ATP Binding Cassette Transporter, Contributes to Nonhost Resistance to Inappropriate Pathogens That Enter by Direct Penetration. The Plant Cell Online **18:** 731-746

Stein N (2007b) Triticeae genomics: advances in sequence analysis of large genome cereal crops. Chromosome Research **15:** 21-31

Stein N, Prasad M, Scholz U, Thiel T, Zhang H, Wolf M, Kota R, Varshney R, Perovic D, Grosse I, Graner A (2007a) A 1,000-loci transcript map of the barley genome: new anchoring points for integrative grass genomics. Theoretical and Applied Genetics **114:** 823 - 839

Stoessl A (1967) The antifungal factors in barley. IV. Isolation, structure, and synthesis of the hordatines. Canadian Journal of Chemistry **45:** 1745-1760

Takemoto D, Hardham AR (2004) The Cytoskeleton as a Regulator and Target of Biotic Interactions in Plants. Plant Physiology **136:** 3864-3876

Takemoto D, Jones DA, Hardham AR (2003) GFP-tagging of cell components reveals the dynamics of subcellular re-organization in response to infection of Arabidopsis by oomycete pathogens. The Plant Journal **33:** 775-792

Takemoto D, Jones DA, Hardham AR (2006) Re-organization of the cytoskeleton and endoplasmic reticulum in the Arabidopsis *pen1*-1 mutant inoculated with the non-adapted powdery mildew pathogen, *Blumeria graminis* f. sp. *hordei*. Molecular Plant Pathology **7:** 553-563

Thiel T, Graner A, Waugh R, Grosse I, Close T, Stein N (2009) Evidence and evolutionary analysis of ancient whole-genome duplication in barley predating the divergence from rice. BMC Evolutionary Biology **9:** 209

Thordal-Christensen H (2003) Fresh insights into processes of nonhost resistance. Current Opinion in Plant Biology **6:** 351-357

Tian M, Chaudhry F, Ruzicka DR, Meagher RB, Staiger CJ, Day B (2009) Arabidopsis Actin-Depolymerizing Factor AtADF4 Mediates Defense Signal Transduction Triggered by the Pseudomonas syringae Effector AvrPphB. Plant Physiology **150:** 815-824

TIBI (2010) Genome sequencing and analysis of the model grass Brachypodium distachyon. Nature **463:** 763-768

Trujillo M, Troeger M, Niks RE, Kogel K-H, HÜCkelhoven R (2004) Mechanistic and genetic overlap of barley host and non-host resistance to Blumeria graminis. Molecular Plant Pathology **5:** 389-396

Underwood W, Somerville SC (2008) Focal accumulation of defences at sites of fungal pathogen attack. Journal of Experimental Botany **59:** 3501-3508

von Röpenack E, Parr A, Schulze-Lefert P (1998) Structural Analyses and Dynamics of Soluble and Cell Wall-bound Phenolics in a Broad Spectrum Resistance to the Powdery Mildew Fungus in Barley. Journal of Biological Chemistry **273:** 9013-9022

Wicker T, Sabot F, Hua-Van A, Bennetzen JL, Capy P, Chalhoub B, Flavell A, Leroy P, Morgante M, Panaud O, Paux E, SanMiguel P, Schulman AH (2007) A unified classification system for eukaryotic transposable elements. Nat Rev Genet **8:** 973-982

Wicker T, Taudien S, Houben A, Keller B, Graner A, Platzer M, Stein N (2009) A whole-genome snapshot of 454 sequences exposes the composition of the barley genome and provides evidence for parallel evolution of genome size in wheat and barley. The Plant Journal **59:** 712-722

Wolter M, Hollricher K, Salamini F, Schulze-Lefert P (1993) The mlo resistance alleles to powdery mildew infection in barley trigger a developmentally controlled defence mimic phenotype. Molecular and General Genetics MGG **239:** 122-128

Xu Z, Escamilla-Treviño L, Zeng L, Lalgondar M, Bevan D, Winkel B, Mohamed A, Cheng C-L, Shih M-C, Poulton J, Esen A (2004) Functional genomic analysis of Arabidopsis thaliana glycoside hydrolase family 1. Plant Molecular Biology **55:** 343-367

Zeyen RJ, Carver TLW, Lyngkjar MF (2002) Epidermal cell papillae. *In* WRB Richard R. Bélanger, Aleid J. Dik and Timothy L.W. Carver, ed, The Powdery Mildews A Comprehensive Treatise. APS Press, USA, p 292

Zhang Z, Henderson C, Perfect E, Carver TLW, Thomas BJ, Skamnioti P, Gurr SJ (2005) Of genes and genomes, needles and haystacks: Blumeria graminis and functionality. Molecular Plant Pathology **6:** 561-575

7. Supplemental Material

Please refer to the "Supplemental CD" for the files regarding this section.

7.1. Genomic sequences from *Pol* (encoding a DNA-directed RNA polymerase I subunit 2) and *Cons* (encoding a protein of unknown function, DUF 1218 family member). The sequences were provided by Nicholas Collins (unpublished data).

7.2. YAC end sequences of isolated clones 87A3, 82B11 and 158C12 used to design primers for chromosome walking with the YAC library.

7.3. YAC end sequences of isolated clones 305A11 and 354G1 used to design primers for chromosome walking with the YAC library.

7.4. Illumina sequencing data from YAC clones 87A3, 82B11 and 158C12.

7.5. Illumina sequencing data from YAC clones 305A11, 72C11 and 354G1.

7.6. Sequences of the *Ror1* candidate genes with DNA polymorphisms between cv. Malteria Heda and cv. Ingrid

7.7. Sequences of the scaffolds from YAC clone 87A3.

7.8. Sequences of the *Ror1* candidate genes with DNA polymorphisms between cv. Malteria Heda and cv. Ingrid. Co-expressed genes approach.

Acknowledgements

I would like to express my gratitude to all people who helped me in achieving my PhD. In especial,

Prof. Dr. Paul Schulze-Lefert for the great opportunity to do my PhD at the Plant-Microbe Interactions Department at the MPIPZ. Many thanks for the stimulating discussions during the departmental seminars and the encouragement to be critical about our work.

Prof. Dr. Ulf-Ingo Flügge and Prof. Dr. Martin Hülskamp for accepting to be members of my PhD examining committee.

Dr. Patrick Schweizer for accepting to be the external examiner of my PhD committee.

My supervisor, Prof. Dr. Ralph Panstruga for making the process of doing a PhD an invaluable personal and professional experience. Thank you for giving me the chance of working in your group and for the support, guidance and enthusiasm to develop this project. I also appreciate all your critical comments and suggestions for my thesis document.

Mariam Benjdia and Nicholas Collins for the plant material and information obtained regarding *Ror1*. Especially to Nick, who was always willing to clarify the data with us. Thanks to Dr. Pietro Spanu, Dr. Peter Nürnberg, Dr. Janine Altmüller, Dr. Nahal Ahmadinejad, Dr. Lu Ma, Dr. Andreas Houben and Dr. Nils Stein for all the scientific collaboration to perform experiments or analysis of data for this project.

My sincere thanks to the Panstruga´s former and present members, for the friendly atmosphere and great discussions at the lab: Amber, Corinna, Katia, Matt, Nana, Przemek, Ralf, Rik, Sandra, Sarah and Shermineh. “Vielen Dank” to Anuschka for all the help inside and outside of the MPIPZ, you are just amazing! and last but not least “Dziękuję” to lady Justine, an incredible person I am glad to have found in this way, thank you for listening, for all the cups of coffee, for your help and for your nice company anytime.

I enjoyed the great year as PhD representative and the work together with Emma, Ben and Stefan. Thanks to you!

I would like to thank those friends outside the lab that made my life here much more enjoyable.

Hay dos ángeles de la guarda a los cuales les dedico un especial agradecimiento: Camila y Johana. Gracias por su compañía, ayuda y apoyo para hacer de ésta, una grata experiencia.

Agradezco a mis amigos y familia en Colombia y los que están en algún otro lugar del mundo, por el constante apoyo para seguir adelante con este proyecto y porque a pesar del tiempo y la distancia sigo contando con ellos.

Un especial agradecimiento va para el Dr. Fernando Rodríguez, Dr. Víctor Núñez y para mi mentor Prof. Dr. Juan José Filgueira, por creer en mí y por haberme brindado las herramientas necesarias para lograr esta posición.

Muchas gracias a mis adorados padres y hermana, por el gran ejemplo de superación, por su apoyo incondicional y sobre todo por su amor, paciencia y fuerza para superar la barrera física que nos separa y sentirlos aquí, cerca de mí.

My deepest “Dank u wel” goes to Mark. My PhD study could never be fulfilled without your unconditional support, care, help and amazing patience. “Muchas Gracias” for your everyday company, for your confidence in me and especially for your love *“because it’s always better if we’re together”.*

Finalmente a Dios, por darme la fortaleza de levantarme cada vez que caí.

Erklärung

Ich versichere, dass ich die von mir vorgelegte Dissertation selbständig angefertigt, die benutzten Quellen und Hilfsmittel vollständig angegeben und die Stellen der Arbeit - einschließlich Tabellen, Karten und Abbildungen -, die anderen Werken im Wortlaut oder dem Sinn nach entnommen sind, in jedem Einzelfall als Entlehnung kenntlich gemacht habe; dass diese Dissertation noch keiner anderen Fakultät oder Universität zur Prüfung vorgelegen hat; noch nicht veröffentlicht worden ist sowie, dass ich eine solche Veröffentlichung vor Abschluss des Promotionsverfahrens nicht vornehmen werde. Die Bestimmungen dieser Promotionsordnung sind mir bekannt. Die von mir vorgelegte Dissertation ist von Prof. Dr. Paul Schulze-Lefert betreut worden.

Köln, 5. Dezember 2011 _____

Johanna Acevedo García